Some Phenomenological Aspects of Topologically Massive Gauge Theories

Thesis submitted for the degree of
Doctor of Philosophy (Science)

in

Physics (Theoretical)

by

Debmalya Mukhopadhyay

Department of Physics
University of Calcutta
May, 2017

To Dear Colleagues.

Acknowledgments

I am very grateful to my supervisor Prof. Amitabha Lahiri for his teaching, helps and questions. His questions always trained me to go into deep in the subjects and helped me find the way to get answer. I want to thank him for keeping patience and tolerating my mistakes with his great kindness. I must thank to the ex-director, Prof. Arup Kumar Raychoudhury and ex-academic dean, Prof. Jayanta Kr. Bhattacharya for giving me the opportunity to pursue my PhD in S. N. Bose Institute. I wish to acknowledge with sincere gratitude Prof. Jayanta Kr. Bhattachriya for his teaching and various academic discussions and non-academic helps.

I would like to thank my seniors Dr. Chandrasekhar Chatterjee and Dr. Sourav Bhattacharya for various academic and non-academic helps. I must be very grateful to our librarian Mr. Soumen Adhikari and library-staffs Mr. Gurudas Ghosh, Mr. Amit Roy, Mr. Ratan Acharya and Mrs. Ananya Sarkar for various academic helps. I will be missing the library where I have spent most of the time in my PhD tenureship.

I am also grateful to all my juniors cum friends, Subhasish, Sayani, Ishita, Anuradha, Abhishek, Pratik, Shauri, Anita, Krishendu and many more for their various academic and non-academic supports in my PhD-life.

Debmalya Mukhopadhyay
Kolkata, India

List of Publications

This thesis is based on the following publications:

1. Unitarity in $WW \to WW$ elastic scattering in topologically massive $SU(2)$ gauge theory.
   Amitabha Lahiri, Debmalya Mukhopadhyay.
   arXiv:1107.1501[hep-ph](2013).

2. β-function for topologically massive gluons.
   Debmalya Mukhopadhyay, Amitabha Lahiri.
   Phys. Rev. **D90**, 025015(2014), arXiv:1407.3148[hep-ph].

Contents

List of Figures

Chapter 1

Introduction

Quantum gauge field theories describe fundamental interactions. The description of the interactions among photons and various charged particles is given by an Abelian gauge theory i.e. quantum electrodynamics (QED) and it is very successful. This success encourages us to describe the electromagnetic, weak and strong interactions in nature by gauge theories. Unlike QED, weak and strong interactions are described by Yang-Mills theory [1]. Unification of electromagnetic and weak interactions [2–4] into the electroweak theory is quite successful in the Standard model of particle physics.

In this thesis, we will consider non-Abelian generalization of a topologically massive model [5–7] in 3+1 dimension where the gauge fields become massive keeping the global symmetry unbroken. This model contains a two form field $B_{\mu\nu}$, known as Kalb Ramond (KR) field [8] which couples with A_μ through a term $mB\wedge F = \frac{m}{4}\epsilon^{\mu\nu\rho\lambda}B_{\mu\nu}F_{\rho\lambda}$ term, where $F_{\rho\lambda}$ is the field strength of one form gauge field A_ρ. This coupling term is four dimensional generalization of Chern Simons term. Massless $B_{\mu\nu}$ field has only one degree of freedom whereas massless A_μ field has two degrees of freedom [8]. But if $B^{\mu\nu}$ is taken to be massive then it has three degrees of freedom like the massive A^μ

field. The fields become massive in this model without a residual degrees of freedom like Higgs field in Higgs mechanism [9–11]. Our convention for the signature of metric is $(+,-,-,-)$.

We will consider the application of the model in quantum chromodynamics (QCD) because it is believed that QCD is described by unbroken $SU(3)$ Yang-Mills (YM) theory [12–15]. The non-Abelian gauge fields in YM theory are the source of themselves i.e. they carry the color charges. As a consequence there are various non-linear interactions among the massless gauge bosons in a YM theory. Instead of taking massless we consider massive gauge fields because mass of the gauge boson plays important roles in the perturbative analysis in QCD. We will consider elastic scatterings among massive non-Abelian gauge bosons and the behaviour of gauge coupling constant with energy scale in the topologically massive model in this thesis which depend on perturbation technique. But there is a limitation in the use of this technique in non-Abelian gauge theory. This technique can be used in YM theory at higher energy because the strength of the strong interaction decreases with increase of energy scale. As a consequence, the interaction becomes weak at high energy and it can be treated in perturbation theory. This behaviour of the coupling strength is known as asymptotic freedom [16–23]. The variation of strong coupling constant α_s with the energy scale Q in massless Yang-Mills theory with matter fields from one loop correction is given by

$$\frac{\partial g}{\partial \ln \mu} = \beta(g) = -\frac{g^3}{16\pi^2}\left(\frac{11}{3}N_c - \frac{2}{3}N_f - \frac{1}{6}N_s\right), \tag{1.1}$$

where g is the gauge coupling constant in Yang-Mills theory. Here N_c is the number of colors, N_f and N_s are the number of flavours of fermions and scalar bosons respectively. From the above expression, we get

$$\alpha_s(Q) = \frac{4\pi}{b\ln\left(\frac{Q^2}{\Lambda^2}\right)}, \tag{1.2}$$

where

$$\alpha_s = \frac{g^2}{4\pi}, \qquad b = \frac{11}{3}N_c - \frac{2}{3}N_f - \frac{1}{6}N_s \ . \tag{1.3}$$

Λ is the energy scale which is defined as

$$\frac{1}{\alpha_s(\Lambda)} = 0, \tag{1.4}$$

which tells that at the energy scale Λ, the coupling strength becomes very large and consequently the quarks are strongly bound or confined in the hadrons. Present value of Λ is few hundred MeV [24] for six flavours of quarks and no scalar. The behaviour of α_s at high energy can be found experimentally where a deep inelastic scattering phenomena takes place between electron and proton. At high energy, the electrons can interact with quarks and gluons in the hadron and produce many particles in the final state. This process is characterised by two kinematic variables: i) the momentum transfer q and ii) the energy E of the virtual photon. If the mass of the nucleon is M, then a dimensionless parameter is constructed in lab frame, which is known as Bjorken x:

$$x = -\frac{q^2}{2ME}. \tag{1.5}$$

Here M is the mass of the proton. The proton is taken to be at rest in the analysis. Since q^2 is a negative quantity in a scattering process, x is positive and we can show from the kinematics that $0 < x < 1$. The scattering cross-section of the process depends on two functions $F_i(q^2, x)$, where $i = 1, 2$, which signify the structure of the nucleon. As $-q^2$ increases, F_i's rapidly lose the dependence on q^2 and becomes the functions of x only:

$$\lim_{-q^2 \to \infty} F_i(q^2, x) = F_i(x). \tag{1.6}$$

So the structure functions become independent of any mass scale. This is known as Bjorken scaling and was first obtained by operator product expansion [25–28]. Experimentally Bjorken scaling is obtained for the value of $Q^2 \geq 2(\text{GeV})^2$. This behaviour of the structure functions can be explained by the Parton model [29] where perturbation theory is used to describe the interactions among virtual photon and quarks. The process is designated as $ep \rightarrow eX$, where X denotes the particles produced due to interactions among electrons and quarks via photon γ. The calculated values of the structure functions from the parton model agree with their experimental values within about $10 - 15\%$. This explanation is only possible when we take the couplings among quarks to be very weak in deep Euclidean region ($-q^2 \rightarrow \infty$), implying asymptotic freedom. Asymptotic freedom also occurs for weak interaction but the weak-coupling strength reduces much more slowly with energy as compared to the coupling strength of strong interaction. But unlike the sources of electromagnetic and weak interaction, the color charges are not found isolated in the experiment, they are confined in hadrons. This confinement cannot be explained in perturbative analysis at high energy. At the energy $Q \sim \Lambda$, α becomes very large and quarks and gluons interact among themselves strongly which leads them to form bound states. In this energy regime, perturbation technique does not work. In the perturbative analysis, we should work in the energy regime $Q \gg \Lambda$.

We have seen from the presence of N_f and N_s in the eqn.(1.2) how interactions among the matter and gauge fields affect the behaviour of α_s with energy scale. Since we will consider a topologically massive model which contains linear and non-linear interactions among A^μ and $B^{\mu\nu}$ fields, it will be interesting to see how the asymptotic freedom will be affected due to the presence of the interactions of the YM and tensor fields. We will see asymptotic freedom in this topologically massive model in the chapter 3 of this thesis.

Confinement of colored particles is due to the behaviour of the strong coupling strength at low energy. Its dynamical mechanism is not understood yet. However, the mass of the gauge boson plays an important role in a possible explanation of confinement of gluons in QCD. That is why we find that the topologically massive model becomes very important for the analysis of QCD. Massive gauge bosons are also important in the analysis of scattering phenomena among gauge bosons in an unbroken non-Abelian gauge theory, which we will consider. I will give now a brief review of some models which were built to explain confinement in non-perturbative regime. Next we will discuss the importance of the mass of gauge boson in scattering theory of non-Abelian gauge bosons.

There are various models built for explaining confinement. Taking the meson to be a bound state of quarks and anti-quarks, Y. Nambu and G. Jona-Lasinio developed their model in 1961 [30] in analogy with the paired state formed by the Cooper pair in superconductivity. In the theory of the superconductivity developed by J. Bardeen, L. N. Cooper, J. R. Schrieffer [31, 32] and N. N. Bogoliubov [33], the ground state of the system does not remain invariant under the global symmetry, i.e. spontaneous symmetry breaking occurs. But the color symmetry is believed to be unbroken in QCD. This implies that all the gluons have equal mass.

One of the very important facts regarding the structure of hadrons was found by T. Regge. The plot of square of mass M^2 vs spin J of hadrons became a possible insight of the structure of hadrons. It is a set of straight lines and each line is called a Regge trajectory [34, 35]. This plot is shown in Fig. 1.1. The straight lines are obtained from the hadronic interaction. An important characteristic of the lines is that they are parallel to one another. This implies that the rate of increase of the square of mass with spin is the same for all resonances. The equation of the lines can

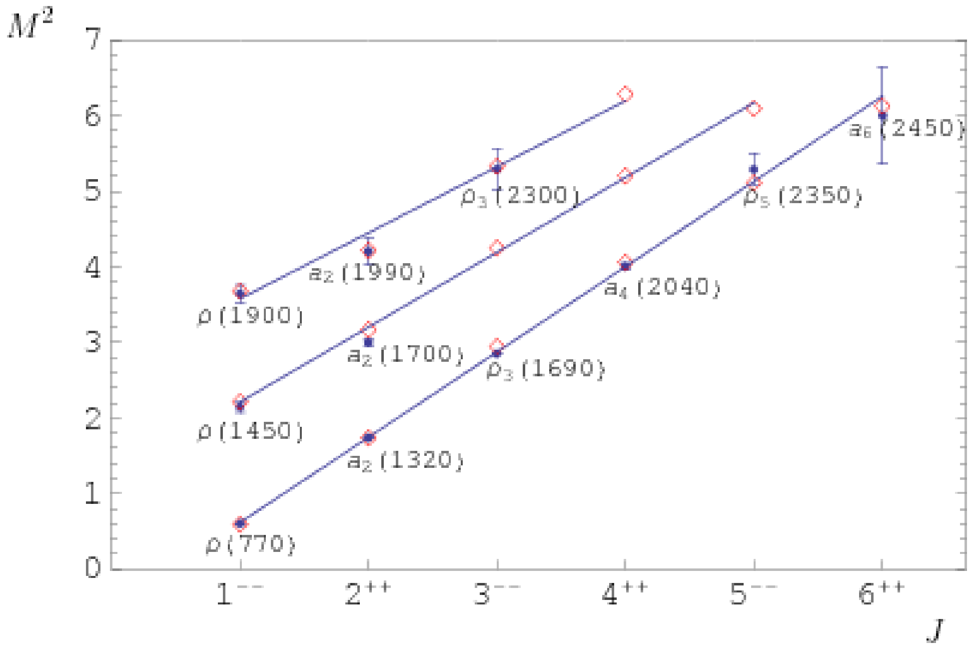

Figure 1.1 Regge trajectories : M^2 vs J^{PC} plot taken from [36] with the authors' permission.

be written as

$$J = \alpha_0 + \alpha' M^2, \tag{1.7}$$

with

$$\alpha' \approx 1 \text{ GeV}^2. \tag{1.8}$$

Here α_0 is the Regge intercept and α' is the Regge slope. A possible explanation of this plot is found if the quarks are taken to be attached by strings. We imagine two massless quarks, connected by a string of length d, rotating with a speed of light. Each point, at a distance r from the centre, has the local velocity $\frac{v}{c} = \frac{2r}{d}$. The total energy or mass of the string is

$$M = 2\int_0^{\frac{d}{2}} \frac{K dr}{(1-v^2)^{1/2}} = \frac{\pi K d}{2}, \tag{1.9}$$

where K is the string tension, and the spin is

$$J = 2\int_0^{\frac{d}{2}} \frac{Krvdr}{(1-v^2)^{1/2}} = \frac{\pi K d^2}{8}. \tag{1.10}$$

Hence we get from eqn.(1.9)-(1.10)

$$J = \frac{1}{2\pi K} M^2. \tag{1.11}$$

Comparing the eqn.(1.7) and eqn.(1.11) we get

$$K = \frac{1}{2\pi\alpha'}. \tag{1.12}$$

Hence taking the value of $\alpha' \approx 1$ GeV^2, we get

$$K \approx 0.16 \text{ GeV}^{-2}. \tag{1.13}$$

Regge trajectories were further investigated deeply by G. Veneziano. He showed in 1968 [37] that the amplitude of $2 \to 2$ meson-meson elastic scattering can be interpreted as the sum of the amplitudes of the interactions among "states" obeying

$$J = \alpha_0 + \alpha' M_J^2, \tag{1.14}$$

where M_J is the mass of particle having spin J. This gives rise to the "dual resonance model". In this model, one calculates the amplitude for elastic scattering of mesons. The basic assumption of the model is that the hadrons interact through the formation of intermediate states (resonances). According to this model the sum of the scattering amplitudes of the $2 \to 2$ meson-meson scattering is

$$A(s,t) = \frac{\Gamma(-\alpha(s))\Gamma(-\alpha(t))}{\Gamma(-\alpha(s)-\alpha(t))}, \tag{1.15}$$

where s and t are the usual Mandelstam variables and

$$\alpha(x) = \alpha_0 + \alpha' x, \tag{1.16}$$

and Γ is the gamma function. It is clear from the expression in eqn.(1.15) that the amplitude $A(s,t)$ is symmetric under the exchange of s and t. It can be shown that the expansion of the amplitude as a power series of s or t yields each term of the expansion to be t or s channel Feynman diagrams. The amplitude has a remarkable property. If one fixes s or t and expands the amplitude in eqn.(1.15) as a power series of t or s, then the amplitude can be written as [38]

$$A(s,t) = \sum_{J=0}^{\infty} \frac{g_J^2 t^J}{s - M_J^2}, \qquad \text{or} \qquad A(s,t) = \sum_{J=0}^{\infty} \frac{g_J^2 s^J}{t - M_J^2}, \tag{1.17}$$

where $g_J^2 = \dfrac{g^2(\alpha')^{J-1}}{J!}$ and M_J is given by eqn.(1.14). We can see from the above eqn.(1.17) that each term in the summation corresponds to an s-channel or t-channel process for having an intermediate resonance of spin J and mass M_J which obey the linear relation, given in eqn.(1.14). We can observe that the amplitude can be represented by either the sum of t or s-channels. This can be interpreted by crossing symmetry. This symmetry implies that if we exchange the incoming momenta with the outgoing momenta in the external legs, t or s, then we can get the amplitude of the other, s or t. On the basis of dual resonance model, Susskind proposed the states to

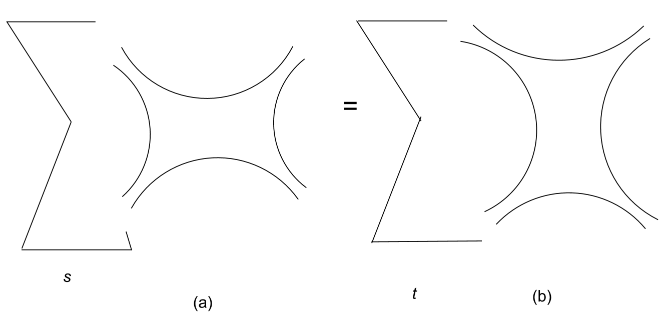

Figure 1.2 (a) Sum of s-channels; (b) sum of t-channels.

be excitations of strings [39]. So if mesons are assumed to be states having quarks and antiquarks attached by strings then we can represent the sum of the s and t channels by the diagram in Fig. 1.2. The strings sweep out a two dimensional surface which is known as string worldsheet. We can see from this figure that topology of t-channel worldsheet can be smoothly deformed into s-channel worldsheet, which shows the local scale invariance of string theory. During the interaction among mesons, the strings also interact with each other. Kalb-Ramond field, $B_{\mu\nu}$ is used in the description of interstring interactions.

A. A. Abrikosov predicted vortex of supercurrent in type II superconductivity when magnetic field overcomes a critical value [40]. This vortex formation is theoretically explained in Ginzburg-Landau model [41]. Motivated by this model, H. B. Nielsen and P. Olesen proposed a way of construction of vortex or flux tube in a Higgs model where $U(1)$ global symmetry is spontaneously broken [42]. The Lagrangian density of the model is

$$\mathscr{L} = -\frac{1}{4}F^{\mu\nu}F_{\mu\nu} + D_\mu\phi\,(D^\mu\phi)^\dagger + \frac{1}{2}\mu^2\left(\phi^\dagger\phi\right) - \frac{1}{4}\lambda\left(\phi^\dagger\phi\right)^2, \tag{1.18}$$

where ϕ is a complex scalar field and μ and λ are the constants. This Lagrangian density remains invariant under $U(1)$ global symmetry. Associated equations of motion are

$$\begin{aligned} \Box A^\mu - \partial^\mu\partial^\nu A_\nu &= j^\mu = -\left[ie(\phi^\dagger\partial^\mu\phi - \phi\partial^\mu\phi^\dagger) + 2e^2A^\mu\phi^\dagger(x)\phi(x)\right], &(1.19)\\ \Box\phi &= \frac{1}{2}(\mu^2 - \lambda|\phi|^2) - ie(2A^\mu\partial_\mu\phi + \phi\partial_\mu A^\mu) + e^2A^\mu A_\mu\phi. &(1.20)\end{aligned}$$

The minimum of the potential

$$V(\phi) = \frac{\mu^2}{2}\left(\phi\phi^\dagger\right) - \frac{1}{4}\lambda\left(\phi\phi^\dagger\right)^2, \tag{1.21}$$

occurs at

$$|\langle\phi\rangle| = v = \sqrt{\frac{\mu}{\lambda}}. \tag{1.22}$$

Let us write

$$\phi(x) = \rho \, e^{i\chi(x)}, \tag{1.23}$$

where ρ and $\chi(x)$ are the real functions of space-time. Invariance of ϕ under the transformation $\chi \to \chi + 2\pi n$, where $n = 1, 2 \ldots$, shows that ϕ is single valued. Assuming cylindrical symmetry around an axis, we can construct a vortex type field configuration at

$$\phi = \rho(r) e^{in\theta}, \tag{1.24}$$

where $\chi(x) = n\theta(x)$ and r is the normal distance from the axis. Here $\rho(r) \to v$ in the limit $r \to \infty$. It follows from the equation of motion of A^μ, given in eqn.(1.19), and eqn.(1.23)

$$A^\mu = -\frac{j^\mu}{2e^2}|\phi|^2 + \frac{1}{e}\partial^\mu \chi(x), \tag{1.25}$$

where

$$j^\mu = \frac{1}{2} ie(\phi^\dagger \partial^\mu \phi - \phi \partial^\mu \phi^\dagger) + e^2 A^\mu \phi^\dagger(x)\phi(x). \tag{1.26}$$

The flux of $F^{\mu\nu}$ through two dimensional surface bounded by a circle at infinity is

$$\Phi = \int F^{\mu\nu}\sigma_{\mu\nu} = \oint A^\mu dx_\mu. \tag{1.27}$$

We assume that j^μ in eqn.(1.25) vanishes at infinity and we get from the eqn.(1.25)

$$\Phi = -\frac{1}{e}\oint dx^\mu A_\mu = \frac{2\pi n}{e}. \tag{1.28}$$

Here n represents the number of winding around the vortex. Thus the magnetic flux of the vortex lines is quantised, to be multiple of $\frac{2\pi}{e}$. Now we are considering the vortex in static configuration. We take temporal gauge $A^0 = 0$ and also $\mathbf{E} = 0$. Then we see that the 'kinetic energy' of the gauge field $\mathbf{E}^2 = 0$, where $E^i = F^{0i}$. In this configuration the vector potential around this vortex at $r \to \infty$ is given by

$$\mathbf{A}(r) = \frac{1}{e}\nabla\chi = \frac{1}{e}\nabla\theta. \tag{1.29}$$

We have taken $n = 1$, in the eqn.(1.24), which signifies that the vortex contains a single unit of quantized flux. The flux is given by through a circle of radius r

$$\Phi(r) = 2\pi r A_\theta(r), \tag{1.30}$$

where $A_\theta(r)$ is the azimuthal component of $\mathbf{A}(r)$. Hence the magnitude of the magnetic field is

$$B(r) = \frac{1}{2\pi r}\frac{d\Phi}{dr} = \frac{1}{r}\frac{d}{dr}(rA(r)). \tag{1.31}$$

The magnetic field is along the z-axis. Taking θ component of eqn.(1.19) and using eqn.(1.24), we have

$$-\frac{ie}{r}2i\rho^2 + 2e^2A\rho^2 = -\partial_i F_{\theta i}, \tag{1.32}$$

which gives

$$\frac{d}{dr}\left(\frac{1}{r}\frac{d}{dr}(rA)\right) - 2e\left(\frac{1}{r} + eA\right)\rho^2 = 0. \tag{1.33}$$

There is no exact solution of the above equation. In the approximation where $\rho = v$ is constant (i.e. for $r \to \infty$), it is found

$$A(r) = -\frac{1}{er} - \frac{k}{e}K_1(|e|vr), \tag{1.34}$$

where K_1 is the modified Bessel function and k is the constant of integration. In the limit $r \to \infty$, the solution becomes

$$A(r) \to -\frac{1}{er} - \frac{k}{e}\sqrt{\frac{\pi}{2evr}}\exp(-evr), \tag{1.35}$$

and $\lim_{r\to\infty} \sqrt{\phi^\dagger \phi} = v$. The magnetic field corresponding to the vector potential becomes

$$|B(r)| \to k\sqrt{\frac{\pi v}{2er}} e^{-evr}, \qquad r \to \infty. \tag{1.36}$$

So we can see that the magnetic field deviates appreciably from zero only near the x^3 axis in a region with characteristic length l, where

$$l = \frac{1}{ev}. \tag{1.37}$$

When the global U(1) symmetry is spontaneously broken, the mass of the gauge boson becomes

$$m_V = ev. \tag{1.38}$$

Therefore the magnetic field and hence the corresponding is confined within the flux tube of radius $r \sim \frac{1}{m_V}$. In the static case, the eqn.(1.20) provides

$$\frac{1}{r}\frac{d}{dr}\left(r\frac{d\rho}{dr}\right) - \left[\left(\frac{1}{r} - eA\right)^2 - \mu^2 + \frac{\lambda}{2}\rho^2\right]\rho = 0. \tag{1.39}$$

Writing $\rho = v + \eta$, where η is a scalar field, we get the asymptotic form for the solution to eqn.(1.39)

$$\rho = v(1 - e^{-\xi r}), \tag{1.40}$$

where ξ is a new characteristic length

$$\xi = \frac{1}{\mu}, \tag{1.41}$$

which measures the distance required for ρ to attain its asymptotic value v. The integration constant k is chosen such a way that flux $\Phi(r) = 2\pi r A(r)$ shall go to zero for $\xi \ll r \ll l$.

Vortex configuration of the field ϕ requires it to be single valued with respect to spatial coordinates. Suppose the field ϕ is in a representation of group G. The vortex configuration of the field defines a mapping of the boundary of the vortex in the physical space onto the group space [15, 25, 44]. But if a vortex configuration is topologically equivalent to a point on a group manifold, then the configuration is not stable. These mappings are unstable in a non-Abelian gauge theory because the first homotopy of the group $\pi_1(G) = 0$. If we take a group $SU(2)$ whose group manifold is a three sphere S^3, then first homotopy group for this case $\pi_1(S^3) = 0$, because this mapping means a map $S^1 \rightarrow S^3$ i.e. a circle winds a three-sphere, which can be shrunk to a point. This is schematically shown in the Fig. 1.3. When a global

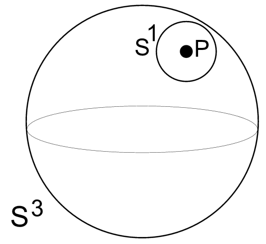

Figure 1.3 S^1 on S^3 can be shrunk to a point P.

symmetry corresponding to a group G symmetry is spontaneously broken down to the to $U(1)$ symmetry, then the vortex is topologically stable, because $\pi_1(U(1)) \neq 0$. But for any gauge theory with unbroken $SU(N)$ global symmetry $\pi_1(SU(N)) = 0$ where $N \geq 2$. Hence unlike the Nielsen-Olesen model, there is no stable Abrikosov flux tube in an unbroken $SU(N)$ gauge theory. These can be formed by the Abelian projection of a non-Abelian gauge theory where spontaneous symmetry breaking occurs [45, 46]. We consider the topologically massive model which contains the Kalb-Ramond field field. The Kalb-Ramond field plays an important role in the interstring interaction [8] which we explain below.

1.1 Kalb-Ramond field in interstring interaction

Abrikosov-Nielsen-Olesen (ANO) string with the quark and anti-quark at the ends are models of mesons. The string contains chromoelectric flux. Flux tubes having very tiny radius are string-like objects sweeping two dimensional world sheets. Such a surface is parametrized by two parameters, say σ and τ. Action for a string is given by Nambu-action [47]

$$S = -\frac{T}{2\pi}\int d\sigma d\tau\sqrt{-h}, \tag{1.42}$$

where h is the determinant of the matrix

$$h_{ab} = \partial_a X^\mu \partial_b X_\mu, \qquad a, b = 0, 1. \tag{1.43}$$

and T is a constant taken to make the action dimensionless. The determinant of the matrix is

$$h = \epsilon_{ab} h^{0a} h^{1b} = \dot{X}^2 X'^2 - \left(\dot{X}\cdot X'\right)^2, \tag{1.44}$$

where $\epsilon_{01} = -\epsilon_{10} = 1$ and $\epsilon_{00} = \epsilon_{11} = 0$. Here $\dot{X}^\mu = \frac{\partial X^\mu}{\partial \tau}$ and $X'^\mu = \frac{\partial X^\mu}{\partial \sigma}$. Hence the Nambu-action, given in eqn.(1.42), becomes

$$S = \int d\sigma d\tau \sqrt{\left(\dot{X}\cdot X'\right)^2 - \dot{X}^2 X'^2}. \tag{1.45}$$

Now suppose we are considering a uniform motion of flux tube. Due to Lorentz contraction, the Lagrangian density $\mathcal{L}_{\text{fluxtube}}$ of a flux tube, having very little width and moving in the transverse direction of its length with three velocity of magnitude $\mathbf{v}_\perp$, is

$$\mathcal{L}_{\text{fluxtube}} \propto \int \sqrt{1-\mathbf{v}_\perp^2}\, d\sigma dt, \tag{1.46}$$

where $\mathbf{v}_\perp = \dot{\mathbf{X}} - \mathbf{X}'(\dot{\mathbf{X}}\cdot\mathbf{X}')$. This is the same as obtained from the Nambu action when the parameter τ is taken to be t. The interaction between two open or closed string is mediated by Kalb-Ramond field and is given by

$$
\begin{aligned}
\mathcal{L}_{\text{int}} &= \int d\sigma d\tau B^{\mu\nu}\dot{X}_{[\mu}X'_{\nu]} && (1.47)\\
&= \int d\sigma d\tau B^{\mu\nu}\sigma_{\mu\nu}(x), && (1.48)
\end{aligned}
$$

where $\sigma_{\mu\nu}(x) = \dot{X}_{[\mu}X'_{\nu]}$ and $B^{\mu\nu}$ is the tensor potential constructed due to another string at y as

$$
B^{\mu\nu}(x) = g_s \int d\sigma d\tau \sigma^{\mu\nu}(y) G\left((x-y)^2\right), \tag{1.49}
$$

where g_s is the coupling constant having dimension of mass and G is the Green's function describing time symmetric interaction. We will not consider string configurations any further as they are not the focus of this thesis. Now we consider the topological model 3+1 dimension containing the KR field.

1.2 Abelian topologically massive model in $3+1$ dimension

The Abelian topologically massive model in 3+1 dimension is given by the Lagrangian density

$$
\mathscr{L} = -\frac{1}{4}F^{\mu\nu}F_{\mu\nu} + \frac{1}{12}H^{\mu\nu\lambda}H_{\mu\nu\lambda} + \frac{m}{4}\epsilon^{\mu\nu\rho\lambda}B_{\mu\nu}F_{\rho\lambda}. \tag{1.50}
$$

Here $F_{\mu\nu} = \partial_\mu A_\nu - \partial_\nu A_\mu$ is the field strength of an Abelian gauge field A_μ, $H_{\mu\nu\lambda} = \partial_\mu B_{\nu\lambda} + \partial_\nu B_{\lambda\mu} + \partial_\lambda B_{\mu\nu}$ is the field strength for the tensor field, m is the coupling constant of the topological term which has dimension of energy. The Lagrangian density is invariant under the two independent gauge transformations

$$
A_\mu \to A_\mu + \partial_\mu\theta, \qquad B_{\mu\nu} \to B_{\mu\nu}, \tag{1.51}
$$

and

$$A_\mu \to A_\mu, \qquad B_{\mu\nu} \to B_{\mu\nu} + \partial_{[\mu}\Lambda_{\nu]}. \tag{1.52}$$

Confinement of the quarks in hadrons can be explained by the formation of chromo-electric flux tube between the quarks at low energy. The presence of the Kalb Ramond field may be used to explain the dynamics of the flux tubes in QCD vacuum. The term $\epsilon^{\mu\nu\alpha\beta}F_{\mu\nu}B_{\alpha\beta}$ has a special characteristic. It does not depend on the topology of the space-time. This can be seen when we write that part of the action in curved space time:

$$\mathcal{S}_{\rm BF} = \int \sqrt{-g}e^{\alpha\beta\mu\nu}B_{\alpha\beta}F_{\mu\nu}d^4x, \tag{1.53}$$

where $e^{\mu\nu\alpha\beta}$ is the Levi-Civita tensor in curved space-time and g is the determinant of the metric tensor $g_{\mu\nu}$ and it is related to $\epsilon^{\mu\nu\alpha\beta}$ as

$$e^{\mu\nu\alpha\beta} = \frac{1}{\sqrt{-g}}\epsilon^{\mu\nu\alpha\beta}. \tag{1.54}$$

where $\epsilon^{0123} = -1$. Using eqn.(1.54), we can rewrite the eqn.(1.53) as

$$\mathcal{S}_{\rm BF} = \int \epsilon^{\alpha\beta\mu\nu}B_{\alpha\beta}F_{\mu\nu}d^4x. \tag{1.55}$$

So $\mathcal{S}_{\rm BF}$ does not depend on the metric of the space-time. As a consequence when we vary the whole action $S = \int \mathscr{L}\sqrt{-g}\ d^4x$ with respect to metric tensor $g_{\mu\nu}$, the contribution from the part $\mathcal{S}_{\rm BF}$ is zero. Hence we can conclude from the definition of energy momentum tensor

$$\theta^{\mu\nu} = -\frac{2}{\sqrt{-g}}\frac{\delta S}{\delta g_{\mu\nu}}, \tag{1.56}$$

that $mB\wedge F$ has no contribution in $\theta^{\mu\nu}$ i.e. the energy momentum tensor does not contain any mass term. That is why the massive bosons in this model are called to be topologically massive bosons. Let us see from equations of motion of the A_μ

and $B_{\mu\nu}$ how this model provides massive A_μ field keeping $U(1)$ symmetry unbroken unlike Higgs mechanism. The equations of motion for A_μ and $B_{\mu\nu}$ are found from the Lagrangian density in eqn.(1.50), and they are

$$\partial_\mu F^{\mu\nu} = -\frac{m}{6}\epsilon^{\nu\mu\rho\sigma}H_{\mu\rho\sigma}, \tag{1.57}$$

$$\partial_\rho H^{\rho\mu\nu} = \frac{m}{2}\epsilon^{\mu\nu\alpha\beta}F_{\alpha\beta}. \tag{1.58}$$

From the eqn.(1.57), we have

$$\frac{1}{m}\epsilon_{\nu\mu\rho\sigma}\partial_\alpha F^{\alpha\nu} = H_{\mu\rho\sigma}. \tag{1.59}$$

Using eqn.(1.58) and eqn.(1.59), we get

$$\frac{1}{m}\epsilon_{\nu\mu\rho\sigma}\partial^\mu\partial_\alpha F^{\alpha\nu} = \frac{m}{2}\epsilon_{\rho\sigma\gamma\tau}F^{\gamma\tau}. \tag{1.60}$$

Putting $F^{\mu\nu} = \partial^\mu A^\nu - \partial^\nu A^\mu$ in the above equation, we get

$$-\epsilon_{\mu\nu\rho\sigma}\Box\partial^\mu A^\nu = \frac{m^2}{2}\epsilon_{\mu\nu\rho\sigma}F^{\mu\nu}. \tag{1.61}$$

Hence

$$\left(\Box + m^2\right)F^{\mu\nu} = 0. \tag{1.62}$$

It is the Klein-Gordon (KG) equation for $F^{\mu\nu}$ with a mass m. Now we will see that how the massive KG equation of the gauge field is found. We can find from eqn.(1.58)

$$\epsilon^{\mu\nu\rho\lambda}\partial_\rho H_\lambda = m\epsilon^{\mu\nu\rho\lambda}\partial_\rho A_\lambda. \tag{1.63}$$

Here H_λ is the dual field of $H^{\mu\nu\rho}$:

$$H_\mu = -\frac{1}{6}\epsilon_{\mu\alpha\beta\gamma}H^{\alpha\beta\gamma}. \tag{1.64}$$

The general solution of eqn.(1.63) is

$$H_\lambda = mA_\lambda + \partial_\lambda\eta, \tag{1.65}$$

where η is a scalar field. Using eqn.(1.64)and eqn.(1.57), we get

$$\Box A^{\nu} - \partial^{\nu}(\partial.A) = -m^2 A^{\nu} - m\partial^{\nu}\eta, \tag{1.66}$$

which gives

$$\left(\Box + m^2\right) A^{\nu} - \partial^{\nu}(\partial \cdot A - m\eta) = 0. \tag{1.67}$$

With the gauge choice $\partial \cdot A = m\eta$, we find

$$\left(\Box + m^2\right) A^{\nu} = 0. \tag{1.68}$$

It is the KG equation of a massive vector field and the coupling constant m of the two-point coupling $B \wedge F$ appears as mass of the Abelian vector field. The mass is not a gauge artifact because it appears in the KG equation of $F^{\mu\nu}$ without being in a particular gauge choice. So the model contains the massive mode of one form gauge field. We can see the coupling constant m plays the role of the mass of the gauge bosons from the eqn.(1.57). E. Cremmer and J. Scherk in their paper [48] show how the dual theory of the model in eqn.(1.50) is equivalent to Stuckelberg Model [49]. Dual of the field strength of Kalb-Ramond field is defined in eqn.(1.64). We can see from the eqn.(1.64), that $\partial_{\mu}H^{\mu} = 0$. This constraint can be taken into consideration for the construction of a dual Lagrangian with the introduction of a Lagrangian multiplier field $\chi(x)$. The introduction is made such a way that the variation of dual Lagrangian with respect to field χ gives $\partial_{\mu}H^{\mu} = 0$. The dual Lagrangian density with the Lagrange multiplier χ in the paper is

$$\mathscr{L}_D = -\frac{1}{4}F^{\mu\nu}F_{\mu\nu} - \frac{1}{2}H^{\mu}H_{\mu} - mA^{\mu}H_{\mu} + \partial_{\mu}\chi H^{\mu}, \tag{1.69}$$

where $\partial_{\mu}\chi H^{\mu}$ and $A^{\mu}H_{\mu}$ are obtained after partial integration. This Lagrangian density remains invariant under the transformation

$$A_{\mu} \to A_{\mu} + \frac{1}{m}\partial_{\mu}f, \qquad \chi \to \chi + mf. \tag{1.70}$$

We can rewrite the dual Lagrangian density as

$$\begin{aligned}\mathscr{L}_D = & -\frac{1}{4}F^{\mu\nu}F_{\mu\nu} - \frac{1}{2}\left(H^\mu H_\mu + 2H_\mu m\left(A^\mu - \frac{1}{m}\partial^\mu\chi\right) + m^2\left(A^\mu - \frac{1}{m}\partial^\mu\chi\right)^2\right) \\ & +\frac{1}{2}m^2\left(A^\mu - \frac{1}{m}\partial^\mu\chi\right)^2 \\ = & -\frac{1}{4}F^{\mu\nu}F_{\mu\nu} - \frac{1}{2}\left\{H^\mu + m\left(A^\mu - \frac{1}{m}\partial^\mu\chi\right)\right\}^2 + \frac{1}{2}m^2\left(A^\mu - \frac{1}{m}\partial^\mu\chi\right)^2 \end{aligned} \tag{1.71}$$

The partition functional for this dual model

$$Z = \int \mathscr{D}\chi\mathscr{D}H_\mu\mathscr{D}A_\mu \exp\left(i\mathscr{L}_D\right). \tag{1.72}$$

Writing

$$H^{'\mu} = H^\mu + m\left(A^\mu - \frac{1}{m}\partial^\mu\chi\right), \tag{1.73}$$

we get $\mathscr{D}H_\mu = \mathscr{D}H'_\mu$. Integrating over the field H^μ we get generating function for the n-point propagator,

$$Z = \int \mathscr{D}\chi\mathscr{D}A_\mu \exp\left(i\int\left(-\frac{1}{4}F^{\mu\nu}F_{\mu\nu} + \frac{1}{2}m^2\left(A^\mu - \frac{1}{m}\partial^\mu\chi\right)^2\right)d^4x\right). \tag{1.74}$$

It is a partition functional for the Abelian Stueckelberg model. So the dual theory of the Abelian topologically massive model is equivalent to a Stueckelberg model [49].

We note that there is a topologically massive model in (2+1) dimensions with mass m as a coupling parameter of a topologically invariant Chern-Simons term [50, 51]

$$\mathscr{L}_{cs} = -\frac{1}{4}F_{\mu\nu}F^{\mu\nu} + \frac{m}{2}\epsilon^{\mu\nu\lambda}F_{\mu\nu}A_\lambda. \tag{1.75}$$

This Lagrangian density is invariant under the gauge transformation

$$A^\mu \rightarrow A^\mu + \partial^\mu\Lambda, \tag{1.76}$$

where Λ is a scalar field which vanishes at infinity. The term $\epsilon^{\mu\nu\lambda}F_{\mu\nu}A_\lambda$ does not depend on the metric of the space-time, just like the $B \wedge F$ term in four dimensions.

The equation of motion of the gauge field becomes

$$\left(\Box + m^2\right) F^{\mu\nu} = 0. \tag{1.77}$$

So we can see that the vector field gets a non-zero pole at tree level which is absent in its energy momentum tensor. The non-Abelian generalization of the model in eqn.(1.75) to the $SU(N)$ gauge group is

$$\mathscr{L}_{cs} = -\frac{1}{4}F_a^{\mu\nu}F_{\mu\nu}^a + \frac{1}{2}m\epsilon^{\mu\nu\alpha}\left(F_{\mu\nu}^a A_\alpha^a - gf_{abc}\frac{2}{3}A_\mu^a A_\nu^b A_\alpha^c\right), \tag{1.78}$$

where $F_a^{\mu\nu} = \partial^\mu A_a^\nu - \partial^\nu A_a^\mu - gf_{abc}A^\mu A^\nu$, g is the gauge coupling constant in the $SU(N)$ gauge theory and f_{abc} is the structure constant of the $SU(N)$ group. This model can be considered as a toy model in understanding the dynamics of color charges in 2+1 dimensions. But the term $F \wedge A$ shows violation of time reversal or CP-symmetry which is not suitable for description of QCD.

1.3 Non-Abelian topologically massive model

Next we consider the non-Abelian generalization of the topologically massive Abelian model in 3+1 dimensions [6,7]. This is given by the Lagrangian density

$$\mathscr{L} \;\; = \;\; -\frac{1}{4}F_a^{\mu\nu}F_{\mu\nu}^a + \frac{1}{12}\tilde{H}_a^{\mu\nu\lambda}\tilde{H}_{\mu\nu\lambda}^a + \frac{m}{4}\epsilon^{\mu\nu\rho\lambda}B_{\mu\nu}^a F_{\rho\lambda}^a. \tag{1.79}$$

Here the field strengths corresponding the Yang-Mills field A_a^μ and the two-form gauge field are respectively

$$F_a^{\mu\nu} \;\; = \;\; \partial^\mu A_a^\nu - \partial^\nu A_a^\mu - gf_{bca}A_b^\mu A_c^\nu, \tag{1.80}$$

and

$$\tilde{H}_{\mu\nu\lambda}^a = D_{[\mu}B_{\nu\lambda]}^a - gf_{bca}F_{[\mu\nu}^b C_{\lambda]}^c, \tag{1.81}$$

where A^μ_a, $B^{\mu\nu}_a$ and C^μ_a are fields in the adjoint representation of the gauge group, taken to be $SU(N)$. Unlike the Abelian model, we have an extra field C^a_μ in this model. It is an auxiliary field [72] which assures the invariance of the Lagrangian density under the transformations,

$$A^a_\mu \rightarrow A^a_\mu, \qquad B^a_{\mu\nu} \rightarrow B^a_{\mu\nu} + \left(D_{[\mu}\theta_{\nu]}\right)^a, \qquad C^a_\mu \rightarrow C^a_\mu + \theta^a_\mu, \tag{1.82}$$

where θ^a_μ is a vector field in adjoint representation of $SU(N)$. Including the ghost fields and Nakanishi-Lautrup fields corresponding to the A^μ and $B^{\mu\nu}$ fields, we get the full action [7] as

$$\begin{aligned} S = S_0 \;\; &+ \;\; \int d^4x [h^a f^a + \frac{\xi}{2} h^a h^a + h^a_\mu (f^{a\mu} + \partial^\mu n^a) \\ &+ \;\; \beta^a (D_\mu \beta^a - g f^{abc} \omega^b_\mu \omega_c) + \frac{1}{2}\eta h^a_\mu h^{\mu a} - \partial_\mu \bar{\omega}^{a\mu} \alpha^a + \bar{\alpha}^a \partial_\mu \omega^{a\mu} \\ &+ \;\; \zeta \bar{\alpha}^a \alpha^a + \bar{\omega^a} \partial_\mu D^\mu \omega^a \\ &+ \;\; \bar{\omega}^a_\mu \{ g f^{abc} \partial_\nu (B^{\mu\nu}_b \omega^c) + \partial_\nu D^{[\mu} \omega^{\nu]a} + \partial_\nu (g f^{abc} F^{\mu\nu}_b \theta^c) \}], \end{aligned} \tag{1.83}$$

where S_0 is the action corresponding to the Lagrangian density in the eqn.(1.79). Here $f^a = \partial^\mu A^a_\mu$, $f^\mu_a = \partial_\nu B^{\nu\mu}_a$ and h and h^μ are the Nakanishi-Lautrup fields corresponding to the A and B fields, ω and $\bar{\omega}$ are the ghost fields of A, ω^μ and $\bar{\omega}^\mu$ are the vector ghost fields of $B^{\mu\nu}$, β and $\bar{\beta}$ are the ghost fields of the vector ghost field, α and $\bar{\alpha}$ are the Grassmann valued auxiliary fields, n and θ are auxiliary fields. This model contains massive non-Abelian gauge field and it was shown to be BRST invariant [6, 73, 74]. In [73, 74], it is seen the model is also invariant under ant-BRST symmetry. CP symmetry is not violated in this model. The parity of the Kalb- Ramond field is found from this coupling in eqn.(1.48). Since under parity transformation $X^0 \rightarrow X^0$ and $X^i \rightarrow -X^i$, the action will be parity invariant if

$$B^{0i} \rightarrow -B^{0i}, \qquad B^{ij} \rightarrow B^{ij}. \tag{1.84}$$

The massless Kalb-Ramond field has only one degree of freedom where massive Kalb-Ramond field has three [8]. This is shown in the following section.

1.4 Degrees of freedom of massless and massive Kalb-Ramond field

The massless two-form gauge field has one degree of freedom. It can be seen from its vector gauge transformation and the Lorenz gauge condition in the following way. If we consider the momentum space and the frame where the momentum $k_\mu = (k_0, 0, 0, k_0)$, we can construct null plane coordinate

$$k^1 = k^2 = 0, \qquad k_- = \frac{k_0 - k_3}{\sqrt{2}} = 0, \qquad k_+ = \frac{k_0 + k_3}{\sqrt{2}} \neq 0. \tag{1.85}$$

Using the null plane coordinates , we can write the vector gauge transformation of the two form field, $B'_{\mu\nu} = B_{\mu\nu} + \partial_\mu \Lambda_\nu - \partial_\nu \Lambda_\mu$, in momentum space with the momentum coordinates given in eqn.(1.85)

$$\tilde{B}'_{+-} = \tilde{B}_{+-} + k_+ \Lambda_-, \tag{1.86}$$

$$\tilde{B}'_{+i} = \tilde{B}_{+i} + k_+ \Lambda_i, \tag{1.87}$$

$$\tilde{B}'_{-i} = \tilde{B}_{-i}, \tag{1.88}$$

$$\tilde{B}'_{12} = \tilde{B}_{12}, \tag{1.89}$$

where $\tilde{B}$ is the Kalb-Ramond field in momentum space and $\Lambda_- = \dfrac{\Lambda_0 + \Lambda_3}{\sqrt{2}}$. Here Λ_i designates Λ_1 and Λ_2. We can observe from the above transformations that B_{-i} and B_{12} remain invariant under the vector gauge transformation. Now using the coordinates in eqn.(1.85) and the four product:

$$k.x = k^0 x^0 - \mathbf{k}.\mathbf{x} = k^+ x^- + k^- x^+, \tag{1.90}$$

where

$$x^{+} = \frac{x^{0}+x^{3}}{\sqrt{2}}, \qquad x^{-} = \frac{x^{0}-x^{3}}{\sqrt{2}}, \tag{1.91}$$

we get from the Lorenz gauge condition $\partial_\rho B^{\rho\sigma} = 0$ that

$$k_{+}\tilde{B}_{-i} = 0, \tag{1.92}$$

$$k_{+}\tilde{B}_{-+} = 0, \tag{1.93}$$

which imply that $B_{-i} = 0$. Now we can see from eqn. (1.89) that $\tilde{B}_{12}$ is the gauge invariant component which remains non-zero under the gauge transformation. Therefore the massless $B^{\mu\nu}$ field has only one degree of freedom. On the other hand, massive $B^{\mu\nu}$ field has three degrees of freedom. This can be seen from the tensor representation of the Lorentz group ([58], Chap. 5) in the following way. The homogeneous Lorentz transformation of the $B^{\mu\nu}$ field is

$$B'^{\mu\nu}(x') = \Lambda^{\mu}{}_{\rho}\Lambda^{\nu}{}_{\sigma}B^{\rho\sigma}(x), \tag{1.94}$$

where $\Lambda^{\mu}{}_{\nu}$ is the Lorentz transformation matrix. For infinitesimal Lorentz transformation

$$\Lambda^{\mu}{}_{\nu} = \delta^{\mu}{}_{\nu} + \omega^{\mu}{}_{\nu}, \tag{1.95}$$

where $\omega^{\mu}{}_{\nu}$ is an infinitesimal antisymmetric matrix. Using eqn.(1.95), we can find a spin matrix $\mathcal{I}$ corresponding to a representation from the transformation of a field

$$\Phi'^{l}(x') - \Phi^{l}(x) = \frac{1}{2}\left(\mathcal{I}_{\rho\sigma}\right)^{l}_{l'}\Phi^{l'}\omega^{\rho\sigma}, \tag{1.96}$$

where $\Phi^{l}(x)$ is a l-type field. In the case of the two form field, the spin matrix becomes

$$\left(\mathcal{I}^{\rho\sigma}\right)^{\mu\nu}_{\alpha\beta} = \left(\eta^{\mu[\rho}\delta^{\sigma]}_{\alpha}\delta^{\nu}{}_{\beta} + \eta^{\nu[\rho}\delta^{\sigma]}_{\beta}\delta^{\mu}_{\alpha}\right). \tag{1.97}$$

The spin of the massive $B^{\mu\nu}$ field can be found from the one-to-one correspondence between the matrix representation of spin-j angular momentum $\mathbf{J}^{(j)}$ in the rest frame of the massive field, and the spin matrix $\mathcal{I}$ as

$$\sum_{\bar{\sigma}} \epsilon^{\mu\nu}(\bar{\sigma}) \left(\mathbf{J}^{(j)}\right)^2_{\bar{\sigma}\sigma} = \left(\mathbf{I}^2\right)^{\mu\nu}_{\rho\lambda} \epsilon^{\rho\lambda}(\sigma), \tag{1.98}$$

where $\epsilon^{\mu\nu}(\sigma)$ is the polarization tensor corresponding to the field $B^{\mu\nu}$ with helicity σ. Here $\mathbf{I}^2 = \mathcal{I}_k\mathcal{I}_k$ and $\mathcal{I}_k = \frac{1}{2}\epsilon_{ijk}\mathcal{I}^{ij}$, $k = 1,2,3$. For the massive field, $\mathbf{J}^{(j)}$ is matrix representation of the generators of $SO(3)$ group. Starting from eqn.(1.97), we can get

$$(\mathcal{I}_k)^{\mu\nu}_{\alpha\beta} = \epsilon_{ijk}\left(\eta^{\mu i}\delta^j_\alpha\delta^\nu_\beta + \eta^{\nu i}\delta^j_\beta\delta^\mu_\alpha\right), \tag{1.99}$$

and

$$(\mathcal{I}_k)^{0l}_{0m} = \epsilon_{lmk}, \quad (\mathcal{I}_k)^{0l}_{mn} = (\mathcal{I}_k)^{mn}_{0l} = 0, \quad (\mathcal{I}_k)^{pq}_{nm} = \left(\epsilon_{pnk}\delta_{qm} + \epsilon_{qmk}\delta_{pn}\right), \tag{1.100}$$

where $m, n, p, q = 1, 2, 3$. As a consequence, we find

$$\left(\mathbf{I}^2\right)^{0m}_{0n} = 2\delta^m_n, \qquad \left(\mathbf{I}^2\right)^{mn}_{0q} = \left(\mathbf{I}^2\right)^{0q}_{mn} = 0, \tag{1.101}$$

$$\left(\mathbf{I}^2\right)^{mn}_{pq} = \left(4\delta_{mp}\delta_{nq} - 2\delta_{m[n}\delta_{q]p}\right), \tag{1.102}$$

which leads us to

$$\sum_{\bar{\sigma}} \left(\mathbf{J}^{(j)}\right)^2_{\bar{\sigma}\sigma} \epsilon^{0m}(\bar{\sigma}) = 2\epsilon^{0m}(\sigma), \tag{1.103}$$

$$\sum_{\bar{\sigma}} \left(\mathbf{J}^{(j)}\right)^2_{\bar{\sigma}\sigma} \epsilon^{pq}(\bar{\sigma}) = 2\epsilon^{pq}(\sigma). \tag{1.104}$$

The eigenvalue of the $\left(\mathbf{J}^{(j)}\right)^2_{\bar{\sigma}\sigma}$ is $j(j+1)\delta_{\sigma\sigma'}$ where $j \geq 0$. From the above equations, we can see that $j = 1$ so that $j(j+1) = 2$. Hence the no. of degrees of freedom of a massive $B_{\mu\nu}$ field $2j + 1 = 3$ exactly like like that for a massive gauge field.

Mass of gauge bosons also gives a possible explanation of confinement of gluons in QCD. K. Nishijima, T. Kugo and I. Ojima gave the explanation from the Becchi-Rouet-Strora-Tyutin (BRST) [52–54] symmetry in a unbroken $SU(N)$ gauge theory. We will discuss the their argument in the next section.

1.5 Massive gauge boson and confinement

The basic argument is that gluon and quarks cannot be physical states defined via BRST symmetry because they are not found to be isolated in the experiments. This interpretation shows that massive gauge boson plays a key role in this interpretation for the unbroken gauge theory. I will discuss their arguments below.

Every gauge theory remains invariant under BRST symmetry even after gauge-fixing. For example, let us consider the Lagrangian density of pure Yang-Mills theory in the Lorenz gauge, including the Nakanishi-Lautrup (NL) field $B^a(x)$ and ghost fields, $\omega^a(x)$ and $\bar{\omega}^a(x)$,

$$\mathscr{L} = -\frac{1}{4} F_a^{\mu\nu} F_{\mu\nu}^a + \frac{\xi}{2} B_a B^a + \partial_\mu A_a^\mu B^a + \partial^\mu \bar{\omega}_a \left(D_\mu \omega\right)_a , \tag{1.105}$$

where ξ is the gauge-fixing parameter. This Lagrangian density is invariant under the transformation

$$\delta A_a^\mu = \epsilon \left(D^\mu \omega\right)_a = \epsilon \left(\partial^\mu \omega^a - g f_{bca} A_b^\mu \omega_c\right), \tag{1.106}$$

$$\delta \omega_a = \frac{1}{2} g \epsilon f_{bca} \omega_b \omega_c, \tag{1.107}$$

$$\delta \bar{\omega}_a = \epsilon B_a, \tag{1.108}$$

$$\delta B_a = 0, \tag{1.109}$$

where ϵ is an infinitesimal Grassmann number and f_{abc} is the structure constant of $SU(N)$ group. The Noether charge corresponding to this symmetry is Q_B which is the generator of BRST symmetry,

$$Q_B = \int d^3x \left[B \cdot \partial_0 \omega + gB \cdot (A_0 \times \omega) + \frac{1}{2} g \partial_0 \bar{\omega} \cdot (\omega \times \omega) \right], \tag{1.110}$$

where we use the notation $X^a Y^a = X \cdot Y$ and $(X \times Y)^a = f^{abc} X_b Y_c$ for any two fields $X, Y = B, \partial_0 \omega, A_0, \partial_0 \bar{\omega}, \omega$. This charge is nilpotent, which means

$$Q_B^2 \left| \Phi \right\rangle = 0 \qquad \forall \left| \Phi \right\rangle \in \mathcal{V}, \tag{1.111}$$

where $\mathcal{V}$ is the Fock space. The physical states $|\text{phy}\rangle$ in the whole Fock space are the states which are annihilated by BRST charge Q_B

$$Q_B \left| \text{phy} \right\rangle = 0, \tag{1.112}$$

but with the condition

$$\left| \text{phy} \right\rangle \neq Q_B \left| \phi \right\rangle, \tag{1.113}$$

where $|\phi\rangle$ is any other state in the Fock space. So physical states belong to a subspace $\mathcal{V}_{\text{phys}}$ of the whole Fock space. Next we consider the equation of motion of the non-Abelian gauge field, in the form obtained by I. Ojima [55]:

$$\partial_\mu F^{\mu\nu} = J_C^\nu + \{Q_B, D^\mu \bar{\omega}\}, \tag{1.114}$$

where the gauge indices are suppressed. Here J_C^μ is the Noether current corresponding to global color symmetry. Now we will see how the eqn.(1.114) is obtained from the Lagrangian density in eqn.(1.105). The Lagrangian density of pure Yang-Mills theory can be written, suppressing the gauge indices as

$$\mathscr{L} = -\frac{1}{4} F^{\mu\nu} \cdot F^a_{\mu\nu} + \frac{\xi}{2} B \cdot B + \partial_\mu A^\mu \cdot B + \partial^\mu \bar{\omega} \cdot D_\mu \omega. \tag{1.115}$$

It can be seen that the Lagrangian density is invariant under global $SU(N)$ transformation of the fields

$$\delta \Phi^a = g f^{bca} \theta_b \Phi_c, \qquad \Phi = A, B, \omega, \bar{\omega}. \tag{1.116}$$

The color current becomes

$$J_C^\mu = g(A_\nu \times F^{\mu\nu}) + g(A^\mu \times B) - g\left(\bar{\omega} \times (D^\mu \omega)\right) - g(\partial^\mu \bar{\omega} \times \omega), \tag{1.117}$$

where the guage index has been suppressed, and the equation of motion of the gauge field is

$$D^\mu F_{\mu\nu} \;\; = \;\; \partial_\nu B - g(\partial_\nu \bar{\omega} \times \omega). \tag{1.118}$$

Now from the BRST transformation of the ghost fields, we can write

$$\{Q_B, D_\mu \bar{\omega}\} = \partial_\mu B - g\left(D_\mu \omega \times \bar{\omega}\right) - g\left(A_\mu \times B\right). \tag{1.119}$$

Substituting $\partial_\nu B$ in eqn.(1.119) from eqn.(1.118) , we get

$$\{Q_B, D_\nu \bar{\omega}\} = D^\mu F_{\mu\nu} + g(\partial_\nu \bar{\omega} \times \omega) - g\left(D_\nu \omega \times \bar{\omega}\right) - g\left(A_\nu \times B\right). \tag{1.120}$$

Using the explicit form of J_C^μ as given in the eqn.(1.117), we have from the above equation

$$\partial_\mu F^{\mu\nu} = J_C^\nu + \{Q_B, D^\nu \bar{\omega}\}, \tag{1.121}$$

which is the eqn.(1.114), as we set out to derive. The global Noether charge in a model will not be broken spontaneously when the Noether current J^μ corresponding to the charge does not contain any massless pole [56]

$$\langle 0 | J^\mu | \psi \rangle = 0, \tag{1.122}$$

where $|\psi\rangle$ is a state of massless particle. In this situation, the vacuum is annihilated by the global color charge. Let us take the matrix element for both side of eqn.(1.114)

$$\langle 0 | \partial_\mu F^{\mu\nu} | \psi \rangle = \langle 0 | \left(J_C^\nu + \{Q_B, D^\nu \bar{\omega}\}\right) | \psi \rangle . \tag{1.123}$$

Since the global charge Q_C is unbroken in QCD, we have $\langle 0|J_C^0|\psi\rangle = 0$. Hence we have from the above equation

$$\langle 0|\partial_\mu F^{\mu\nu} - \{Q_B, D^\nu\bar{\omega}\}|\psi\rangle = 0. \tag{1.124}$$

So either each individual matrix element is zero or the contribution of massless pole from one is cancelled by the other. If we consider the first case where the individual matrix elements are zero, then we have

$$\langle 0|\partial_\mu F^{\mu\nu}|\psi\rangle = \langle 0|\left(\Box A^\nu - \partial_\mu\partial^\nu A^\mu - \partial_\mu(gA^\mu \times A^\nu)\right)|\psi\rangle = 0. \tag{1.125}$$

If the gluon state $|g\rangle$ is a massless state, then $\langle 0|\partial_\mu F^{\mu\nu}|g\rangle \neq 0$, it provides a massless pole. As a consequence $\langle 0|J_C^\nu|\psi\rangle$ becomes non-zero, which implies that the color symmetry is broken spontaneously which is not our requirement. Hence we can say if color symmetry is to be an unbroken symmetry, $\langle 0|\partial_\mu F^{\mu\nu}|\psi\rangle = 0$. So we can conclude that $|g\rangle$ should be massive. Now we consider the next matrix-element

$$\langle 0|\{Q_B, D^\nu\bar{\omega}\}|\psi\rangle = 0. \tag{1.126}$$

Kugo-Ojima showed that [57] the left hand side of the above equation satisfies

$$\langle 0|\{Q_B, (D^\nu\bar{\omega})^a\}|\psi, c\rangle = -(\delta_c^a + u_c^a)\partial^\nu D_+(x-y), \tag{1.127}$$

where $|\psi, c\rangle$ is massless particle state with the gauge index c and u_c^a is a dynamical parameter defined as the residue of the pole of $g\,(A_\mu \times \bar{\omega})$ at $p^2 = 0$ and $D_+(x-y)$ is the correlation function of the massless asymptotic fields of anti-ghost and ghost fields:

$$\langle 0|\bar{\gamma}^a(x)\gamma^b(y)|0\rangle = -i\delta^{ab}D_+(x-y). \tag{1.128}$$

where γ^a and $\bar{\gamma}^a$ are defined as the free-field limits of ω^a and $\bar{\omega}^a$ respectively

$$\lim_{x^0 \pm\infty} \omega^a(x) \;=\; \gamma^a(x) + \ldots \tag{1.129}$$

$$\lim_{x^0 \pm\infty} \bar{\omega}^a(x) \;=\; \bar{\gamma}^a(x) + \ldots \tag{1.130}$$

So the matrix-element $\langle 0|\{Q^B, (D^\nu\bar{\omega})^a\}|\psi, c\rangle = 0$, if $u^a_b = -\delta^a_b$. Hence the global charge Q_C remains unbroken according to our requirement only if $u^a_b = -\delta^a_b$. Now we consider the second case where massless poles from the matrix elements $\langle 0|\partial_\mu F^{\mu\nu}|\psi\rangle$ and $\langle 0|\{Q_B, D^\nu\bar{\omega}\}|\psi\rangle = 0$ cancel each other so that $\langle 0|J^\nu|\psi\rangle = 0$. In this situation the gluons are massless. But the massless gauge field is not compatible with the cluster decomposition principle that I will explain below.

1.5.1 Mass gap and cluster decomposition property in gauge theory

The mass of the gauge boson plays a very important role in the analysis of scattering phenomena among gauge bosons. The inner-product of the polarization vectors of a one-form gauge field is given by

$$\epsilon^\mu_r \epsilon_{s\mu} = -\eta_{rs}, \qquad r, s = 0, 1, 2, 3. \tag{1.131}$$

It is not positive definite. For the case of a vector space with positive indefinite metric, mass gap [78] plays a role in the cluster decomposition property [58–60, 75] in the theory. Cluster decomposition principle says that two events separated by very large space-like distance are uncorrelated, i.e. one events cannot affect the other. H. Araki, K. Hepp and D. Ruelle [59, 76] established cluster decomposition property in scattering theory considering the axioms :

(i) **translational invariance** : this implies the existence of conservation of energy and momentum in a physical process. This implies the S-matrix operator commutes with four momentum $\mathcal{P}^\mu$ operator in inhomogeneous Lorentz group

$$[S, \mathcal{P}^\mu] = 0. \tag{1.132}$$

(b)**local commutativity**: this means if $\mathcal{O}_1(x)$ and $\mathcal{O}_2(y)$ are two observables measured at the space-time point x and y, then they commute with each other at spatial infinity:

$$\lim_{|\mathbf{x}-\mathbf{y}|\to\infty}[\mathcal{O}_1(x), \mathcal{O}_1(y)] = 0. \tag{1.133}$$

This implies that the measurement of one observable is unrelated with the measurement of the other observable when the measurements are made at spacelike separated points.

(c) **uniqueness of vacuum**: this means the ground state of the system does not have degenerate eigenvalues of Hamiltonian.

(d) **spectrum condition**: this means the energy spectrum of the system is bounded from the below.

Using these properties they have shown that

$$\begin{cases} \text{(a) With a mass gap} \\ \\ \text{or} \\ \\ \text{(b) without a mass gap} \end{cases}$$

The function $h_{12}(\xi)$ defined as

$$h_{12} = |\, \langle 0|B_1(x_1)B_2(x_2)|0\rangle - \langle 0|B_1(x_1)|0\rangle \, \langle 0|B_1(x_2)|0\rangle \,|, \tag{1.134}$$

$$\tag{1.135}$$

where

$$B_i(x_i) = \int f_i(x'_1, x'_2, \ldots, x'_r) \prod_{n=1}^{r} d^4x'_n \Phi(x_i + x_n), \tag{1.136}$$

where f_i is a rapidly decreasing C^∞ test function with compact support and Φ is a generic designation of field operator or product of field operators. From the properties mentioned in (a)-(d), they showed that h_{12} satisfies the inequality:

$$h_{12} \leq \begin{cases} C[\xi]^{-\frac{3}{2}} \exp(-m[\xi])\xi^{2N} \left(1 + \frac{\xi^0}{\xi}\right) \\ \text{or} \\ C'[\xi]^{-2}[\xi]^{2N} \left(1 + \frac{|\xi^0|}{[\xi]^2}\right), \end{cases} \tag{1.137}$$

where $\xi = |\mathbf{x}_1 - \mathbf{x}_2|$ and $[\xi]$ is the shortest space-like distance between ξ and a certain compact set which depends on the compact supports and ξ^0 is the time component of ξ. N is a certain non negative integer , which is non-zero and non-negative for positive indefinite metric and $N = 0$ for positive definite metric, C and C' are the constants which do not depend on ξ. We can see from the eqn.(1.137), that only for the case of mass gap, $h_{12} \to 0$ if $\xi \to \infty$, where $\xi = |\mathbf{x}_1 - \mathbf{x}_2|$. Now we will see how it affects S-matrix. Perturbative analysis of the scattering phenomena depends on the definition of the S-matrix.

$$S = \lim_{\epsilon \to 0} \mathcal{T} \left[\exp\left(\int_{-\infty}^{\infty} dt H^{\epsilon}(t) \right) \right], \tag{1.138}$$

where the $\mathcal{T}$ signifies the time-ordered product of the operators and $H_I^{\epsilon}(t)$ is the interaction Hamiltonian in the interaction picture, with an adiabatic switching factor $e^{-\epsilon|t|}$

$$H_I^{\epsilon}(t) = e^{-\epsilon|t|} \int d^3x \mathcal{H}_I(x), \tag{1.139}$$

where $\mathcal{H}_I$ is the interaction Hamiltonian density. Due to presence of a mass gap in the gauge theory the correlation between two interactions placed at a infinitely spacelike distance becomes

$$\lim_{|\mathbf{x}-\mathbf{y}| \to \infty} \langle \mathcal{T} \mathcal{H}_I(x) \mathcal{H}_I(y) \rangle = \langle \mathcal{H}_I(x) \rangle \langle \mathcal{H}_I(y) \rangle \tag{1.140}$$

hence they are uncorrelated. Thus the S matrix of a process at a point x cannot be related to the S matrix of a process at another y when the spatial separation of x and

y becomes infinite. This is the requirement in a causal theory. Hence the causality required by the Lorentz invariance of the S-matrix is maintained in a gauge theory with a mass gap.

In summary, we see that massiveness of gauge field plays an important role in the analysis of confinement as well as in the scattering phenomena of gluons. Hence we do not consider the case where massless Yang-Mills gauge bosons are present with unbroken color charge $Q_C = \int J^0_C d^3x$ i.e. the case where massless poles from the matrix element $\langle 0|\partial_\mu F^{\mu\nu}|\psi\rangle$ are cancelled by massless poles in $\langle 0|\{Q_B, D^\nu\bar{\omega}\}|\psi\rangle$.

There are other possibilities of having massive Yang-Mills gauge bosons in 3+1 dimension which we will discuss now.

1.6 Some other models for massive gauge bosons in 3+1 dimension

The non-Abelian Stuckelberg model in 3+1 dimension, given by the Lagrangian density

$$\mathscr{L} = -\frac{1}{4}F_a^{\mu\nu}F^a_{\mu\nu} + \frac{1}{2}m^2\left(A^\mu_a - \frac{1}{m}b^\mu_a\left(\Theta\right)\right)^2, \tag{1.141}$$

contains a massive A^μ_a field, where

$$b^\mu_a = E_{ab}\partial_\mu\Theta^b, \tag{1.142}$$

$$E^{ab}(\theta) = \sum_{n=0}^{\infty}\frac{1}{(n+1)!}\left[\left(\frac{ig\bar{\Theta}}{m}\right)^n\right]^{ab}. \tag{1.143}$$

where $\Theta^a(x)$ is a scalar field. Here $\bar{\Theta}^{ab} = if^{abc}\Theta^c$. This model is invariant under the gauge transformations:

$$A^a_\mu \to A^a_\mu + D^{ab}_\mu E^{bc}(\Theta)\delta\theta^c, \qquad \Theta^a \to \Theta^a + m\delta\theta^a, \tag{1.144}$$

where $D^{ab}_{\mu} = \delta^{ab}\partial_{\mu} - gf^{bca}A^{c}_{\mu}$ and $\delta\theta^{a}$ is infinitesimal transformation parameter. But this model is not renormalizable in 3+1 dimension [64–67], whereas the topologically massive model in 3+1 dimension is renormalizable [7].

One of the possibilities is that the mass of the gauge boson has purely chromodynamic origin i.e. the mass is generated due to non-linear interactions among gauge bosons and among gauge bosons and ghosts. This mass is known as dynamically generated mass. This is found by truncating the Schwinger-Dyson equation for the propagator of the gluon field at low energy i.e. in the non-perturbative regime. The propagator of non-Abelian gauge field can be written from truncation of the Schwinger- Dyson equation [68, 69]

$$\Delta^{\mu\nu} = -\frac{1}{k^2 - m^2(k^2)}\left[g^{\mu\nu} - (1-\xi)\frac{k^{\mu}k^{\nu}}{k^2}\right]. \tag{1.145}$$

The pole of scalar part of the propagator should depend on the momentum scale $m(k^2)$. But we know that at higher energy scale , the propagator must behave like a propagator of massless particle , so that the theory can describe renormalizablility. Hence the dynamical mass $m(k^2) \to 0$ with the increase of momentum scale. But the topologically massive model in 3+1 dimension is renormalizable [7] with a mass which does not vanish in the limit $k^2 \to \infty$.

There is another model where mass $m \nrightarrow 0$ in the limit $k^2 \to 0$. The model was developed by Curci and Ferrari [70], and it contains a Proca-massive gauge boson and is given by the Lagrangian

$$\begin{aligned}\mathscr{L}_{CF} = \quad & -\frac{1}{4}F^{\mu\nu}_{a}F^{a}_{\mu\nu} - \frac{1}{2}\left[(A^{a}_{\mu})^2 + 2\xi\bar{\omega}^{a}\omega^{a}\right] + \frac{1}{2}\bar{\omega}^{a}\left(\partial^{\mu}D_{\mu} + D^{\mu}\partial_{\mu}\right)\omega^{a} \\ & -\frac{1}{2\xi}(\partial_{\mu}A^{\mu}_{a})^2 + \frac{1}{8}g^2(\bar{\omega}\times\omega)^2. \end{aligned} \tag{1.146}$$

This model is invariant under the global transformations

$$\delta A^{\mu}_{a} = (D^{\mu}\omega)_{a}, \quad \delta\omega^{a} = -i\frac{1}{2}(\omega\times\omega)^{a}, \quad \delta\bar{\omega}^{a} = -\frac{1}{\xi}\partial^{\mu}A^{a}_{\mu} + \frac{g}{2}(\bar{\omega}\times\omega)^{a}. \tag{1.147}$$

Here b and c are ghost fields. But these transformations are not BRST transformations. I. Ojima showed that [71] the Noether charge corresponding to the global transformations in eqn.(1.147) is not nilpotent. But the four dimensional topologically massive model is BRST invariant [6].

We will consider $2 \to 2$ elastic scatterings among topologically massive gauge bosons in the next chapter. This analysis needs the complete propagators of A and B fields which we are going to derive below.

1.7 Complete propagators of A and B fields

We will consider the elastic scatterings among topologically massive bosons in this thesis. This analysis requires the propagators of A and B fields. We get the propagators of the A and B fields when we introduce the gauge fixing terms in the Lagrangian density for Abelian fields in eqn.(1.50). Then we have

$$\mathscr{L}_{gf} = \frac{1}{4}F^{\mu\nu}F_{\mu\nu} + \frac{1}{12}H^{\mu\nu\lambda}H_{\mu\nu\lambda} - \frac{1}{2\xi}(\partial_\mu A^\mu)^2 + \frac{1}{2\eta}(\partial_\mu B^{\mu\nu})^2. \tag{1.148}$$

where ξ and η are the gauge fixing parameters. The topological term is also a quadratic term containing both the A and B fields. If we want to calculate the propagator of the fields we should take all the quadratic terms in the Lagrangian density. First we exclude $B \wedge F$ coupling from our consideration and get the propagators of A^a_μ and $B^{\rho\lambda}_a$ fields :

$$i\Delta_{\mu\nu} = -\frac{i}{k^2}\left(g^{\mu\nu} - (1-\xi)\frac{k^\mu k^\nu}{k^2}\right), \tag{1.149}$$

$$i\Delta_{\mu\nu,\rho\lambda} = \frac{i}{k^2}\left(g_{\mu[\rho}g_{\lambda]\nu} - (1-\eta)\frac{k_\mu k_{[\lambda}g_{\rho]\nu} - k_\nu k_{[\lambda}g_{\rho]\mu}}{k^2}\right). \tag{1.150}$$

Then we consider the quadratic derivative coupling term in the $B \wedge F$ term as an interaction

$$\mathcal{L}_{\text{quad}} = \frac{m}{2}\epsilon^{\mu\nu\rho\lambda}B_{\mu\nu}\partial_\rho A_\lambda, \tag{1.151}$$

and obtain the vertex rule for the $B - A$ coupling, for the vertex, shown in the

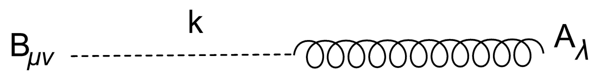

Figure 1.4 $B - A$ vertex from the $B \wedge F$ term

Fig. 1.4

$$iV_{\mu\nu,\lambda} = -m\epsilon_{\mu\nu\lambda\rho}k^{\rho}. \tag{1.152}$$

Hence we get the complete propagator of the A field by taking an infinite number

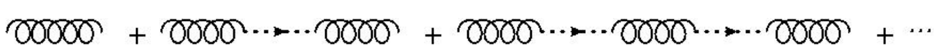

Figure 1.5 Massive A propagator by summing over B insertions

of insertions of the $B - A$ vertex and the B propagator, given in eqn.(1.150). This process is shown in the Fig. 1.5 and the sum of diagrams can be written as the infinite sum

$$\begin{aligned} iD_{\mu\nu} &= i\Delta_{\mu\nu} + i\Delta_{\mu\mu'}\frac{1}{2}iV_{\sigma\rho,\mu'}i\Delta_{\sigma\rho,\sigma'\rho'}\frac{1}{2}iV_{\sigma'\rho',\nu'}i\Delta_{\nu'\nu} + \cdots \\ &= -i\left[\frac{g_{\mu\nu} - (1-\xi)\frac{k_\mu k_\nu}{k^2}}{(k^2 - m^2)} - \xi m^2 \frac{k_\mu k_\nu}{k^4(k^2 - m^2)}\right], \end{aligned} \tag{1.153}$$

which is the propagator of a massive vector boson of mass m. The factors of $\frac{1}{2}$ compensate for double-counting due to the anti-symmetrization of the indices. Similarly for the tensor field we have

$$iD_{\mu\nu,\rho\lambda} = \left[\frac{g_{\mu[\rho}g_{\lambda]\nu} + (1-\eta)\frac{k_{[\mu}k_{[\lambda}g_{\rho]\nu]}}{k^2}}{k^2 - m^2} - \eta m^2 \frac{k_{[\mu}k_{[\lambda}g_{\rho]\nu]}}{k^4(k^2 - m^2)}\right]. \tag{1.154}$$

The propagators of A and B fields show power counting renormalizablity in the non-Abelian topologically massive model. The reason is the following. The superficial degree of divergence d for a loop diagram is given by

$$d = 4 - n_l E_l - \sum_i \delta_i. \tag{1.155}$$

Here n_l is the mass dimension corresponding to the l type fields and E_l is the number of their external lines. δ_i is the mass dimension of the coupling constant present at i-th vertex. In Yang-Mills theory, the mass dimension of the gauge coupling constant [g]=0 in 3+1 dimension. So if we include more loops in a loop diagram keeping number of the external lines fixed, then we should have the same d. We can rewrite the propagator of $B_{\mu\nu}$ field as

$$iD_{\mu\nu,\rho\lambda} = i\left[\frac{g_{\mu[\rho}g_{\lambda]\nu} + \frac{k_{[\mu}k_{[\lambda}g_{\rho]\nu]}}{k^2}}{k^2 - m^2} - \eta\frac{k_{[\mu}k_{[\lambda}g_{\rho]\nu]}}{k^4}\right]. \tag{1.156}$$

We can see from the eqn.(1.153) and eqn.(1.156) that the propagators of A and B fields behave as k^{-2} in the limit $k \to \infty$. So for example in the diagram shown in Fig. 1.6, we get the same d with the increase of loops. So the model becomes power

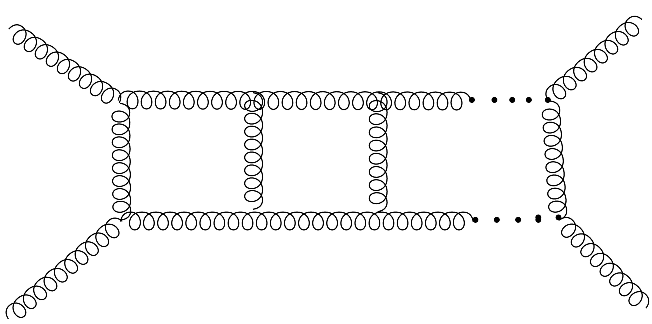

Figure 1.6 Many loop correction of quartic coupling $AAAA$.

counting renormalizable for $d \leq 0$.

Quantum corrections are generally infinite in quantum field theory. So we require counterterms for removing those infinities. If the cancellations of infinities are obtained from an infinite number of counter-terms, then the theory is not renormalizable. But the theory becomes renormalizable if the counterterms are finite in number.

The classical Lagrangian density of Yang-Mills gauge theory obey BRST symmetry. J. Zinn-Justin found that if the quantum effective action Γ of a model is to remain invariant under global symmetry, then the condition

$$\int d^4x \, \langle \Delta^l(x) \rangle_{J_\chi} \frac{\delta_L \Gamma[\chi]}{\delta \chi^l} = 0 \tag{1.157}$$

must be obeyed. Here $\chi^l(x)$ is any field present in the Lagrangian density and the $\Delta^l(x)$ is the change of the field under BRST transformation

$$\delta \chi^l(x) = \theta \Delta^l(x). \tag{1.158}$$

Here θ is the anticommutating parameter for the BRST transformation. $\langle \ldots \rangle_{J_\chi}$ denotes a vacuum expectation value taken in the presence of the current J_χ. The current is defined as

$$J_\chi = \frac{\delta_L \Gamma}{\delta \chi}. \tag{1.159}$$

$\dfrac{\delta}{\delta_L \chi}$ is the functional derivative acting from the left on the Γ. The eqn.(1.157) is known as Zinn-Justin equation. It is used to analyse the renormalization of a gauge theory. It can be shown in a renormalizable non-Abelian gauge theory that at every order the quantum effective action obeying the eqn.(1.157) contains the terms which are proportional to the term present in the classical Lagrangian density [25, 81–83]. So the counterterms needed are finite in number. As a consequence, the couplings among fields in the classical Lagrangian density are 'rescaled'. The renormalization of the massless Yang-Mills theory is shown algebraically in [25,83,84]. The non-Abelian topologically massive model in eqn.(1.83) is shown to be renormalizable algebraically in [7] with the BRST invariance [6].

In the next chapter, we have considered unitarity of S-matrix in $2 \to 2$ elastic scattering process among massive gluons at tree level. We have considered $SU(2)$

gauge theory to see the unitarity in the $2 \to 2$ elastic scattering processes of longitudinally polarized massive gauge bosons. We consider two different cases. The mass of the gauge boson can be generated by Higgs mechanism or they are topologically massive. The $2-2$ elastic scattering process involving longitudinally polarized bosons at tree-level is not unitary if we consider only the tri-linear and quartic interactions considered from the pure Yang-Mills Lagrangian density, which we will see in the chapter 2. We will see how the interaction among Higgs field and gauge bosons assure the unitarity of S-matrix in $SU(2)$ gauge theory. Next we will consider the action, given in the eqn.(1.83) to check the unitarity for topologically massive bosons. We have calculated the Feynman amplitudes of $2 \to 2$ scattering using various couplings among $B_a^{\mu\nu}$ and A_a^{μ} and see if unitarity at tree-level survives.

In chapter 3, we consider the behaviour of the gauge coupling constant g by varying the energy scale. The two-form field has one degree of freedom like a scalar field has. We have seen from the eqn.(1.2) and eqn.(1.3) that the contribution of scalar field is positive. So we would like to see if the contribution from the two form field is the same as the scalar field provides in the β function. This leads us to work out one loop β function. We will discuss the result there.

Chapter 2

Unitarity of $A_L A_L \to A_L A_L$ scattering at tree level.

2.1 Tree level calculation

In this chapter we will see the unitarity in the $2-2$ scattering process between two longitudinally polarized massive gauge bosons i.e. $A_L A_L \to A_L A_L$ at tree level. In the electroweak sector of the standard model, Higgs mechanism plays an important role in providing unitarity of S-matrix of various tree level processes involving longitudinally polarized W and Z bosons and fermions, for example $e^+e^- \to W^+W^-$, $W^+W^- \to W^+W^-$ etc. which are shown explicitly in [87–89]. But among these scattering processes, we see unitarity is maximally violated in the $2 \to 2$ processes involving only longitudinally polarized vector bosons because without the Higgs mediated channels, their scattering amplitudes grow with square of energy of the centre of momentum frame i.e. $\mathcal{M} \sim E^2$, which we will see in this chapter. On the scattering process involving fermions with same helicity, it was found that the amplitude grows as $\mathcal{M} \sim E$ [87–89].

We have mentioned in the previous chapter that we consider a non-Abelian topologically massive model in 3+1 dimensions where Yang-Mills gauge bosons are massive with unbroken $SU(N)$ global symmetry. We will see in this chapter whether unitarity of $2 \to 2$ elastic scattering process among topologically massive Yang-Mills gauge bosons is violated. We will take the gauge group to be $SU(2)$ group for simplicity and first show how unitarity of the elastic scattering process $A_L A_L \to A_L A_L$ is assured when the mass of A is generated by Higgs mechanism. Next we will consider the scattering process in the non-Abelian topologically massive model in 3+1 dimension based on the work in [90].

The polarization vector of the longitudinal mode of a massive gauge boson is given by

$$\epsilon_L^\mu \equiv \frac{1}{m}(P, E\hat{n}), \tag{2.1}$$

where P is the magnitude of the three-momentum vector, E is the energy and $\hat{n}$ is the direction of the propagation of the mode. In the high energy limit $E \gg m$, we can expand ϵ_L in inverse powers of energy as

$$\epsilon_L^\mu \approx \frac{p^\mu}{m} + v^\mu, \tag{2.2}$$

where $p^\mu \equiv (E, P\hat{n})$ is the four-momentum vector and $v^\mu \approx \left(-\frac{m}{2E}, \frac{m}{2E}\hat{n}\right)$. We know that the $F_a^{\mu\nu}F^a_{\mu\nu}$ term in the non-Abelian Lagrangian density contains the couplings AAA and $AAAA$. Using them, we get the Feynman diagrams for the $2 \to 2$ tree level scattering, shown in Fig. 2.1. The Yang-Mills Lagrangian density is

$$\begin{aligned} \mathscr{L}_{YM} = & - \frac{1}{2}\{(\partial^\mu A_a^\nu - \partial^\nu A_a^\mu)\partial_\mu A^a_\nu + g f_{bca} A_b^\mu A_c^\nu(\partial^\mu A_a^\nu - \partial^\nu A_a^\mu)\} \\ & - \frac{1}{4} g^2 f_{bca} f_{b'c'a} A_b^\mu A_c^\nu A_\mu^{b'} A_\nu^{c'}. \end{aligned} \tag{2.3}$$

The AAA coupling contains the derivative of gauge fields, so the corresponding vertex rule contains momenta of the gauge fields. Using eqn.(2.1), we get the total power of

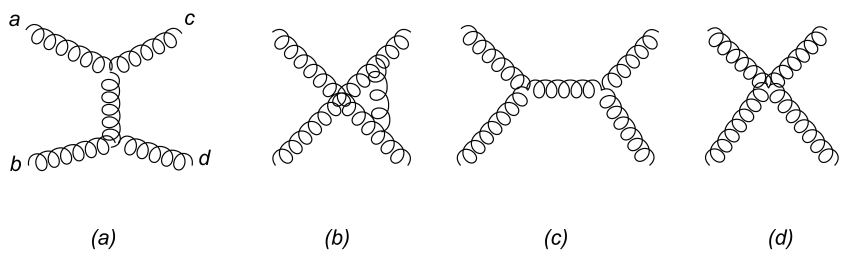

Figure 2.1 (a) t-channel, (b) u-channel, (c) s -channel and (d)quartic interaction.

the momentum of the external legs of Feynman diagrams, shown in Fig. 2.1a–2.1d. Each gauge boson in the legs of Feynman diagrams has the longitudinal polarization, given in eqn.(2.2). So multiplication of the four polarization vectors $\epsilon_L\epsilon_L\epsilon_L\epsilon_L$ provides the term: $pppp$, $pppv$, $ppvv$, $pvvv$, $vvvv$. Now we consider t, u and s channels where the contributions from two AAA vertices are present. The vertex rules for the AAA coupling, shown in Fig. 2.2a, is

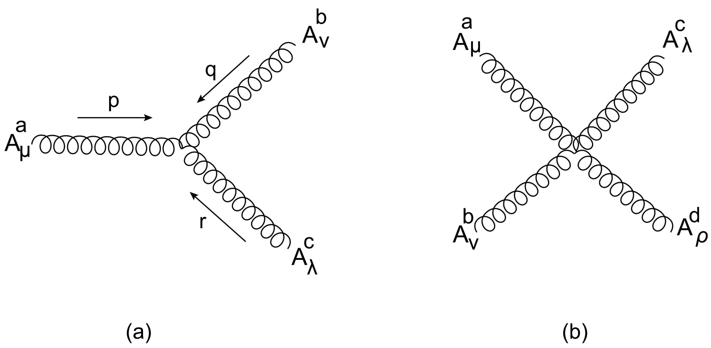

Figure 2.2 (a)AAA vertex; (b)$AAAA$ vertex.

$$V^{abc}_{\mu\nu\lambda} = -gf_{abc}\left[(p-q)_\lambda g_{\mu\nu} + (q-r)_\mu g_{\nu\lambda} + (r-p)_\nu g_{\lambda\mu}\right], \tag{2.4}$$

which contains the incoming four momentum assigned to external boson legs. So the two AAA vertices in the t, u and s channels in Fig. 2.1 contribute $\mathscr{O}(p^2)$ at large

p. But due to the presence of the propagator of gauge field behaving as $\mathscr{O}(p^{-2})$, the resultant contribution from the vertices and the propagator is $\mathscr{O}(p^0)$. The vertex rule for the quartic coupling $AAAA$, shown in Fig.2.2b, is

$$\begin{aligned} V^{abcd}_{\mu\nu\lambda\rho} = & - ig^2[f_{abe}f_{cde}\,(g_{\mu\lambda}g_{\nu\rho} - g_{\mu\rho}g_{\nu\lambda}) - f_{ace}f_{bde}\,(g_{\mu\rho}g_{\lambda\nu} - g_{\mu\nu}g_{\lambda\rho}) \\ & + f_{ade}f_{bce}\,(g_{\mu\nu}g_{\rho\lambda} - g_{\mu\lambda}g_{\rho\nu})], \end{aligned} \tag{2.5}$$

which does not contain any momentum of the external legs. Thus for all diagrams in Fig. 2.1 the vertices do not contribute any power of momentum. Consequently it becomes sufficient to consider the contributions from the polarization vectors at external legs of the diagrams in Fig. 2.1 in counting the power of energy. Since each leg goes as p, we can generally say that the amplitude $\mathcal{M}$ of each channel of the scattering process has the dependence on the energy as [87–89, 92]

$$\mathcal{M} = aE^4 + bE^2 + C + \mathscr{O}(E^{-n}), \qquad n = 2, 4, \dots \tag{2.6}$$

where a, b and C are functions of the scattering angle. We need to check if the total amplitude of this form violates unitarity of the S-matrix. This is based on the following argument.

Unitarity of the S-matrix in a tree level scattering involving a total of n particles requires the corresponding amplitude to vary with the energy of the process in the centre of momentum frame as [94, 95]

$$\mathcal{M} \sim E^{4-n}, \tag{2.7}$$

where $\mathcal{M}$ is the amplitude of the scattering process. In the $2 \to 2$ scattering process, the total number of particles involved is $n = (2+2) = 4$. Hence according to eqn.(2.7),

$$\mathcal{M} \sim E^0. \tag{2.8}$$

But we can now see from eqn.(2.6) that the amplitude of each channel $\mathcal{M}$ violates the condition in eqn.(2.8). Now we are going to see explicitly if their sum violates unitarity. We will consider the scattering $A^a A^b \to A^c A^d$ in $SU(N)$ gauge theory. The amplitudes of the t, u and s channels are[1],

$$\mathcal{M}_t \approx g^2 f_{ace} f_{bde} \left[\frac{P^4}{m^4}(3+c)(1-c) + \frac{P^2}{2m^2}(9+7c-4c^2) \right], \tag{2.9}$$

$$\mathcal{M}_u \approx g^2 f_{ade} f_{bce} \left[\frac{P^4}{m^4}(3-c)(1+c) + \frac{P^2}{2m^2}(9-7c-4c^2) \right], \tag{2.10}$$

$$\mathcal{M}_s \approx -g^2 f_{abe} f_{cde} \left[\frac{4P^4}{m^4} + \frac{9P^2}{m^2} + 9 \right] c, \tag{2.11}$$

where $c = \cos\theta$, θ is the scattering angle in the centre of momentum frame. The amplitude of the quartic diagram, shown in Fig. 2.1d, is

$$\begin{aligned} \mathcal{M}_q \approx -\Bigg[& g^2 f_{ace} f_{bde} \left\{ \frac{P^2}{m^2}(3+c)(1-c) + (1-c)(1+c) \right\} \left(\frac{P^2}{m^2} + 1 \right) \\ + & g^2 f_{ade} f_{bce} \left\{ \frac{P^2}{m^2}(3-c)(1+c) + (1+c)(1-c) \right\} \left(\frac{P^2}{m^2} + 1 \right) \\ - & g^2 f_{abe} f_{cde} \frac{4P^2 c}{m^2} \left(\frac{P^2}{m^2} + 1 \right) \Bigg]. \end{aligned} \tag{2.12}$$

Thus the sum of the scattering amplitudes of t, u and s-channels and quartic interaction is

$$\mathcal{M}_T^{abcd} \approx \left[g^2 f_{ace} f_{bde} \frac{P^2}{2m^2}(1+11c) + g^2 f_{ade} f_{bce} \frac{P^2}{2m^2}(1-11c) - g^2 f_{abe} f_{cde} \, \frac{5P^2}{m^2} c \right]. \tag{2.13}$$

We will use $\mathcal{M}_T^{abcd}$ to find scattering amplitudes of various $2 \to 2$ scattering processes among gauge bosons in $SU(2)$ gauge theory.

Instead of taking $SU(N)$, we consider $SU(2)$ gauge theory for simplicity. The structure constants for the $SU(2)$ group are $f_{abc} = \epsilon_{abc}$. Taking the contraction rule of the structure constants for ϵ_{abc}

$$\epsilon_{abe} \epsilon_{cde} = (\delta_{ac}\delta_{bd} - \delta_{ad}\delta_{bc}), \tag{2.14}$$

[1]See appendix A for the derivation of the amplitudes

we get the total amplitude at the leading order of energy in the form

$$\mathcal{M}^{abcd} = \frac{g^2}{4m^2}\left(s\ \delta_{ab}\delta_{cd} + u\ \delta_{ac}\delta_{bd} + t\ \delta_{ad}\delta_{bc}\right), \tag{2.15}$$

where

$$s = 4E^2, \qquad t = -2P^2(1-c), \qquad u = -2P^2(1+c), \tag{2.16}$$

for this elastic scattering at high energy. This amplitude is same as that of the pion-pion scattering $\pi^a\pi^b \to \pi^c\pi^d$, which is expressed by a single function of Mandelstam variables $\mathcal{M}(s,t,u)$ at low energy [91–93] as

$$\mathcal{M}_T^{\pi^a\pi^b\to\pi^c\pi^d} = \left(\mathcal{M}(s,t,u)\ \delta_{ab}\delta_{cd} + \mathcal{M}(u,t,s)\delta_{ac}\delta_{bd} + \mathcal{M}(t,s,u)\ \delta_{ad}\delta_{bc}\right), \tag{2.17}$$

where,

$$\mathcal{M}(s,t,u) = \frac{g^2 s}{4m^2}, \quad \mathcal{M}(u,t,s) = \frac{g^2 u}{4m^2}, \quad \mathcal{M}(t,s,u) = \frac{g^2 t}{4m^2}. \tag{2.18}$$

The function $\mathcal{M}(s,t,u)$, $\mathcal{M}(u,t,s)$ and $\mathcal{M}(t,s,u)$ are symmetric under the exchange of last two arguments given in the parenthesis. For example

$$\mathcal{M}(s,t,u) = \mathcal{M}(s,u,t). \tag{2.19}$$

The total amplitude in eqn.(2.15) is clearly increasing with the square of energy, E^2 at high energy [87–89,92]. Hence it violates unitarity according to the condition given in eqn.(2.8).

Before we discuss the solution of this problem of unitarity, let us first see how the amplitudes of different elastic scattering processes are connected with each other. For this purpose, we consider a conventional representation of gauge fields:

$$A_\mu^\pm = \frac{(A^1 \mp iA^2)_\mu}{\sqrt{2}} = \frac{(\delta_a^1 \mp i\delta_a^2)\ A_\mu^a}{\sqrt{2}} = \varsigma_a^\pm A_\mu^a, \tag{2.20}$$

where we have written

$$\varsigma_a^{\pm} = \frac{(\delta_a^1 \mp i\delta_a^2)}{\sqrt{2}}. \tag{2.21}$$

The three massive gauge bosons $A^{\pm}$ and A^3 may be treated as an exact triplet under the unbroken global $SU(2)$ symmetry, so that all elastic $2 \to 2$ scattering processes which are possible among these triplet states conserve the associated isospin quantum number I. We will remove the subscript L. The scattering amplitudes of all $2 \to 2$ scattering processes among the triplet states, $|A^{\pm}\rangle$ and $|A^3\rangle$, can now be related to each other because of the conservation of $SU(2)$ isospin $\vec{I}$. The conservation of isospin $\vec{I}$ implies that the scattering matrix S must commute with the isospin operator:

$$[S, \vec{I}] = 0 \Rightarrow [S, I_{\pm}] = 0, \quad [S, I_3] = 0, \tag{2.22}$$

with the ladder operator $I_{\pm}$ built up from the first two components of $\vec{I}$ as usual

$$I_{\pm} = \frac{I_1 \pm iI_2}{\sqrt{2}}. \tag{2.23}$$

The two-particle state is designated as $|I_1, I_2; M_1 M_2\rangle$, where I_1 and I_2 are the isospins of the particles and M_1 and M_2 are their components along I_3 axis in the isospin space. For example,

$$|A^{\pm}A^{\pm}\rangle \equiv |1,1;\pm1,\pm1\rangle\,,\ |A^3A^3\rangle \equiv |1,1;0,0\rangle\,,\ |A^{\pm},A^3\rangle \equiv |1,1;\pm1,0\rangle\,,\ \text{etc.} \tag{2.24}$$

Generally the S matrix element can be written as

$$S_{fi} = \delta_{fi} + T_{fi}. \tag{2.25}$$

But we will drop the first term δ_{fi} which signifies no scattering. It is irrelevant to our discussion given below. Thus for our purpose

$$S_{fi} = T_{fi} \tag{2.26}$$

The amplitude of the process $A^-A^- \to A^-A^-$ is obtained from eqn.(2.13) using lowering operator and the commutation relation in eqn.(2.22)

$$\begin{aligned}
\mathcal{M}(A^-A^- \to A^-A^-) &= \big\langle A^-A^- \,\big|\, S \,\big|\, A^-A^- \big\rangle \\
&= \frac{1}{\sqrt{2}} \big\langle A^-A^- \,\big|\, SI^- \,\big|\, A^-A^3 \big\rangle \\
&= \frac{1}{\sqrt{2}} \langle A^-A^- | I^- S | A^-A^3 \rangle \\
&= \langle A^-A^3 | S | A^-A^3 \rangle + \langle A^3A^- | S | A^-A^3 \rangle \,. \qquad (2.27)
\end{aligned}$$

Here we have used that

$$I^- \, |A^-A^3\rangle = \sqrt{2}\, |A^-A^-\rangle \,, \qquad \big\langle A^-A^- \big|\, I^- = \sqrt{2}\, \big(\big\langle A^-A^3\big| + \langle A^3A^- |\big) \,. \qquad (2.28)$$

The amplitude $i\mathcal{M}(A^3A^3 \to A^3A^3)$ is derived using the action of the weak isospin operator I^+ on the state $|A^-A^3\rangle$

$$I^+ \, |A^-A^3\rangle = \sqrt{2}\, \big(|A^3A^3\rangle + |A^-A^3\rangle\big) \,, \qquad (2.29)$$

in the matrix element $\langle A^3A^3|S|A^3A^3\rangle$:

$$\begin{aligned}
\langle A^3A^3|S|A^3A^3\rangle &= \frac{1}{\sqrt{2}} \langle A^3A^3|SI^+|A^-A^3\rangle - \langle A^3A^3|S|A^-A^+\rangle \\
&= \langle A^-A^3|S|A^-A^3\rangle + \langle A^3A^-|S|A^-A^3\rangle - \langle A^-A^+|S|A^3A^3\rangle \,.
\end{aligned} \qquad (2.30)$$

Left hand side of the eqn.(2.30) is zero at tree level. Using eqn.(2.27), we find from eqn.(2.30) that

$$\langle A^3A^3|S|A^3A^3\rangle = \big\langle A^-A^- \,\big|\, S \,\big|\, A^-A^- \big\rangle - \langle A^-A^+|S|A^3A^3\rangle \,. \qquad (2.31)$$

Here we have used the time reversal or CP symmetry so that $\langle A^3A^3|S|A^-A^+\rangle = \langle A^-A^+|S|A^3A^3\rangle$, since under the time reversal symmetry of a scattering process, the role of the initial and final states are interchanged.

So we have seen from the relation in eqn.(2.30), that the amplitudes of various scattering are related to each other. This relation holds at every order of quantum correction in a renormalizable gauge theory. At tree level $\langle A^3A^3|S|A^3A^3\rangle = 0$. So we can write from eqn.(2.31) that at tree level

$$\left\langle A^-A^- \,\middle|\, S \,\middle|\, A^-A^- \right\rangle = \langle A^-A^+|S|A^3A^3\rangle \,. \tag{2.32}$$

We can find the amplitude of $A^-A^- \to A^-A^-$ at tree level from eqn.(2.13) using eqn.(2.27) and eqn.(2.21) as

$$\begin{aligned} \mathcal{M}(A^-A^- \to A^-A^-) &= \mathcal{M}(A^-A^3 \to A^-A^3) + \mathcal{M}(A^3A^- \to A^-A^3) \\ &= (\varsigma_a^-\delta_b^3\varsigma_c^+\delta_d^3 + \delta_a^3\varsigma_b^-\varsigma_c^+\delta_d^3)\mathcal{M}_T^{abcd}. \end{aligned} \tag{2.33}$$

Here $\mathcal{M}_T^{abcd}$ is given in eqn.(2.13) and we use δ's and ς's in the above equation taking all the momenta at the two vertices to be incoming. Using eqn.(2.21) and eqn.(2.18), we get from the above equation

$$\mathcal{M}(A^-A^- \to A^-A^-) = (\mathcal{M}(t,s,u) + \mathcal{M}(u,s,t))\,. \tag{2.34}$$

In a similar way, we can find the amplitude of the scattering process $A^+A^- \to A^3A^3$ as

$$\mathcal{M}(A^+A^- \to A^3A^3) = \varsigma_a^+\varsigma_b^-\delta_c^3\delta_d^3\mathcal{M}_T^{abcd} = \mathcal{M}(s,t,u). \tag{2.35}$$

We also calculate

$$\mathcal{M}(A^-A^+ \to A^3A^3) = \varsigma_a^-\varsigma_b^+\delta_c^3\delta_d^3\mathcal{M}_T^{abcd} \tag{2.36}$$

$$= -\mathcal{M}(u,s,t). \tag{2.37}$$

Since in the high energy limit $(s \gg 4m^2)$ $s+t \approx -u$, we can write amplitude in eqn.(2.37) using eqn.(2.18)

$$\mathcal{M}(A^-A^+ \to A^3A^3) = \mathcal{M}(s,t,u) + \mathcal{M}(t,s,u). \tag{2.38}$$

Hence we can rewrite the eqn.(2.30) using eqn.(2.34) and eqn.(2.37)

$$\mathcal{M}(A_3A_3 \to A_3A_3) \;=\; \mathcal{M}(s,t,u) + \mathcal{M}(t,s,u) + \mathcal{M}(u,s,t). \tag{2.39}$$

We can also find at tree level

$$\mathcal{M}(A^+A^- \to A^+A^-) = \varsigma_a^+ \varsigma_b^- \varsigma_c^+ \varsigma_d^- \mathcal{M}_T^{abcd} = -\mathcal{M}(u,s,t), \tag{2.40}$$

which can be written as a sum of two amplitudes at high energy as

$$-\mathcal{M}(u,t,s) = \mathcal{M}(s,t,u) + \mathcal{M}(t,s,u), \tag{2.41}$$

according to the eqn.(2.18), because in the high energy limit we have $-u \approx s+t$. We can also get the amplitude of the scattering process $A^-A^3 \to A^-A^3$

$$\mathcal{M}(A^-A^3 \to A^-A^3) = \varsigma_a^- \delta_b^3 \varsigma_c^- \delta_d^3 \mathcal{M}_T^{abcd} = \mathcal{M}(t,s,u). \tag{2.42}$$

So we have

$$\mathcal{M}(A^+A^- \to A_3A_3) \;=\; \mathcal{M}(s,t,u), \tag{2.43}$$

$$\mathcal{M}(A^+A^- \to A^+A^-) \;=\; \mathcal{M}(s,t,u) + \mathcal{M}(t,s,u), \tag{2.44}$$

$$\mathcal{M}(A_3A_3 \to A_3A_3) \;=\; \mathcal{M}(s,t,u) + \mathcal{M}(t,s,u) + \mathcal{M}(u,s,t). \tag{2.45}$$

It is now straightforward to rewrite these results for the isospin product states in the basis of irreducible states of total isospin. We use the Clebsch-Gordan coefficients for decomposition $3 \otimes 3 = 5 \oplus 3 \oplus 1$ [100] to get the reduced amplitudes $\mathcal{M}_{I=0,1,2}$ corresponding to the different isospin channels[2] in $SU(2)$ gauge theory which are possible in principle. They are at leading order in the high energy limit

$$\mathcal{M}_0 \;=\; 3\mathcal{M}(s,t,u) + \mathcal{M}(t,s,u) + \mathcal{M}(u,s,t), \tag{2.46}$$

$$\mathcal{M}_1 \;=\; \mathcal{M}(t,s,u) - \mathcal{M}(u,s,t), \tag{2.47}$$

$$\mathcal{M}_2 \;=\; \mathcal{M}(t,s,u) + \mathcal{M}(u,s,t). \tag{2.48}$$

[2] See Appendix A for the calculations.

Using the expression of $\mathcal{M}(s,t,u)$ we then have in the high energy limit

$$\mathcal{M}_0 = \frac{g^2 s}{2m^2}, \tag{2.49}$$

$$\mathcal{M}_1 = \frac{g^2(t-u)}{4m^2}, \tag{2.50}$$

$$\mathcal{M}_2 = -\frac{g^2 s}{4m^2}. \tag{2.51}$$

Expanding $\mathcal{M}_I$ in partial waves we can write

$$\mathcal{M}_I^J = 32\pi \int \sum_J (2J+1) a_I^J(s) P_J(\cos\theta), \tag{2.52}$$

where $P_l(x)$ is Legendre polynomial of first kind. Using the orthonormality condition of the Legendre polynomial we have

$$a_I^J = \frac{1}{2\cdot 32\pi}\int_{-1}^{1} d(\cos\theta) P_J(\cos\theta)\mathcal{M}_I. \tag{2.53}$$

The partial wave amplitude for $I=0$, $J=0$ mode is

$$a_0^0 = \frac{1}{2\cdot 32\pi}\int_{-1}^{1} d(\cos\theta) P_0(\cos\theta)\mathcal{M}_0. \tag{2.54}$$

The condition for unitarity is $\mathrm{Re}|a_0^0| \leq \frac{1}{2}$. Hence we find the maximum limit of energy scale up to which unitarity is valid in the $I=0$, $J=0$ channel

$$s \leq \frac{32\pi m^2}{g^2} = \frac{4\sqrt{2}\pi}{G_F}, \tag{2.55}$$

where G_F is Fermi coupling constant in the electroweak sector. Here we have used the relation

$$\frac{G_F}{\sqrt{2}} = \frac{g^2}{8m^2}. \tag{2.56}$$

If we take $G_F \approx 1.66\times 10^{-5}$ GeV^{-2} and the mass of the gauge boson $m \approx 80$ GeV, as for weak interactions, then we have from eqn.(2.55) that

$$s \leq 1.071\text{TeV}. \tag{2.57}$$

This means that the energy for the scattering process must not exceed the above limit, but the total amplitude grows with E^2. For weak interactions this growth of the amplitude has to be removed before the TeV scale. This bad behaviour of the scattering amplitude was studied by the J. S. Bell [96] and C. H. Llewellyn Smith [97]. They showed how this behaviour can be removed if spontaneous breaking of global symmetry is included or new interactions with scalar fields are considered. We know that spontaneous breaking of symmetry is required for the Higgs mechanism [102,103] in electroweak theory. Now we see how the interaction with the Higgs particle saves the unitarity of $A^a A^b \to A^c A^d$ process. If we consider the Higgs mechanism, then we need to include the trilinear coupling among Higgs and massive gauge fields:

$$\mathscr{L}_{\text{int}} = \frac{g}{2}\, m h A_a^\mu A_\mu^a, \tag{2.58}$$

where m is the mass of the gauge boson and h is the Higgs particle. There is also a quartic coupling $hhAA$ but this does not take part in the $A^a A^b \to A^c A^d$ elastic scattering at tree level. The tree level diagrams for the process $A^a A^b \to A^c A^d$ due to the interaction among Higgs and gauge bosons are shown in Fig. 2.3. So if we calculate the amplitude of the Higgs-mediated channels and add them up, we find the total amplitude in leading order[3]

$$\mathcal{M}_h = \frac{g^2}{4m^2}\left(s\ \delta_{ab}\delta_{cd} + t\ \delta_{ac}\delta_{bd} + u\ \delta_{ad}\delta_{bc}\right). \tag{2.59}$$

In order to get the total amplitude of the tree level scattering process at leading order of energy, we have to add eqn.(2.15) and eqn.(2.59), which yields

$$\begin{aligned}\mathcal{M}_T + \mathcal{M}_h = \quad & -\frac{g^2}{4m^2}\left(s\ \delta_{ab}\delta_{cd} + t\ \delta_{ac}\delta_{bd} + u\ \delta_{ad}\delta_{bc}\right) \\ & + \frac{g^2}{4m^2}\left(s\ \delta_{ab}\delta_{cd} + t\ \delta_{ac}\delta_{bd} + u\ \delta_{ad}\delta_{bc}\right) = 0.\end{aligned} \tag{2.60}$$

[3] See the details of the calculation in appendix A.

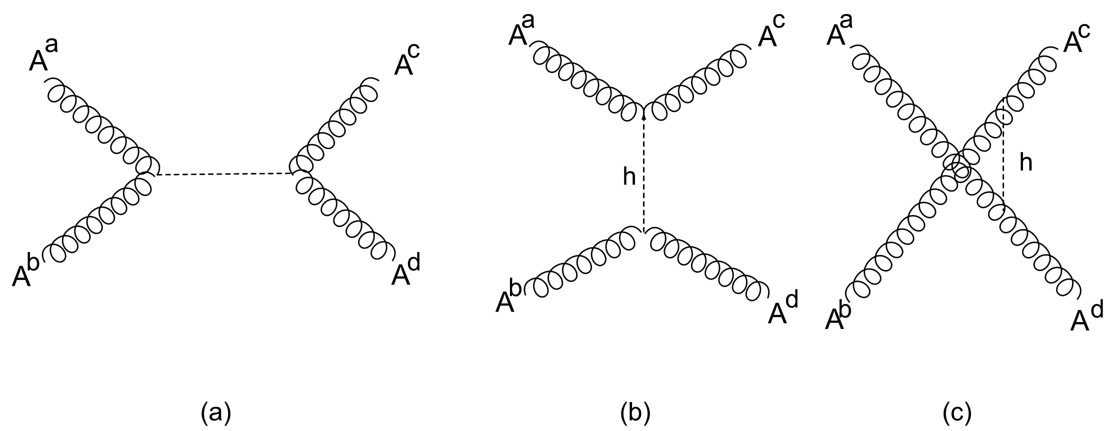

Figure 2.3 Higgs mediated (a) s-channel, (b) t-channel, (c)u-channel of $A^aA^b \to A^cA^d$ scattering ; dotted line represents the propagator of Higgs particle

The next to leading order term, which survives, does not depend on energy, being $\mathscr{O}(E^0)$. Thus the unitarity of the S-matrix is assured.

Now we consider the non-Abelian topologically massive model, given in eqn.(1.83). The model is taken in the place of Higgs mechanism. Construction of the tree diagrams require two-point coupling AB, various trilinear couplings: AAA, AAB, ABB and quartic couplings: $AAAA$ and $AABB$. Since the auxiliary fields: C^μ, θ and n do not enter in any tree level diagrams of $A^aA^b \to A^cA^d$ scattering process, we do not consider them. The couplings $\omega\bar{\omega}A$, $\bar{\omega}_\mu\partial_\nu B^{\mu\nu}\omega$ are also irrelevant to our analysis because we consider only tree level process. We consider only the part of the full Lagrangian density which is relevant in the computation of Feynman amplitude of the tree level scattering process. So we only consider

$$\begin{aligned}\mathscr{L} = & -\frac{1}{4}F_a^{\mu\nu}F^a_{\mu\nu} + \frac{1}{12}H_a^{\mu\nu\lambda}H^a_{\mu\nu\lambda} + \frac{m}{4}\epsilon^{\mu\nu\rho\lambda}B^a_{\mu\nu}F^a_{\rho\lambda} \\ & - \frac{1}{2\xi}(\partial_\mu A_a^\mu)^2 + \frac{1}{2\eta}(\partial_\mu B_a^{\mu\nu})^2. \end{aligned} \tag{2.61}$$

Here $H^a_{\mu\nu\lambda} = \left(D_{[\mu} B_{\nu\lambda]}\right)^a$, where D^μ is the gauge covariant derivative. The first term $F^{\mu\nu}_a F^a_{\mu\nu}$ in the Lagrangian density in eqn.(2.61) provides the 3-point and quartic couplings between the gauge fields. The second term leads to ABB and $AABB$ couplings, whereas the $B \wedge F$ term provides a two point derivative coupling between B and A and a three-point coupling, AAB. The vertex rules for AB and AAB couplings are

$$iV^{ab}_{\mu\nu,\lambda} = -m\epsilon_{\mu\nu\lambda\rho} k^\rho \delta^{ab}, \tag{2.62}$$

$$iV^{abc}_{\mu,\nu,\lambda\rho} = -igmf^{bca}\epsilon_{\mu\nu\lambda\rho} \ , \tag{2.63}$$

for the two point AB vertex and the three-point AAB vertex, respectively. The cor-

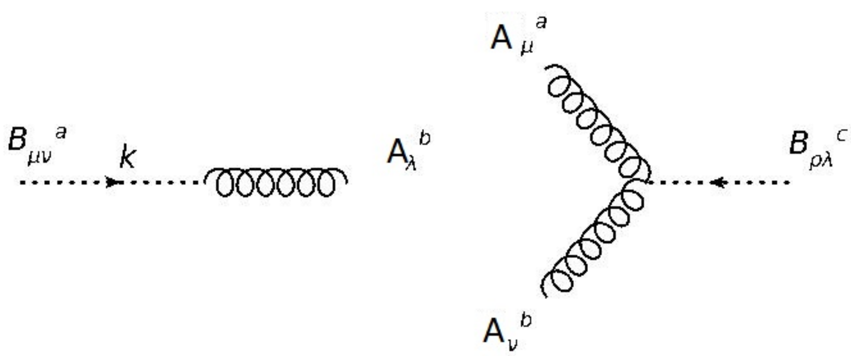

Figure 2.4 Vertices from the $B \wedge F$ term

responding vertices are shown in Fig. 2.4 where the momenta are all directed towards the vertex. In order to use these vertices in a diagram, we need propagators of the fields, which come from kinetic terms, $-\frac{1}{4}F^a_{\mu\nu}F^{a\mu\nu}$ for the A bosons, and $\frac{1}{12}H^a_{\mu\nu\lambda}H^{a\mu\nu\lambda}$ for the B field. We have already found the complete propagator of the vector field(at the tree level) in the previous chapter, which is

$$iD_{\mu\nu} = -i\left[\frac{g_{\mu\nu} - (1-\xi)\frac{k_\mu k_\nu}{k^2}}{(k^2 - m^2)} - \xi m^2 \frac{k_\mu k_\nu}{k^4(k^2 - m^2)}\right]\delta^{ab}. \tag{2.64}$$

Similarly for the tensor field we have

$$iD^{ab}_{\mu\nu,\rho\lambda} = i\left[\frac{g_{\mu[\rho}g_{\lambda]\nu} + (1-\eta)\frac{k_{[\mu}k_{[\lambda}g_{\rho]\nu]}}{k^2}}{k^2-m^2} + \eta m^2\frac{k_{[\mu}k_{[\lambda}g_{\rho]\nu]}}{k^4(k^2-m^2)}\right]\delta^{ab}. \tag{2.65}$$

These are shown diagrammatically in Fig. 2.5. These propagators show a good high energy behaviour, varying as $\sim k^{-2}$ as $k \to \infty$ which shows the power-counting renormalizability of the model. The terms $\xi m^2 \frac{k_\mu k_\nu}{k^4(k^2-m^2)}$ and $\eta m^2 \frac{k_{[\mu}k_{[\lambda}g_{\rho]\nu]}}{k^4(k^2-m^2)}$ in the propagators in eqn.(2.64) and eqn.(2.65) behave as $\sim k^{-4}$ at high energy. So they do not contribute in the divergent part of the tree-level amplitude and we can safely ignore them. The particle interpretation of quantum fields comes from the quadratic

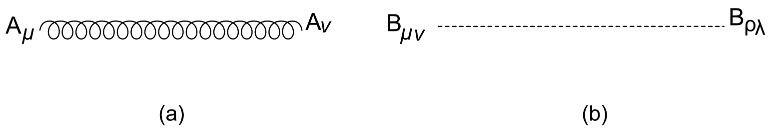

Figure 2.5 (a) Propagator of gluon field; (b) propagator of B field.

part of the Lagrangian. However, the kinetic term for the B field contains non-linear

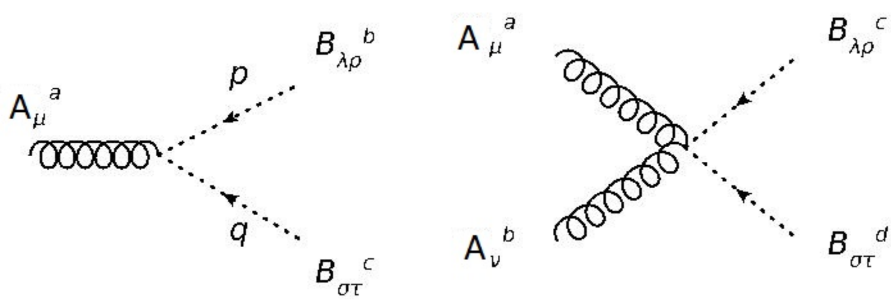

Figure 2.6 Vertices from the $H_{\mu\nu\lambda}H^{\mu\nu\lambda}$ term

interactions among the B and the A fields. From $H^a_{\mu\nu\lambda}H^{\mu\nu\lambda}_a \sim D_\mu B_{\nu\lambda}D^{[\mu}B^{\nu\lambda]}_a$, we get the couplings ABB and $ABBB$. The ABB coupling contains derivatives of B fields but $AABB$ does not have them. So the vertex rule of ABB contains the momentum of B field. The diagrams corresponding to the vertex rules for those couplings are shown in Fig. 2.6. The vertex rules are respectively

$$
\begin{aligned}
iV^{abc}_{\mu,\lambda\rho,\sigma\tau} &= gf^{abc}\left[(p-q)_\mu g_{\lambda[\sigma}g_{\tau]\rho} + p_{[\sigma}g_{\tau][\lambda}g_{\rho]\mu} - q_{[\lambda}g_{\rho][\sigma}g_{\tau]\mu}\right], &(2.66)\\
iV^{abcd}_{\mu,\nu,\lambda\rho,\sigma\tau} &= ig^2\left[f^{ace}f^{bde}\left(g_{\mu\nu}g_{\lambda[\sigma}g_{\tau]\rho} + g_{\mu[\sigma}g_{\tau][\lambda}g_{\rho]\nu}\right) + f^{ade}f^{bce}\left(g_{\mu\nu}g_{\lambda[\sigma}g_{\tau]\rho} + g_{\mu[\lambda}g_{\rho][\sigma}g_{\tau]\nu}\right)\right]. &(2.67)
\end{aligned}
$$

Considering the linear and non-linear interactions among A and B fields, we find several new diagrams corresponding to $A^+A^- \to A^+A^-$ scattering at the tree level in $SU(2)$ gauge theory. We have grouped the diagrams into Fig. 2.7, Fig. 2.8 and Fig. 2.10, according to the number of internal B propagators. The amplitudes for all of these diagrams go as $\mathscr{O}(P^2)$.

In Fig. 2.7, diagrams (a) and (b) appear only once, but diagrams (c) and (d) have twins, obtained by exchanging the internal B and A lines. Similarly, the B line can be on any of the external legs in each of diagrams (e) and (f), leading to a multiplicity of 4. We have calculated the amplitudes corresponding to these diagrams using the vertex rules and propagators given before.

The amplitudes for the diagrams in Fig. 2.7, including their multiplicities, are

$$
\begin{aligned}
\mathcal{M}_{2.7a} + \mathcal{M}_{2.7b} &= -\frac{3g^2P^2}{2m^2}(1+c) + \mathscr{O}(P^0) &(2.68)\\
2\left(\mathcal{M}_{2.7c} + \mathcal{M}_{2.7d}\right) &= \frac{3g^2P^2}{m^2}(1+c) + \mathscr{O}(P^0) &(2.69)\\
4\left(\mathcal{M}_{2.7e} + \mathcal{M}_{2.7f}\right) &= -\frac{2g^2P^2}{m^2}(1+c) + \mathscr{O}(P^0), &(2.70)
\end{aligned}
$$

Each of the diagrams in Fig. 2.7 contains only one propagator of the B field. We consider the couplings AAA, AB and AAB here . Now we are going to consider the diagrams having the couplings in the diagrams in Fig. 2.8 where we have used AAA, AB and ABB and $AABB$ couplings.

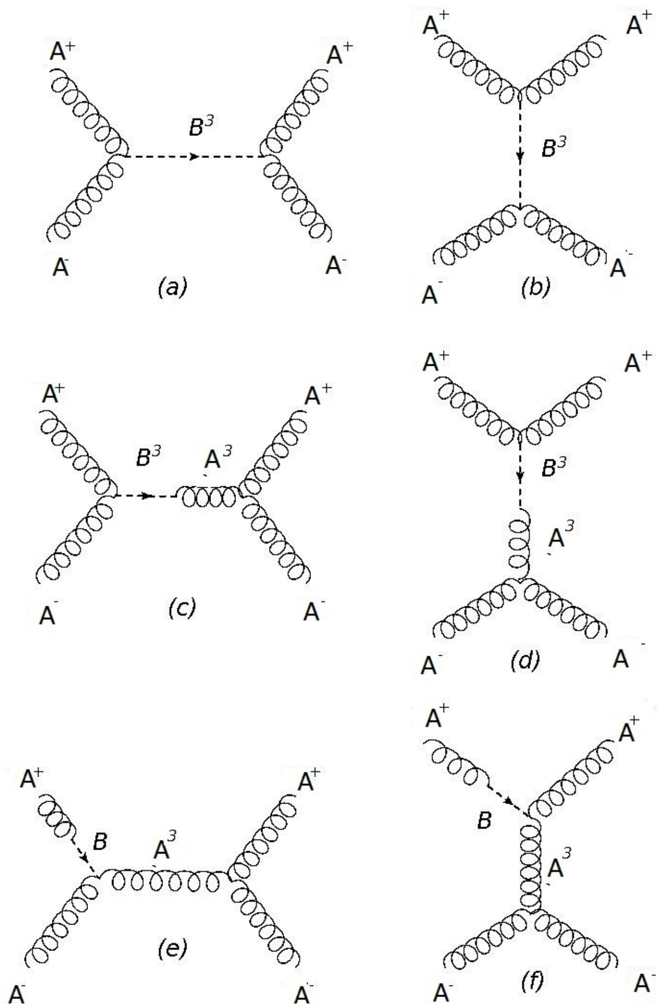

Figure 2.7 Scattering diagrams with P^2 behavior: I

Now consider the diagrams in Fig. 2.8c and Fig. 2.8d. We can place the AB coupling in any one of the legs. Due to this placement of AB, we get different Feynman diagrams but with an internal B-propagator joining two ABB vertices. We find that each of them provides the same amplitude. Hence we get a multiplicity of 4 for these diagrams. Similar reason is behind the appearance of the multiplicity factor 4 for the amplitudes in eqn.(2.72)-(2.73) due to the four placements of the AB couplings on the external legs in the Fig. 2.8c-2.8f.

But in the case of Fig. 2.8a, if we place the AB coupling at different legs as shown in

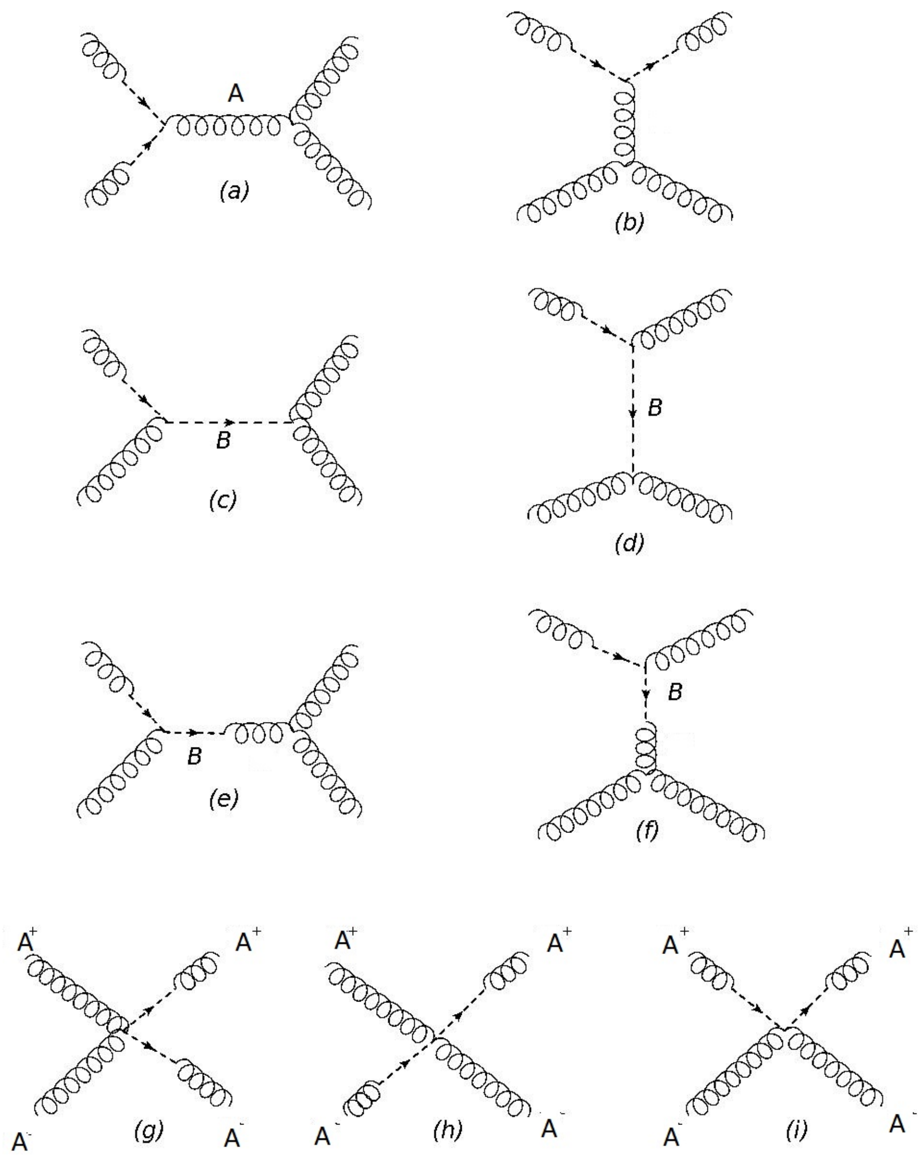

Figure 2.8 Scattering diagrams with P^2 behavior: II

Fig. 2.9, then we find their contribution is $\mathscr{O}(P^0)$. There are other diagrams which also have two propagators of B field. These are constructed using the quartic couplings $AABB$ and AB as shown in Fig. 2.8g-2.8i.Including multiplicities, the amplitudes of

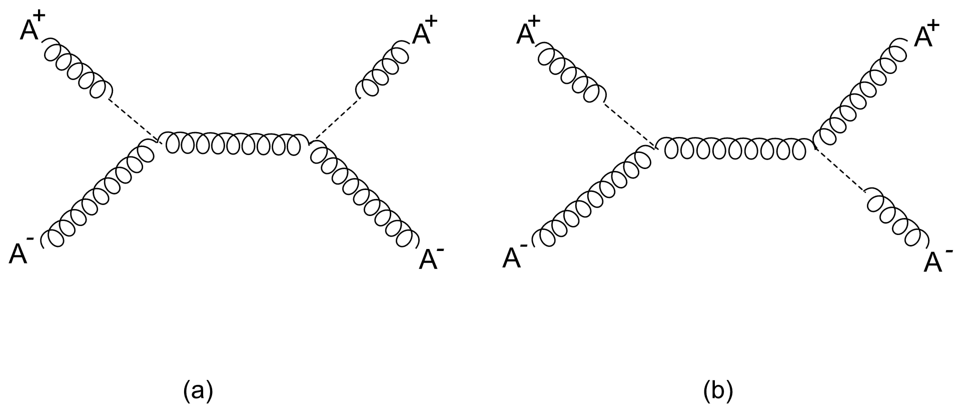

Figure 2.9 Scattering diagrams with P^0 behaviour.

the diagrams in Fig.2.8 are

$$2\left(\mathcal{M}_{2.8a}+\mathcal{M}_{2.8b}\right) = \frac{2g^2P^2}{m^2}(1+c)+\mathscr{O}(P^0) \tag{2.71}$$

$$4\left(\mathcal{M}_{2.8c}+\mathcal{M}_{2.8d}\right) = \frac{4g^2P^2}{m^2}(1+c)+\mathscr{O}(P^0) \tag{2.72}$$

$$4\left(\mathcal{M}_{2.8e}+\mathcal{M}_{2.8f}\right) = -\frac{4g^2P^2}{m^2}(1+c)+\mathscr{O}(P^0) \tag{2.73}$$

$$2\left(\mathcal{M}_{2.8g}+\mathcal{M}_{2.8h}+\mathcal{M}_{2.8i}\right) = \frac{2g^2P^2}{m^2}(1+3c+2c^2)+\mathscr{O}(P^0)\,. \tag{2.74}$$

We have shown detailed calculations of amplitudes of the diagrams in Fig. 2.7b, Fig. 2.7e-2.7f and Fig. 2.8e-2.8f in appendix B. There are remaining diagrams which contains three propagators of B field, shown in Fig. 2.10. There are two of each diagram, corresponding to exchanging the B line between the incoming lines and simultaneously between the outgoing lines. The amplitudes for these are

$$2\left(\mathcal{M}_{2.10a}+\mathcal{M}_{2.10b}+\mathcal{M}_{2.10c}+\mathcal{M}_{2.10d}\right) = -\frac{4g^2P^2}{m^2}(1+2c+c^2)+\mathscr{O}(P^0)\,. \tag{2.75}$$

Adding the amplitudes of the diagrams in Fig. 2.7, Fig. 2.8 and Fig. 2.10, we get

$$\mathcal{M}_T = -\frac{g^2P^2}{2m^2}(1+c)+\mathscr{O}(P^0)\,, \tag{2.76}$$

There are other diagrams containing four internal propagators of the Kalb-Ramond field. These are shown in Fig.2.11. They are irrelevant to our concern because they

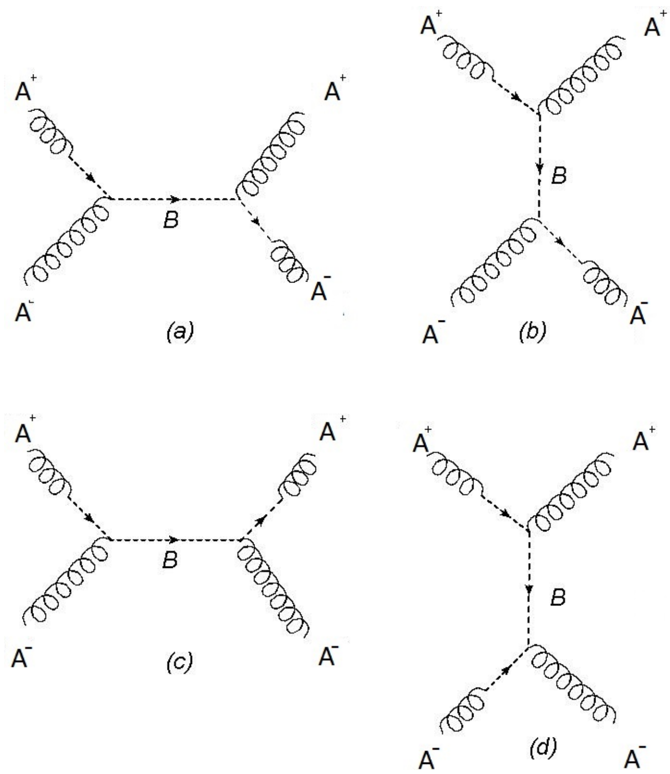

Figure 2.10 Scattering diagrams with P^2 behaviour: III

contribute $\mathscr{O}(P^0)$ at the leading order. We have found the scattering amplitude of $A_L^+ A_L^- \to A_L^+ A_L^-$ in eqn.(2.40) based only on the interactions in Yang-Mills Lagrangian density. The amplitude of the diagrams in Fig. 2.12 is found to be

$$\mathcal{M}_G = \frac{g^2 P^2}{2m^2}(1+c) + \mathscr{O}(P^0). \tag{2.77}$$

If we add to it the total amplitude of the B-mediated tree level scattering process $A^+A^- \to A^+A^-$, given in eqn.(2.76), we find

$$\mathcal{M}_T + \mathcal{M}_G = -\frac{g^2 P^2}{2m^2}(1+c) + \frac{g^2 P^2}{2m^2}(1+c) + \mathscr{O}(P^0) = \mathscr{O}(P^0). \tag{2.78}$$

Hence cancellation of the P^2 divergence occurs exactly and unitarity survives. The tree level amplitude for $A_L^+ A_L^- \to A_L^+ A_L^-$ elastic scattering remains finite as $P \to \infty$, and unitarity is not violated. We note that there are tree level diagrams other than the

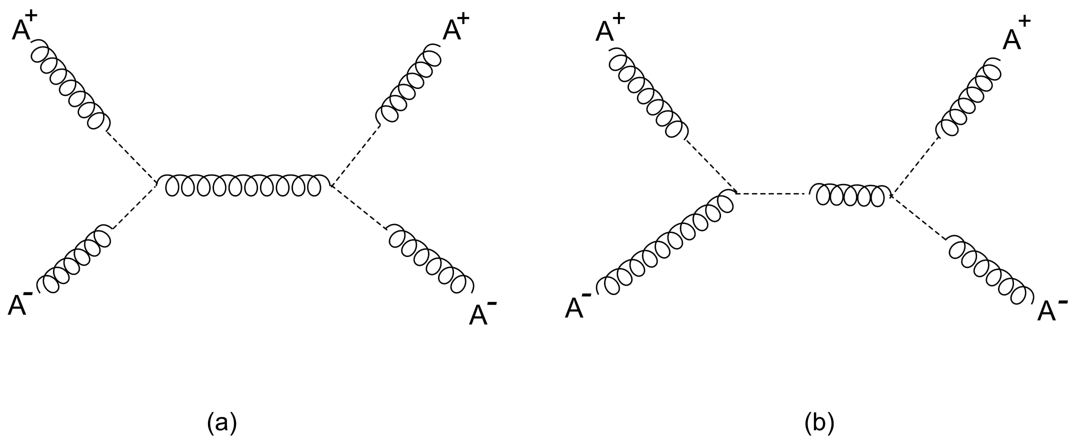

Figure 2.11 Scattering diagrams with P^0 behaviour.

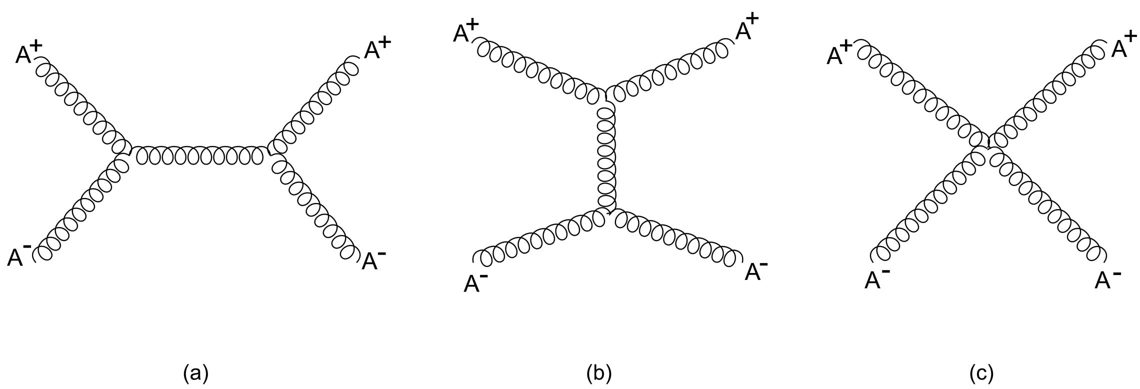

Figure 2.12 Scattering diagrams of $A_L^+ A_L^- \to A_L^+ A_L^-$ from $F^{\mu\nu} F_{\mu\nu}$ term.

diagrams shown in Fig. 2.11 in this model for the $A_L^+ A_L^- \to A_L^+ A_L^-$ elastic scattering process, but all those are of the order P^0, so do not affect our argument.

Now we are going to check the unitarity of the tree level scattering process $A_L^+ A_L^+ \to A_L^+ A_L^+$. Considering the AAA and $AAAA$ couplings in $F_a^{\mu\nu} F_{\mu\nu}^a$, we get the diagrams, shown in Fig. 2.13. The amplitude of the scattering process $A^+ A^+ \to$

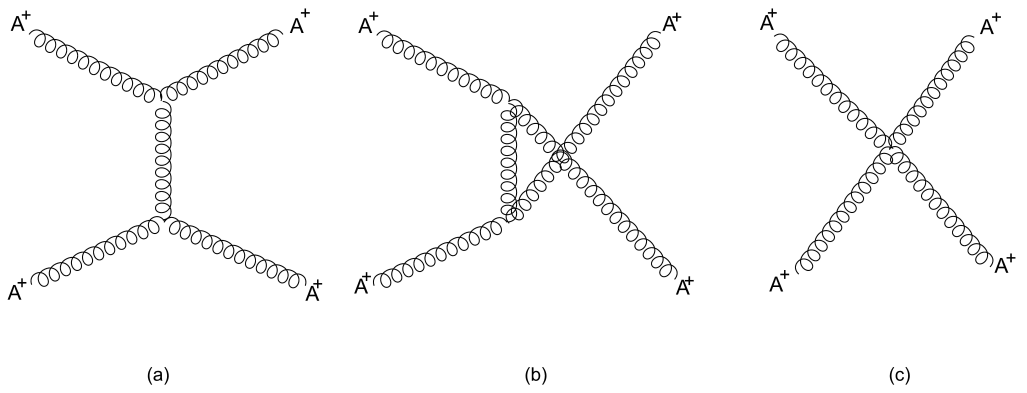

Figure 2.13 (a) t-channel; (b) u channel; (c) quartic interaction of $A^+A^+ \to A^+A^+$ process.

A^+A^+ can be obtained in the high energy limit using eqn.(2.13) and eqn.(2.21)

$$\begin{aligned}\mathcal{M}_{2.13} &= \mathcal{M}_{2.13a} + \mathcal{M}_{2.13b} + \mathcal{M}_{2.13c} \\ &= \varsigma_a^+ \varsigma_b^+ \varsigma_c^- \varsigma_d^- \mathcal{M}_T^{abcd} \\ &= -\frac{g^2 s}{4m^2}. \end{aligned} \tag{2.79}$$

Now including the couplings among the A and B fields, we get the diagrams with a single B propagator shown in the Fig. 2.14 The total amplitude of the t channels is

$$\mathcal{M}_{2.14}^t = (\mathcal{M}_{2.14a} + 2\mathcal{M}_{2.14b} + 4\mathcal{M}_{2.14c}) = \frac{g^2 P^2}{2m^2}(1 + 11c) + \mathscr{O}(P^0). \tag{2.80}$$

There are u-channel diagrams corresponding to the t channel diagrams of Fig. 2.14 which I do not draw here. We can easily get the amplitude of the u-channel diagrams from the corresponding t channel amplitude exchanging the legs of the Feynman diagram carrying the momentum p' and q'. As a consequence, if a term in a amplitude of the t-channel depends on c, we can get the amplitude of the u channel then by replacing c by $-c$ in the t-channel amplitude. Hence the amplitude from the u channels corresponding to the t-channels in Fig. 2.14

$$\mathcal{M}_{2.14}^u = \frac{g^2 P^2}{2m^2}(1 - 11c) + \mathscr{O}(P^0). \tag{2.81}$$

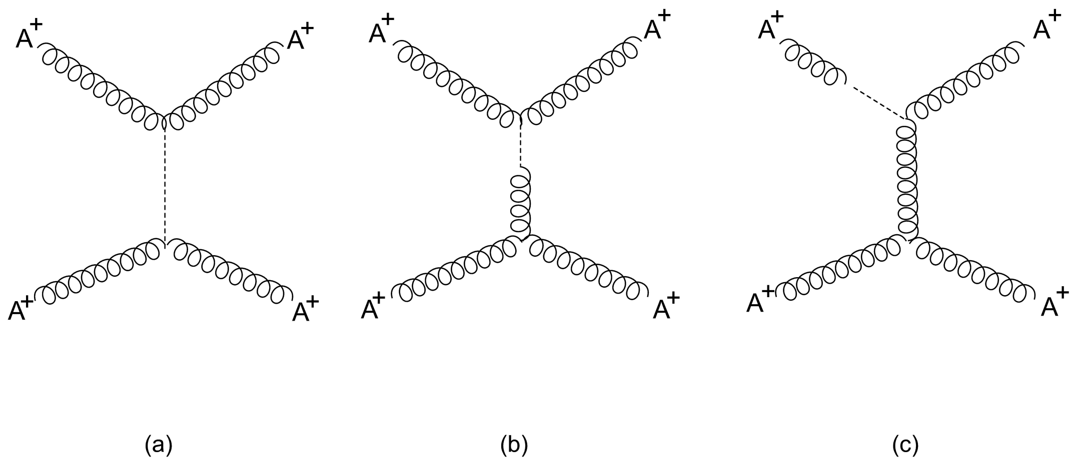

Figure 2.14 (a)t-channels with single B propagator.

So the total amplitude of the t and u channels corresponding to Fig. 2.14 is

$$\mathcal{M}_{2.14} = \mathcal{M}^t_{2.14} + \mathcal{M}^u_{2.14} = \frac{g^2 P^2}{m^2} + \mathscr{O}(P^0). \tag{2.82}$$

Next, we come to the t-channel diagrams with two propagators of the B field are shown in the Fig. 2.15. The total amplitude for the diagrams in Fig. 2.15 is

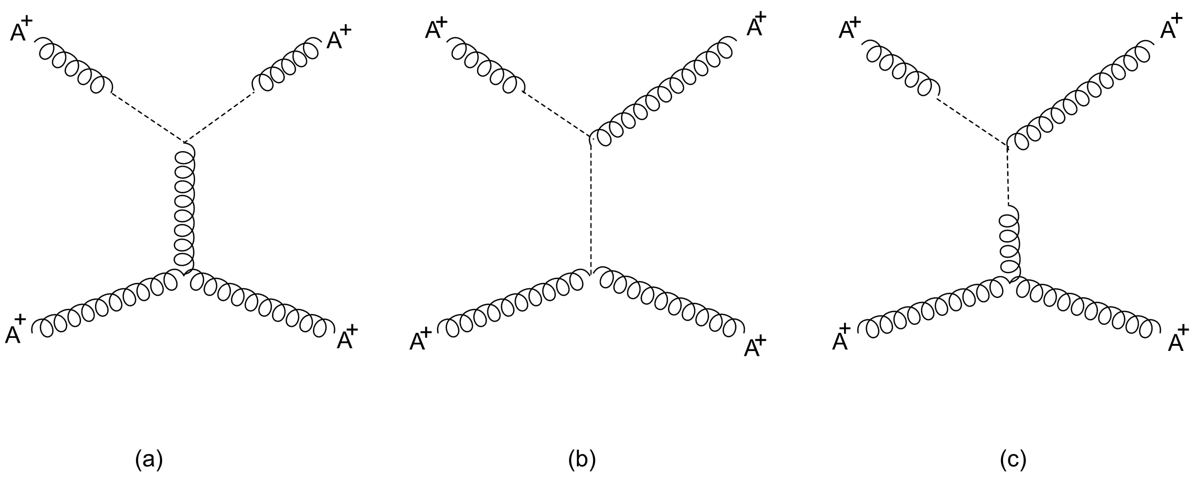

Figure 2.15 t-channels of $A^+A^+ \to A^+A^+$ process with two B propagators.

$$\mathcal{M}^t_{2.15} = \left(2\mathcal{M}^t_{2.15a} + 4\mathcal{M}^t_{2.15b} + 4\mathcal{M}^t_{2.15c}\right) = -\frac{2g^2P^2}{m^2}(1+3c) + \mathscr{O}(P^0). \tag{2.83}$$

Using the same arguments as in the previous case, we get the total amplitude for the corresponding u channel diagrams as

$$\mathcal{M}^u_{2.15} = -\frac{2g^2P^2}{m^2}(1-3c) + \mathscr{O}(P^0). \tag{2.84}$$

So the total amplitude of t and u channels corresponding to Fig. 2.15 becomes

$$\mathcal{M}_{2.15} = -\frac{4g^2P^2}{m^2} + \mathscr{O}(P^0). \tag{2.85}$$

Now we are considering the 'contact' diagrams which contains two B propagators. They are shown in Fig. 2.16. The sum of their amplitudes is

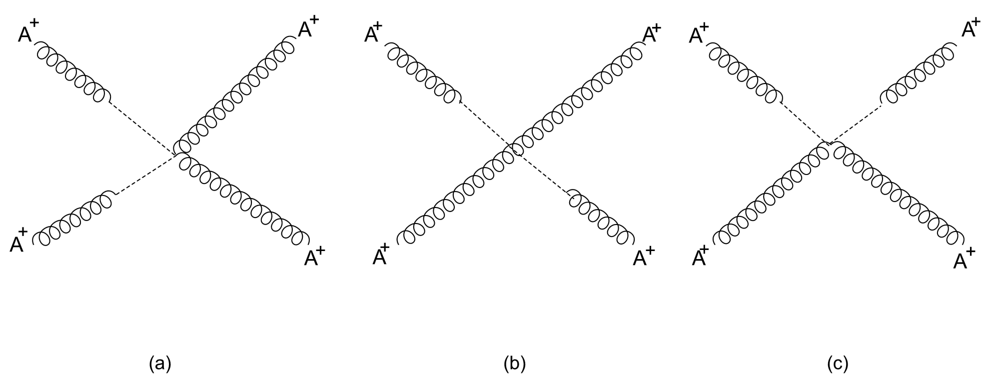

Figure 2.16 Quartic interaction of the process $A^+A^+ \to A^+A^+$ with two B propagators.

$$\mathcal{M}_{2.16} = 2\left(\mathcal{M}_{2.16a} + \mathcal{M}_{2.16b} + \mathcal{M}_{2.16c}\right) = -\frac{4g^2P^2}{m^2}(1+2c^2) + \mathscr{O}(P^0). \tag{2.86}$$

Each of the remaining relevant diagrams contains three propagators of B field. These are shown in Fig. 2.17. The total amplitude of the t and u channels corresponding to the diagrams, shown in Fig. 2.17, is

$$\mathcal{M}_{2.17} = \frac{8g^2P^2}{m^2}(1+c^2) + \mathscr{O}(P^0) \tag{2.87}$$

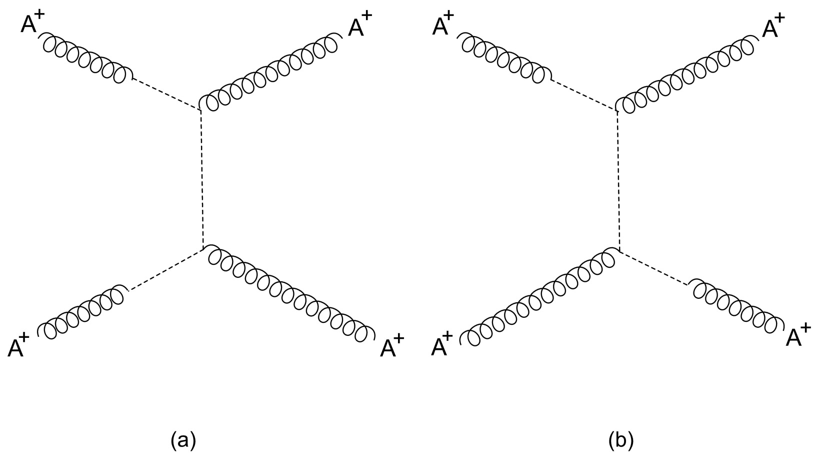

Figure 2.17 (a)Diagrams contains three B propagators.

If we add eqn.(2.82), eqn.(2.85), eqn.(2.86) and eqn.(2.87), we get

$$\begin{aligned} \mathcal{M} &= \mathcal{M}_{2.14} + \mathcal{M}_{2.15} + \mathcal{M}_{2.16} + \mathcal{M}_{2.17} \\ &= \frac{g^2P^2}{m^2} - \frac{4g^2P^2}{m^2} - \frac{4g^2P^2}{m^2}(1+2c^2) + \frac{8g^2P^2}{m^2}(1+c^2) + \mathscr{O}(P^0) \\ &= \frac{g^2P^2}{m^2} + +\mathscr{O}(P^0) \approx \frac{g^2s}{4m^2} + \mathscr{O}(E^0) \end{aligned} \tag{2.88}$$

The total amplitude in eqn.(2.88) comes from the interactions among A and B field in the topologically massive model. So the sum of the amplitudes in eqn.(2.79) and eqn.(2.88) is

$$\mathcal{M}^{A^+A^+\to A^+A^+} = -\frac{g^2s}{4m^2} + \frac{g^2s}{4m^2} + \mathscr{O}(E^0) = \mathscr{O}(E^0). \tag{2.89}$$

Hence we can see that the divergent part of the scattering amplitude is cancelled when we consider the non-Abelian topologically massive model. In similar way, we can find the unitarty of $A^-A^- \to A^-A^-$ scattering. Considering eqn.(2.32) we see that

$$\mathcal{M}(A^-A^- \to A^-A^-) = \mathcal{M}(A^-A^+ \to A^3A^3) \tag{2.90}$$

holds in the high energy limit. So we can easily say from the above relation that the unitarity of the process $A^-A^+ \to A^3A^3$ is assured. We conclude that the topological mass generation mechanism for $3+1$ dimensional SU(2) gauge theory with the Lagrangian as given in eqn.(2.61) does not violate tree level unitarity of scattering amplitude of longitudinal gauge bosons. Various couplings among the B and A fields in $H^{\mu\nu\lambda_a}H^a_{\mu\nu\lambda}$ and $B\wedge F$ terms plays important roles in obtaining the unitarity.

Appendices

Appendix A

Derivation of the isospin amplitudes

The third component of weak-isospin I_3 of A^-, A^3 and A^+ are respectively -1, 0 and $+1$. So the two particle product state $|I_1 I_2, m_1 m_2\rangle$ can be decomposed into total isospin states $|I, M\rangle$ using Clebsch-Gordan coefficients, i.e.,

$$|I_1 I_2, m_1 m_2\rangle = \sum_{IM} |I, M\rangle \langle I, M|I_1, I_2; m_1, m_2\rangle , \tag{A.1}$$

where m_1 runs from $-I_1$ to I_1 and m_2 from $-I_2$ to I_2. The Clebsch-Gordan coefficients $\langle IM|I_1, I_2; m_1, m_2\rangle$ are non-zero only if $m_1 + m_2 = M$. For example

$$\left\langle A^+A^-\right| \equiv \langle 1, 1; 1, -1| = -\left(\sqrt{\frac{1}{6}}\,\langle 2, 0| + \sqrt{\frac{1}{2}}\,\langle 1, 0| + \sqrt{\frac{1}{3}}\,\langle 0, 0|\right), \tag{A.2}$$

$$\left|A^3A^3\right\rangle \equiv |1, 1; 0, 0\rangle = \sqrt{\frac{2}{3}}\,|2, 0\rangle - \sqrt{\frac{1}{3}}\,|0, 0\rangle . \tag{A.3}$$

Hence using the orthogonality of the state vector we have

$$\begin{aligned}\left\langle A^+A^-\right| S \left|A^3A^3\right\rangle &= -\left(\sqrt{\frac{1}{6}}\,\langle 2, 0| + \sqrt{\frac{1}{2}}\,\langle 1, 0| + \sqrt{\frac{1}{3}}\,\langle 0, 0|\right) S \left(\sqrt{\frac{2}{3}}\,|2, 0\rangle - \sqrt{\frac{1}{3}}\,|0, 0\rangle\right) \\ &= \frac{1}{3}\left(\mathcal{M}_0 - \mathcal{M}_2\right), \end{aligned} \tag{A.4}$$

where the we have defined

$$\langle 0,0|\,S\,|0,0\rangle = \mathcal{M}_0, \tag{A.5}$$

$$\langle 1,M|\,S\,|1,M\rangle = \mathcal{M}_1, \tag{A.6}$$

$$\langle 2,M|\,S\,|2,M\rangle = \mathcal{M}_2. \tag{A.7}$$

The S-matrix is Poincare invariant, therefore it is invariant under $SO(3)$ group. Then we can say using Wigner-Eckart theorem that the matrix elements in eqn.(A.5)-eqn.(A.7) are independent of M [98–101]. In a similar way we get

$$\left\langle A^-A^-\right|S\left|A^-A^-\right\rangle = \left\langle A^+A^+\right|S\left|A^+A^+\right\rangle = \mathcal{M}_2 \tag{A.8}$$

and

$$\begin{aligned}\left\langle A^-A^3\right|S\left|A^-A^3\right\rangle &= \left(\sqrt{\frac{1}{2}}\langle 2,-1| + \sqrt{\frac{1}{2}}\langle 1,-1|\right) S \left(\sqrt{\frac{1}{2}}|2,-1\rangle + \sqrt{\frac{1}{2}}|1,-1\rangle\right) \\ &= \frac{1}{2}\left(\mathcal{M}_1 + \mathcal{M}_2\right)\end{aligned} \tag{A.9}$$

and

$$\begin{aligned}\left\langle A^+A^3\right|S\left|A^+A^3\right\rangle &= \left(\sqrt{\frac{1}{2}}\langle 2,1| + \sqrt{\frac{1}{2}}\langle 1,1|\right) S \left(\sqrt{\frac{1}{2}}|2,1\rangle + \sqrt{\frac{1}{2}}|1,1\rangle\right) \\ &= \frac{1}{2}\left(\mathcal{M}_1 + \mathcal{M}_2\right).\end{aligned} \tag{A.10}$$

Using eqn.(2.34), eqn.(2.35) and eqn.(2.32), we can express eqn.(A.4), eqn.(A.8) and eqn.(A.10) as

$$\mathcal{M}(t,s,u) + \mathcal{M}(u,s,t) = \mathcal{M}_2 \tag{A.11}$$

$$\mathcal{M}(s,t,u) = \frac{1}{3}\left(\mathcal{M}_0 - \mathcal{M}_2\right) \tag{A.12}$$

$$\mathcal{M}(t,s,u) = \frac{1}{2}\left(\mathcal{M}_1 + \mathcal{M}_2\right). \tag{A.13}$$

Solving eqn.(A.11)-(A.13), we have

$$\mathcal{M}_0 = 3\mathcal{M}(s,t,u) + \mathcal{M}(t,s,u) + \mathcal{M}(u,s,t) \tag{A.14}$$

$$\mathcal{M}_1 = \mathcal{M}(t,s,u) + \mathcal{M}(u,s,t) \tag{A.15}$$

$$\mathcal{M}_2 = \mathcal{M}(t,s,u) + \mathcal{M}(u,s,t) \tag{A.16}$$

as given in the eqn.(2.46)-(2.48).

A.1 Kinematics

In the centre of momentum frame for the elastic scattering process $A^aA^b \to A^cA^d$, the gauge bosons A^a and A^b are moving along z-axis as shown in Fig. A.1. The diagram

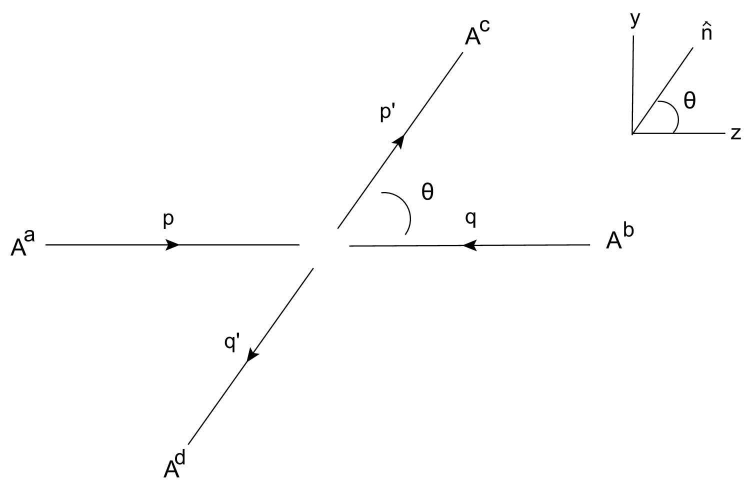

Figure A.1 Kinematical diagram in the centre of momentum frame.

is in the y-z plane. The four momenta of the gauge bosons A^a and A^b in initial state are respectively

$$p^\mu \equiv (E, P\hat{z}) \qquad q^\mu \equiv (E, -P\hat{z}). \tag{A.17}$$

where P is magnitude of the three momentum. The four momenta of the gauge bosons in the final states are

$$p'^{\mu} \equiv (E, P\hat{n}) \qquad q'^{\mu} \equiv (E, -P\hat{n}). \tag{A.18}$$

Here $\hat{n}$ is the unit vector along the direction of the scattered gauge boson and it makes an angle θ with the z-axis i.e.

$$\hat{z}.\hat{n} = \cos\theta, \tag{A.19}$$

which will be abbreviated as c in our analysis of the scattering process. The longitudinal polarization vectors of the initial states are

$$\epsilon_p^{\mu} \equiv \frac{1}{m}(P, E\hat{z}), \qquad \epsilon_q^{\mu} \equiv \frac{1}{m}(P, -E\hat{z}), \tag{A.20}$$

which satisfy $p_\mu \epsilon_p^\mu = 0$ and $q_\mu \epsilon_q^\mu = 0$. The longitudinal polarization vectors for the final states are

$$\epsilon_{p'}^{\mu} \equiv \frac{1}{m}(P, E\hat{n}), \qquad \epsilon_{q'}^{\mu} \equiv \frac{1}{m}(P, -E\hat{n}), \tag{A.21}$$

satisfying $p'_\mu \epsilon_{p'}^\mu = 0$ and $q'_\mu \epsilon_{q'}^\mu = 0$. We use Mandelstam variables s, t and u in terms of the four momenta as

$$s = (p+q)^2, \qquad t = (p-p')^2, \qquad u = (p-q')^2, \tag{A.22}$$

which is in the high energy limit i.e. $E \gg m$, becomes

$$s \approx 4E^2, \qquad t \approx -2P^2(1-c), \qquad u \approx -2P^2(1+c). \tag{A.23}$$

A.2 Amplitude of $A_L^a A_L^b \to A_L^c A_L^d$ scattering.

Here we show the calculation of the amplitude for the t, u and s channels and quartic interaction of the scattering process of longitudinally polarized gauge bosons $A^a A^b \to$

$A^c A^d$ where they are taken to be massive in $SU(N)$ gauge theory. The result is used in eqn.(2.13). The t-channel diagram of the scattering process is shown in Fig. 2.1a and also in Fig. A.2. First we consider the non-linear interactions among massive gauge bosons in pure Yang-Mills Lagrangian density and show how the scattering amplitude violates unitarity. We calculate in the Feynman-'t Hooft gauge for the

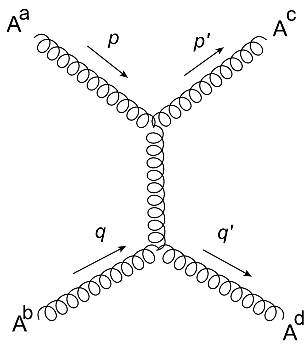

Figure A.2 t-channel for $A^a A^b \to A^c A^d$ scattering.

propagator of the gauge boson A. The Feynman amplitude is given by

$$i\mathcal{M}_t = \epsilon_\mu^p \epsilon_\nu^{p'} V_{aec}^{\mu\nu\lambda} iD_{\lambda\lambda'}^t V_{bed}^{\alpha\beta\lambda'} \epsilon_\alpha^q \epsilon_\beta^{q'}, \tag{A.24}$$

where the ϵ are the polarizations of the external gauge bosons, and

$$iD_{\lambda\lambda'}^t = -\frac{ig_{\lambda\lambda'}}{(p-p')^2 - m^2} = -\frac{ig_{\lambda\lambda'}}{t - m^2}, \tag{A.25}$$

$$V_{aec}^{\mu\nu\lambda} = -g f_{ace}\left[(p+p')_\lambda g_{\mu\nu} - (2p'-p)_\mu g_{\nu\lambda} - (2p-p')_\nu g_{\mu\lambda}\right]. \tag{A.26}$$

The $V_{aec}^{\mu\nu\lambda}$ is obtained from eqn.(2.4). Applying the condition of the longitudinal polarization vector $p^\mu \epsilon_\mu^p = 0$, I find after some algebraic manipulations

$$\mathcal{M}_t = g^2 \frac{f_{ace} f_{bde}}{(t-m^2)} \left[(p+p')_\lambda \epsilon_p \cdot \epsilon_{p'} - 2p' \cdot \epsilon_p (\epsilon^p + \epsilon^{p'})_\lambda\right] \tag{A.27}$$

$$\times \left[(q+q')^\lambda \epsilon_q \cdot \epsilon_q' - 2q' \cdot \epsilon_q (\epsilon^q + \epsilon^{q'})^\lambda\right]$$

$$= g^2 \frac{f_{ace} f_{bde}}{(t-m^2)} B_\lambda^t C^{t\lambda}, \tag{A.28}$$

where for the convenience we have defined the 4-vectors

$$B^t \equiv \left(-\frac{2P^2E}{m^2}(1-c) - 2Ec, \left\{-\frac{P^3}{m^2}(1-c) - P(2-c)\right\}(\hat{z}+\hat{n})\right), \quad \text{(A.29)}$$

$$C^t \equiv \left(-\frac{2P^2E}{m^2}(1-c) - 2Ec, \left\{\frac{P^3}{m^2}(1-c) + P(2-c)\right\}(\hat{z}+\hat{n})\right). \quad \text{(A.30)}$$

We have used

$$p' \cdot \epsilon_p = p \cdot \epsilon_{p'} = q' \cdot \epsilon_q = q \cdot \epsilon_{q'} = \frac{PE}{m}(1-c) \quad \text{(A.31)}$$

and

$$\epsilon^p \cdot \epsilon^{p'} = \left\{\frac{P^2}{m^2}(1-c) - c\right\} = \epsilon^q \cdot \epsilon^{q'} \quad \text{(A.32)}$$

from eqn.(A.17)-(A.21) to get eqn.(A.28) from eqn.(A.27). Now taking the high energy limit $P \gg m$, we can write

$$\begin{aligned} \frac{1}{t-m^2} = \frac{1}{-2P^2(1-c)-m^2} &= -\frac{1}{2P^2(1-c)}\left[1+\frac{m^2}{2P^2(1-c)}\right]^{-1} \\ &= -\frac{1}{2P^2(1-c)}\left[1-\frac{m^2}{2P^2(1-c)}+\cdots\right]. \end{aligned} \quad \text{(A.33)}$$

Hence the Feynman amplitude becomes in the high energy limit

$$\mathcal{M}_t \approx g^2 f_{ace} f_{bde}\left[\frac{P^4}{m^4}(3+c)(1-c) + \frac{P^2}{2m^2}(9+7c-4c^2)\right] \quad \text{(A.34)}$$

$$\approx -g^2 f_{ace} f_{bde}\left[\frac{E^4}{m^4}(3+c)(1-c) - \frac{E^2}{2m^2}(3-15c)\right]. \quad \text{(A.35)}$$

Similarly we can calculate the amplitude for the u and s-channels and quartic interactions shown in Fig. A.3. The amplitude of the u-channel is

$$\mathcal{M}_u = g^2 \frac{f_{ade} f_{bce}}{(u-m^2)}\left[(p+q')_\lambda \epsilon_p \cdot \epsilon_{q'} - 2q' \cdot \epsilon_p(\epsilon_p + \epsilon_{q'})_\lambda\right] \quad \text{(A.36)}$$

$$\times \left[(q+p')^\lambda \epsilon_q \cdot \epsilon_{p'} - 2q \cdot \epsilon_q(\epsilon_q + \epsilon_{p'})^\lambda\right]$$

$$= g^2 \frac{f_{ace} f_{bde}}{(u-m^2)} B^u_\lambda C^{u\lambda}, \quad \text{(A.37)}$$

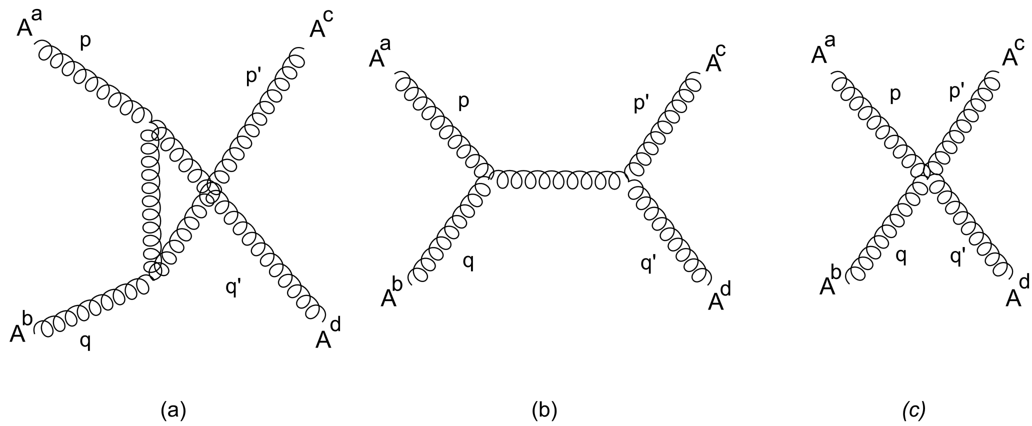

Figure A.3 (a) u-channel; (b) s-channel; (c) quartic interaction.

where

$$B^u \equiv \left(-\frac{2P^2E}{m^2}(1+c)+2Ec, \left\{-\frac{P^3}{m^2}(1+c)-P(2+c)\right\}(\hat{z}-\hat{n})\right), \tag{A.38}$$

$$C^u \equiv \left(-\frac{2P^2E}{m^2}(1+c)-2Ec, \left\{\frac{P^3}{m^2}(1+c)+P(2+c)\right\}(\hat{z}-\hat{n})\right). \tag{A.39}$$

In the high energy limit, we get the amplitude of $A^aA^b \to A^cA^d$ scattering process in $SU(N)$ gauge theory

$$\mathcal{M}_u \approx g^2 f_{ade}f_{bce}\left[\frac{P^4}{m^4}(3-c)(1+c)+\frac{P^2}{2m^2}(9-7c-4c^2)\right] \tag{A.40}$$

$$\approx -g^2 f_{ade}f_{bce}\left[\frac{E^4}{m^4}(3-c)(1+c)-\frac{E^2}{2m^2}(3+15c)\right]. \tag{A.41}$$

The amplitude of the s-channel is similarly calculated to be

$$\mathcal{M}_s = -g^2\frac{f_{abe}f_{dce}}{(s-m^2)}\left[(p-q)_\lambda \epsilon_p\cdot\epsilon_q - 2q\cdot\epsilon_p(\epsilon_p-\epsilon_q)_\lambda\right] \tag{A.42}$$

$$\times \left[(q'+p')^\lambda \epsilon_{q'}\cdot\epsilon_{p'} - 2p'\cdot\epsilon_{q'}(\epsilon_{p'}-\epsilon_{q'})^\lambda\right]$$

$$= g^2\frac{f_{abe}f_{cde}}{(s-m^2)}B^s_\lambda C^{s\lambda}, \tag{A.43}$$

where

$$B^s \equiv \left(0, \left(\frac{4P^3}{m^2} + 6P\right)\hat{z}\right), \tag{A.44}$$

$$C^s \equiv \left(0, \left(\frac{4P^3}{m^2} + 6P\right)\hat{n}\right). \tag{A.45}$$

In the high energy limit the amplitude of the s-channel in $SU(N)$ Yang-Mills theory becomes

$$\mathcal{M}_s \approx -g^2 f_{abe} f_{cde}\left[\frac{4P^4}{m^4} + \frac{9P^2}{m^2} + 9\right]c \tag{A.46}$$

$$\approx -g^2 f_{ace} f_{bde}\left[\frac{4E^4}{m^4} + \frac{E^2}{m^2} + 4\right]c. \tag{A.47}$$

The amplitude of the quartic coupling is calculated similarly to be

$$\begin{aligned}\mathcal{M}_q \approx & -\Bigg[g^2 f_{ace} f_{bde}\left\{\frac{P^2}{m^2}(3+c)(1-c) + (1-c)(1+c)\right\}\left(\frac{P^2}{m^2}+1\right) \\ & + g^2 f_{ade} f_{bce}\left\{\frac{P^2}{m^2}(3-c)(1+c) + (1+c)(1-c)\right\}\left(\frac{P^2}{m^2}+1\right) \\ & - g^2 f_{abe} f_{cde}\frac{4P^2 c}{m^2}\left(\frac{P^2}{m^2}+1\right)\Bigg]\end{aligned} \tag{A.48}$$

$$\begin{aligned}\approx & -\Bigg[g^2 f_{ace} f_{bde}\left\{\frac{E^2}{m^2}(3+c)(1-c) + 2(1-c-c^2)\right\}\frac{E^2}{m^2} \\ & + g^2 f_{ade} f_{bce}\left\{\frac{E^2}{m^2}(3-c)(1+c) + 2(1+c-c^2)\right\}\frac{E^2}{m^2} \\ & - g^2 f_{abe} f_{cde}\left(\frac{4E^2 c}{m^2} - 4c\right)\frac{E^2}{m^2}\Bigg].\end{aligned} \tag{A.49}$$

These amplitudes in eqn.(A.34), eqn.(A.40), eqn.(A.46) and eqn.(A.48) are shown in eqn.(2.9), eqn.(2.10), eqn.(2.11) and eqn.(2.12) respectively. We now calculate the Feynman amplitude of the elastic scattering with the Higgs mediator in the $SU(N)$ gauge theory. There are three channels corresponding to s, t and u. The vertex rule corresponding to the hAA vertex is

$$iV_{\mu\nu,ab} = im\delta_{ab}\eta_{\mu\nu}. \tag{A.50}$$

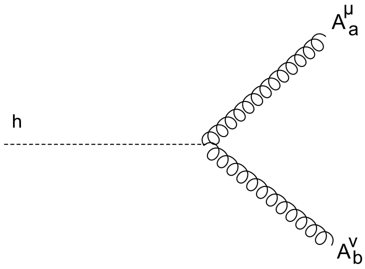

Figure A.4 Vertex rule for hAA.

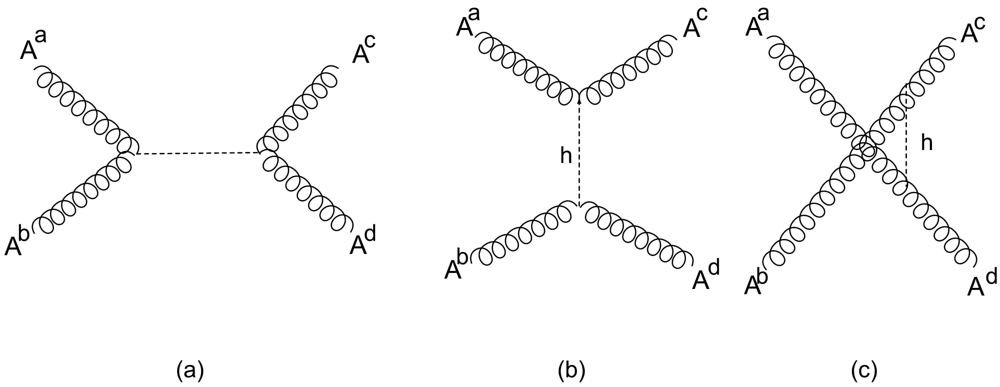

Figure A.5 (a) s-channel,(b) t-channel, (c) u-channel for Higgs mediated diagrams.

Using the vertex rule we can find the amplitude of the diagrams.

The Feynman amplitude for the s-channel in Fig. A.5c is

$$\begin{aligned}\mathcal{M}_s^h &= (igm)\delta_{ab}\frac{1}{s-m_h^2}(igm)\delta_{cd}(\epsilon_p\cdot\epsilon_q)^2 \\ &= -\delta_{ab}\delta_{cd}\frac{g^2m^2}{(s-m_h^2)}\left(\frac{2P^2}{m^2}+1\right)^2. \end{aligned}\tag{A.51}$$

In the high energy limit, it becomes

$$\mathcal{M}_s^h \approx -\delta_{ab}\delta_{cd}\frac{g^2P^2}{m^2} \approx -\delta_{ab}\delta_{cd}\frac{g^2 s}{4m^2}. \tag{A.52}$$

The Feynman amplitude for the t-channel in Fig. A.5a is

$$\begin{aligned}\mathcal{M}_t^h &= (gm)\delta_{ac}\frac{1}{t-m_h^2}(gm)\delta_{bd}(\epsilon_{p'}\cdot\epsilon_p)^2 \\ &= -\delta_{ac}\delta_{bd}\frac{g^2m^2}{(t-m_h^2)}\left(\frac{P^2}{m^2}(1-c)-c\right)^2 . \end{aligned} \tag{A.53}$$

In the high energy limit,

$$\mathcal{M}_t^h \approx \delta_{ac}\delta_{bd}\tfrac{g^2P^2}{2m^2}(1-c) \approx -\delta_{ac}\delta_{bd}\tfrac{g^2t}{4m^2}. \tag{A.54}$$

The Feynman amplitude for the u-channel in Fig. A.5b is

$$\begin{aligned}\mathcal{M}_u^h &= (igm)\delta_{ad}\frac{1}{u-m_h^2}(igm)\delta_{bc}(\epsilon_p\cdot\epsilon_{q'})^2 \\ &= \delta_{ad}\delta_{bc}\frac{g^2m^2}{(u-m_h^2)}\left(\frac{P^2}{m^2}(1+c)+c\right)^2 . \end{aligned} \tag{A.55}$$

In the high energy limit,

$$\mathcal{M}_u^h \approx \delta_{ad}\delta_{bc}\frac{g^2P^2}{2m^2}(1+c) \approx -\delta_{ad}\delta_{bc}\frac{g^2u}{4m^2}. \tag{A.56}$$

Thus the total amplitude of Higgs mediated $A^aA^b \to A^cA^d$ scattering, shown in Fig. A.5a, in the high-energy limit is

$$\mathcal{M}_t^h + \mathcal{M}_u^h + \mathcal{M}_s^h \approx -\frac{g^2}{4m^2}\left(s\ \delta_{ab}\delta_{cd} + t\ \delta_{ac}\delta_{bd} + u\ \delta_{ad}\delta_{bc}\right). \tag{A.57}$$

Appendix B

Amplitude of some B-mediated $A_L A_L \to A_L A_L$ scattering-channels.

Here we show some tricks which we use in the calculation of the amplitudes of B-mediated diagrams for $A^+A^- \to A^+A^-$ and give some examples to show how the tricks help us in the calculations. We now show explicitly how the amplitude of t-channel Feynman diagram in the Fig. 2.7b is calculated. It is redrawn in the Fig. B.1 with the four momenta shown on the legs. The four momenta, p, q, p' and q' are specified in eqn.(A.17) and eqn.(**??**). The Feynman amplitude for the diagram is

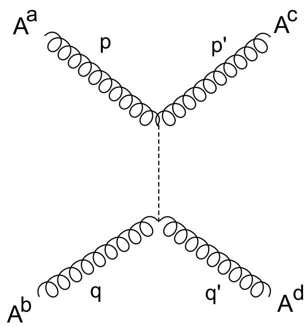

Figure B.1 t-channel Scattering diagrams with B-propagator then given by

$$\mathcal{M} = \epsilon^\mu_p \epsilon^\nu_{p'}(-igmf_{ace}\epsilon_{\nu\mu\alpha\beta})\frac{1}{4}\frac{ig^{\alpha[\alpha'}g^{\beta']\beta}}{t-m^2}(-igmf_{ebd})\epsilon_{\rho\sigma\alpha'\beta'}\epsilon^\rho_q\epsilon^\sigma_{q'} \quad \text{(B.1)}$$

$$= \frac{g^2m^2}{(t-m^2)}f_{ace}f_{bde}\left(\epsilon_p\cdot\epsilon_q\epsilon'_p\cdot\epsilon'_q - \epsilon_p\cdot\epsilon_{q'}\epsilon_{p'}\cdot\epsilon_q\right). \quad \text{(B.2)}$$

We use some tricks to find the amplitude of the Feynman diagrams containing the AB two point function Fig. B.2a. The calculation of the t-channel diagrams in

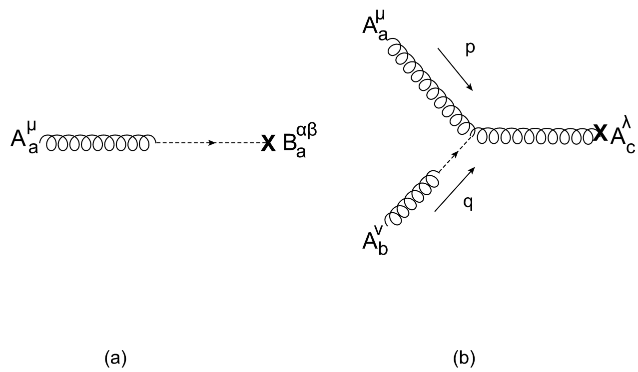

Figure B.2 (a) Diagram corresponding to vertex tensor $\mathcal{A}^{\alpha\beta}$; (b)diagram corresponding to vertex vector V^λ

Fig. B.1 and its corresponding s-channel diagram, shown in Fig. 2.7, are the simplest B-mediated diagrams among all the other diagrams shown in the Fig. 2.7-Fig. 2.10. We have already seen that except the diagrams in the Fig. 2.7a and Fig. 2.7b, all the diagrams contain AB couplings. So we calculate the contraction of AB-vertex rule, given in the eqn.(2.62), with the longitudinal polarization vector of the massive gauge boson moving along the z axis. We have excluded the propagator of B field which is shown in the Fig. B.2a by the **X** mark where the B-lines end. We get a 'vertex tensor'

$$\mathcal{A}^{\alpha\beta} = \epsilon^{\alpha\beta\gamma\mu}p_\gamma\epsilon^p_\mu = m\epsilon^{\alpha\beta03} \quad \text{(B.3)}$$

according to eqn.(A.17) and eqn.(A.20). The calculation of the amplitudes of the diagrams in Fig. 2.7e and Fig. 2.7f with the placement of AB coupling on different legs, becomes easier if we use some tricks. Excluding the propagator of B field, we contract the two point vertex rule, given in eqn.(2.62), by the longitudinal polarization of the gauge boson along the z axis to get

$$\begin{aligned} V^\lambda &= \epsilon^p_\mu(-igmf_{cab}\epsilon^{\lambda\mu\rho\sigma})\frac{ig_{\rho[\rho'}g_{\sigma']\sigma}}{4m^2}m\epsilon^{\rho'\sigma' s\nu}q_s\epsilon^q_\nu \\ &= -gf_{cab}[q^\lambda\ \epsilon_p.\epsilon_q - q.\epsilon_p\ \epsilon^\lambda_q] \qquad \text{(B.4)} \\ &= -gf_{cab}(E, P\hat{z}) = -gf_{abc}p^\lambda. \qquad \text{(B.5)} \end{aligned}$$

Similarly we can find the 'vertex-vector' for the diagrams in Fig. B.3 using eqn.(2.21),

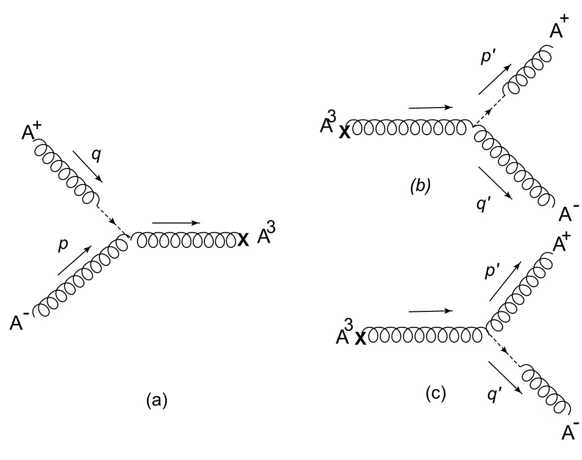

Figure B.3 Diagrams for vertex vectors.

$$(a)\ V^\lambda_{B.3a} = gq^\lambda, \qquad \text{(B.6)}$$

$$(b)\ V^\lambda_{B.3b} = -gq'^\lambda, \qquad \text{(B.7)}$$

$$(c)\ V^\lambda_{B.3c} = gp'^\lambda, \qquad \text{(B.8)}$$

and for the diagrams in Fig. B.4

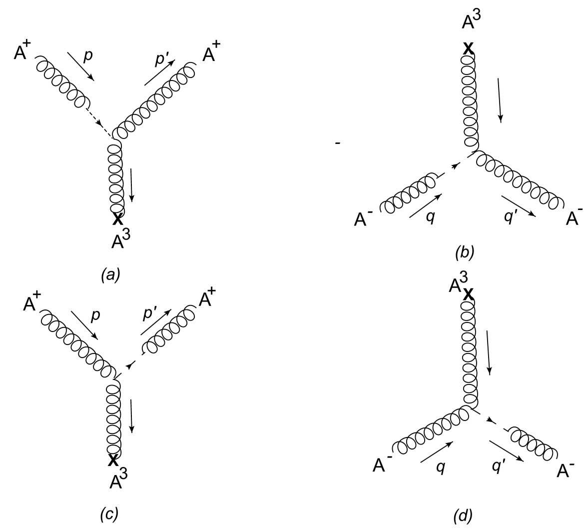

Figure B.4 Diagrams for vertex vectors $V^{\lambda}_{B.4a} - V^{\lambda}_{B.4d}$.

$$
\begin{aligned}
(a)\ V^{\lambda}_{B.4a} &= g(Ec, P\hat{z}), && \text{(B.9)}\\
(b)\ V^{\lambda}_{B.4b} &= -g(Ec, -P\hat{z}), && \text{(B.10)}\\
(c)\ V^{\lambda}_{B.4c} &= g(Ec, P\hat{n}), && \text{(B.11)}\\
(d)\ V^{\lambda}_{B.4d} &= -g(Ec, -P\hat{n}). && \text{(B.12)}
\end{aligned}
$$

We can use these results to calculate the amplitude of the diagrams in the Fig. B.5. These are diagrams shown in Fig. 2.7e and Fig. 2.7f. For the s-channel diagram, we have

$$
\begin{aligned}
\mathcal{M}_s &= V^{\mu}_{B.3a} \frac{-ig_{\mu\nu}}{s-m^2} C^s_{\nu} \\
&= \frac{g^2}{s-m^2}\left(\frac{4P^4}{m^2} + 6P^2\right) c, && \text{(B.13)}
\end{aligned}
$$

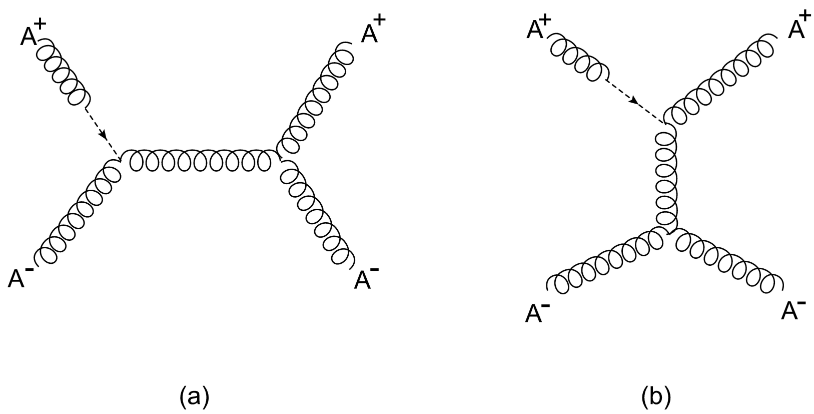

Figure B.5 (a) s-channel and (b) t channel with one B-propagator, which are also shown in Fig. 2.7e and Fig. 2.7f.

where C_s^ν is given in eqn.(A.45). For the t-channel

$$\begin{aligned}\mathcal{M}_t &= V^\lambda_{B.4a}\frac{-g_{\mu\nu}}{s-m^2}C_t^\nu \\ &= ig(Ec, P\hat{z})\frac{-i}{t-m^2}g\left(-\frac{2P^2E}{m^2}(1-c)-2Ec, \left\{\frac{P^3}{m^2}(1-c)+P(2-c)\right\}(\hat{z}+\hat{n})\right) \\ &= \frac{ig}{t-m^2}\left[\frac{P^4}{m^2}(1-c)(1+3c)+p^2(2-c)(1+3c)+2m^2c\right], \qquad \text{(B.14)}\end{aligned}$$

where C_t^ν is given in eqn.(A.30). In the high energy limit

$$\mathcal{M}_s \approx \frac{g^2P^2c}{m^2}, \qquad \mathcal{M}_t \approx -\frac{g^2P^2}{2m^2}(1+3c). \qquad \text{(B.15)}$$

Hence the total amplitude for the diagram in Fig. B.5 is

$$\mathcal{M}_s + \mathcal{M}_t = -\frac{g^2P^2}{2m^2}(1+c), \qquad \text{(B.16)}$$

which is used in eqn.(2.70). We also find the vertex-vectors for the diagrams shown

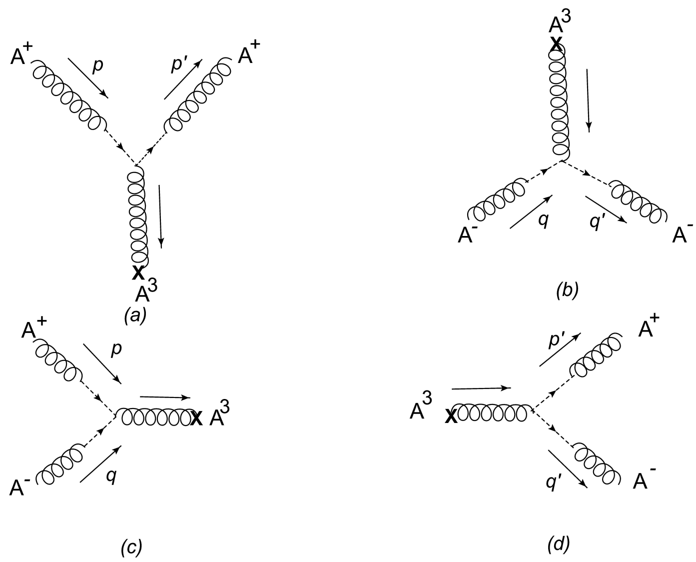

Figure B.6 Diagrams for the 'vertex vectors' containing two B propagators

in Fig. B.6 as

$$(a\ )V^{\lambda}_{B.6a} = g(2Ec, P(\hat{z}+\hat{n})), \tag{B.17}$$

$$(b)\ V^{\lambda}_{B.6b} = -g(2Ec, -P(\hat{z}+\hat{n})), \tag{B.18}$$

$$(c)\ V^{\lambda}_{B.6c} = g(p-q)^{\lambda}, \tag{B.19}$$

$$(d)\ V^{\lambda}_{B.6d} = g(p'-q')^{\lambda}. \tag{B.20}$$

We can use them to calculate the scattering amplitude of the diagrams in Fig. B.7, which are the diagrams in Fig. 2.8a and Fig. 2.8b. The amplitude of the s-channel, shown in Fig. B.7 is

$$\begin{aligned}
\mathcal{M}_{B.7a} &= V^{\lambda}_{B.6c}\frac{-ig_{\lambda\rho}}{s-m^2}C^{\rho}_{s} \\
&= (0, 2P\hat{z})\,\frac{1}{s-m^2}\left(0, \left(\frac{4P^3}{m^2}+6P\right)\hat{n}\right) \\
&= -\frac{g^2}{s-m^2}\left(\frac{8P^4}{m^2}+12P^2\right)c.
\end{aligned}\tag{B.21}$$

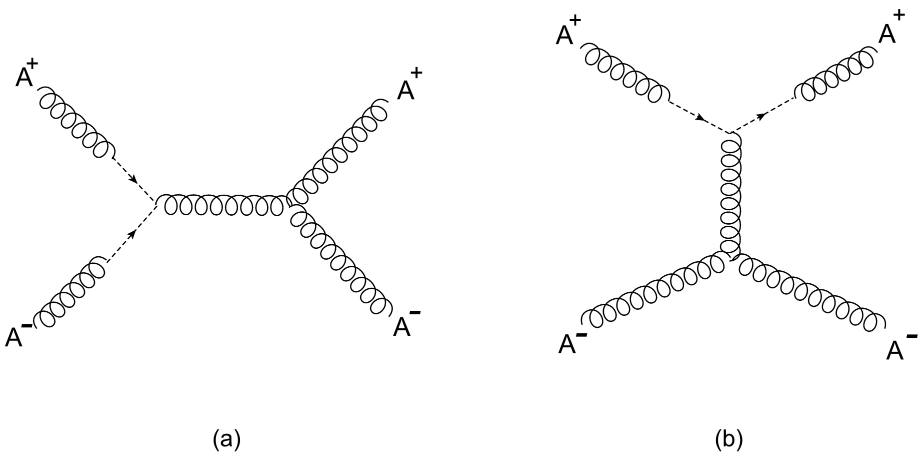

Figure B.7 Feynman diagrams with two B-propagators:(a) s-channel; (b) t-channel corresponding to Fig. 2.8a and Fig. 2.8b.

The amplitude of the t-channel diagram in Fig. B.7b is

$$\begin{aligned}\mathcal{M}_{B.7b} &= V^{\lambda}_{B.6a}\frac{-ig_{\lambda\rho}}{t-m^2}C^{\rho}_{t} \\ &= \frac{-g^2}{t-m^2}\left[\frac{2P^4}{m^2}(1+3c)(1-c)+4P^2c(1-c)+4E^2c+2P^2(2-c)(1+c)\right].\end{aligned} \tag{B.22}$$

Thus, in the high energy limit we find

$$\mathcal{M}_{B.7a} \approx -\frac{2g^2P^2}{m^2}c, \qquad \mathcal{M}_{B.7b} \approx \frac{g^2P^2}{m^2}(1+3c). \tag{B.23}$$

Hence if we sum up the amplitudes of the s and t channels, we get in the high energy limit

$$\mathcal{M}_{B.7} \approx \frac{g^2P^2}{m^2}(1+c), \tag{B.24}$$

which is used in eqn.(2.71).

Chapter 3

β function in topologically massive theory

In this chapter we will see the behaviour of gauge coupling constant g with the change of the energy scale in a topologically massive gauge theory based on the work in [105]. We know that perturbative technique can be used at high energies in non-Abelian gauge theory due to asymptotic freedom. Asymptotic freedom was shown in [16, 17] assuming the gauge bosons to be massless. To begin with, we consider Yang-Mills Lagrangian density, shown in eqn.(2.3). Taking the Lorenz-gauge condition, we have to add a Lagrangian density for the ghost field to eqn.(2.3), and we get

$$\mathscr{L} = -\frac{1}{4}F^{\mu\nu} \cdot F_{\mu\nu} - \frac{1}{2\xi}\left(\partial_\mu A^\mu\right)^2 + \partial^\mu \bar{\omega} \cdot D_\mu \omega, \tag{3.1}$$

where ω and $\bar{\omega}$ are the ghost fields and D_μ is the covariant derivative. The propagator of the ghost field is

$$iD^{ab}_{\bar{\omega}\omega}(k) = \frac{i}{k^2}\delta^{ab}, \tag{3.2}$$

which is shown diagrammatically by a solid line, as in Fig. 3.1.

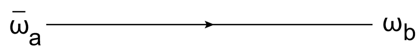

Figure 3.1 Ghost propagator is represented by unbroken line.

Using the self couplings among gauge field and the three point coupling among gauge field and the ghost fields, we can calculate the one-loop correction to the two-point function of the gauge field. The one-loop diagrams are shown in Fig. 3.2. The behaviour of the gauge coupling constant g with the energy scale μ can be expressed by the "beta function", which is defined as

$$\beta = \frac{\partial g}{\partial \ln \mu}. \tag{3.3}$$

In the case of $SU(N)$ Yang-Mills theory, with the Lagrangian density given in the

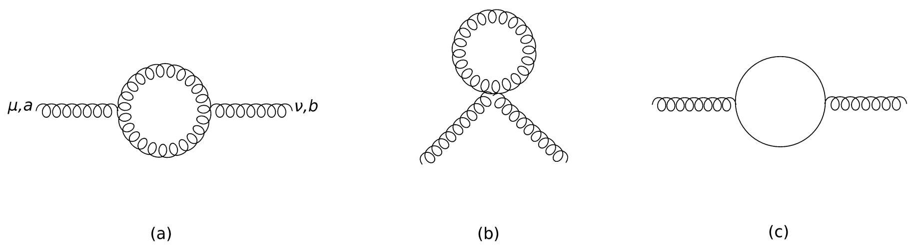

Figure 3.2 One loop diagrams, contributed from (a) 3-point couplings among gauge fields; (b)quartic couplings among gauge field; (c) 3-point interaction among gauge and ghost fields.

eqn.(3.1), it is known [16, 17] that

$$\beta_{YM} = -\frac{g^3 N}{16\pi^2}\frac{11}{3}. \tag{3.4}$$

If we consider the inclusion of matter fields (fermions and scalar) in the Lagrangian density then the one-loop β function becomes

$$\beta(\alpha) = -\left(\frac{11}{3}N - \frac{2}{3}N_f - \frac{1}{6}N_s\right)\alpha^2. \tag{3.5}$$

Here $\alpha = \frac{g^2}{4\pi}$, N_f and N_s are the number of flavours of fermion and scalar fields respectively interacting with the gauge fields. We can see from the above eqn.(3.5) that the β function has positive terms due to the presence of the matter fields in the theory. The β function for Curci-Ferrari model was calculated by Boer et al at one loop order [109] where the Yang-Mills field where the Yang-Mills gauge bosons are Proca massive. The β function becomes the same as the β function of massless Yang-Mills theory i.e.

$$\beta(\alpha) = -\frac{11N}{3}\frac{\alpha^2}{2\pi}. \tag{3.6}$$

We are now treating a topologically massive model, where various non-linear couplings among gauge and two-forms fields are present, we are curious to see how the β function is modified in the model. We have taken the Lagrangian density

$$\begin{aligned} \mathscr{L}' &= -\frac{1}{4}F^a_{\mu\nu}F^{\mu\nu}_a + \frac{1}{12}H^{\mu\nu\lambda}_a H^a_{\mu\nu\lambda} + \frac{m}{4}\epsilon^{\mu\nu\alpha\beta}F^a_{\mu\nu}B^a_{\alpha\beta} \\ &\quad +\partial_\mu\bar{\omega}_a\partial^\mu\omega^a - gf_{bca}A^b_\mu\partial^\mu\bar{\omega}^a\omega_c - \frac{1}{2\xi}(\partial_\mu A^\mu_a)^2 + \frac{1}{2\eta}\left\{(D_\mu B^{\mu\nu})^a\right\}^2, \end{aligned} \tag{3.7}$$

where $B^{\mu\nu}$ field is now treated like a matter field. In particular, we do not consider the vector gauge symmetry of $B^{\mu\nu}$ field. Hence the vector ghost and ghosts of the vector ghosts fields do not take part in our calculation. Here $H^a_{\mu\nu\lambda} = \left(D_{[\mu}B_{\nu\lambda]}\right)^a$. The term $\frac{1}{2\eta}\left\{(D_\mu B^{\mu\nu})^a\right\}^2$ is added to get the propagator of B field, where η is an arbitrary parameter. We will take $\xi = 1$ and $\eta = 1$ as in Feynman-'t Hooft gauge for our calculation. The two form field is often compared to a scalar, so it necessary to check how the interactions between gauge field A and the two form field B contribute in the behaviour of the gauge coupling constant with the energy scale. With this purpose, we are going to calculate the one loop correction of the gauge boson propagator. The loop diagrams are constructed from various couplings in this model. The propagators of A and B fields as shown in eqn.(1.153) and eqn.(1.154), are

$$iD^{ab}_{\mu\nu} = -i\left[\frac{g_{\mu\nu} - (1-\xi)\frac{k_\mu k_\nu}{k^2}}{(k^2-m^2)} - \xi m^2 \frac{k_\mu k_\nu}{k^4(k^2-m^2)}\right]\delta^{ab}, \tag{3.8}$$

$$iD^{ab}_{\mu\nu,\rho\lambda} = \left[\frac{g_{\mu[\rho}g_{\lambda]\nu} + (1-\eta)\frac{k_{[\mu}k_{[\lambda}g_{\rho]\nu]}}{k^2}}{k^2-m^2} + \eta m^2 \frac{k_{[\mu}k_{[\lambda}g_{\rho]\nu]}}{k^4(k^2-m^2)}\right]\delta^{ab}. \tag{3.9}$$

The square of the covariant derivative of the B field contains the terms $g\partial_\alpha B^{\alpha\nu}A_\mu B^{\mu\nu}$, which contain the partial derivative of B field. On the other hand we can also have the derivative coupling ABB from the $H^{\mu\nu\lambda}H_{\mu\nu\lambda}$ as we found in the previous chapter. Hence the ABB vertex rule for the ABB coupling shown in Fig. 3.3a becomes

$$iV^{abc}_{\mu,\lambda\rho,\sigma\tau} = gf^{abc}\left[(p-q)_\mu g_{\lambda[\sigma}g_{\tau]\rho} + (p+q/\eta)_{[\sigma}\, g_{\tau][\lambda}g_{\rho]\mu} - (q+p/\eta)_{[\lambda}\, g_{\rho][\sigma}g_{\tau]\mu}\right]. \tag{3.10}$$

The term $\frac{1}{2\eta}\left\{(D_\mu B^{\mu\nu})^a\right\}^2$ in the Lagrangian density also has the coupling $AABB$. So taking the contribution from the $H^{\mu\nu\lambda}H_{\mu\nu\lambda}$ and $\frac{1}{2\eta}\left\{(D_\mu B^{\mu\nu})^a\right\}^2$, we get the vertex

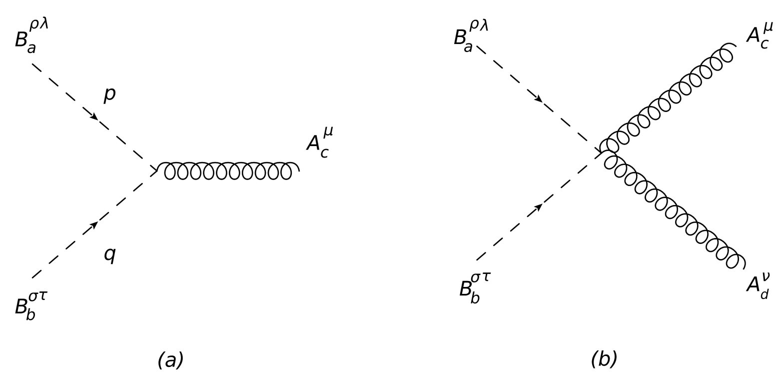

Figure 3.3 ABB and AABB vertices;

rule

$$\begin{aligned} iV^{abcd}_{\mu,\nu,\lambda\rho,\sigma\tau} = \; & ig^2 \; \Bigg[f_{ace}f_{bde}\left(g_{\mu\nu}g_{\lambda[\sigma}g_{\tau]\rho} + g_{\mu[\sigma}g_{\tau]g[\lambda}g_{\rho]\nu} - \frac{1}{\eta}g_{\mu[\lambda}g_{\rho][\sigma}g_{\tau]\nu}\right) \\ & + \; f_{ade}f_{bce}\left(g_{\mu\nu}g_{\lambda[\sigma}g_{\tau]\rho} + g_{\mu[\lambda}g_{\rho]g[\sigma}g_{\tau]\nu} - \frac{1}{\eta}g_{\mu[\sigma}g_{\tau]g[\lambda}g_{\rho]\nu}\right)\Bigg]. \end{aligned} \tag{3.11}$$

This vertex is shown in Fig. 3.3b. We will use the vertex rules in eqn.(3.10) and eqn.(3.11) in the one-loop calculations. We will calculate the β function of the gauge coupling constant at one loop order. The dimensional regularization procedure is used to work out the loop integration in $(4-\epsilon)$ dimensions, where ϵ is an infinitesimal number. In $(4-\epsilon)$ dimension, the gauge coupling constant has mass dimension $\frac{\epsilon}{2}$ and can be written as $\mu^{\frac{\epsilon}{2}}g$, where μ has the dimension of mass or energy. We define the bare Lagrangian density at one-loop order as

$$\begin{aligned}\mathscr{L}_{\mathscr{B}} = & - Z_3\frac{1}{4}F_a^{\mu\nu}F_{\mu\nu}^a + Z_1\frac{1}{12}H_a^{\mu\nu\lambda}H_{\mu\nu\lambda}^a + Z_m\frac{m}{4}\epsilon^{\mu\nu\rho\lambda}F_{\mu\nu}^aB_{\rho\lambda}^a \\ & + Z_2'\partial_\mu\bar{\omega}_a\partial^\mu\omega^a - Z_1'gf_{bca}A_\mu^b\partial^\mu\bar{\omega}^a\omega_c - Z_3\frac{1}{2\xi}(\partial_\mu A_a^\mu)^2 \\ & - Z_1\frac{1}{2\eta}\left\{(D_\mu B^{\mu\nu})^a\right\}^2, \end{aligned} \tag{3.12}$$

where the Z's are the factors which appear due to one-loop corrections of the kinetic terms of the fields, and of various couplings, and the subscript '$\mathscr{B}$' designates the bare Lagrangian density. It contains divergent contributions from the loop calculations. The bare fields, mass, and gauge coupling constants are related to renormalized fields, mass, and gauge coupling constants as

$$A_{\mathscr{B}} = Z_3^{\frac{1}{2}}A \tag{3.13}$$

$$B_{\mathscr{B}} = Z_1^{\frac{1}{2}}B \tag{3.14}$$

$$\omega_{\mathscr{B}} = Z_{2'}^{\frac{1}{2}}\omega \tag{3.15}$$

$$m_{\mathscr{B}} = \frac{Z_m}{Z_3^{\frac{1}{2}}Z_1^{\frac{1}{2}}}m \tag{3.16}$$

$$g_{\mathscr{B}} = \mu^{\frac{\epsilon}{2}}\frac{Z_1'}{Z_3^{\frac{1}{2}}Z_2'}g \tag{3.17}$$

where the subscript '$\mathscr{B}$' indicates that the fields and coupling constants in the left hand side of above equations are bare fields and the bare constants respectively. To find Z_3, our next task will be to get the exact propagator of the gauge field taking the infinite insertion of the sum of one loop contributions to the gluon propagator. The sum of one loop contribution is designated as $i\Pi^{\alpha\beta}$. This sum is diagrammatically shown in Fig. 3.4 where the solid black blob represents $i\Pi^{\alpha\beta}$. The complete gluon propagator including one loop correction can be written as

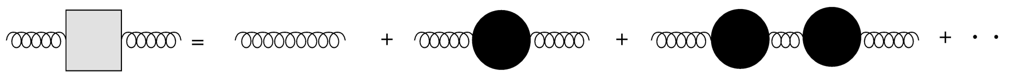

Figure 3.4 Exact propagator at one loop.

$$\tilde{\Delta}_{\mu\nu} = iD_{\mu\nu} + iD_{\mu\alpha} i\Pi^{\alpha\beta} iD_{\beta\nu} + iD_{\mu\alpha} i\Pi^{\alpha\beta} iD_{\beta\gamma} i\Pi^{\gamma\delta} iD_{\delta\nu} + \dots \tag{3.18}$$

We will see that $\Pi^{\alpha\beta}$ will take the form $\{\pi_1(p^2, m^2)(g^{\alpha\beta}p^2 - p^\alpha p^\beta) + \pi_2(p^2, m^2)m^2 g^{\alpha\beta}\}$. The result of the infinite sum is

$$i\tilde{\Delta}_{\mu\nu} = -i\left[\frac{g_{\mu\nu} - \frac{k_\mu k_\nu}{k^2}}{(1-\pi_1)k^2 - m^2(1+\pi_2)} + \xi \frac{k_\mu k_\nu}{k^2}\left(\frac{1}{k^2 - \xi\pi_2 m^2}\right)\right]. \tag{3.19}$$

Including the counterterms, the first term of $i\tilde{\Delta}_{\mu\nu}$ is modified as

$$iD'^{\mathscr{B}}_{\mu\nu} = -i\left[\frac{g_{\mu\nu} - \frac{k_\mu k_\nu}{k^2}}{k^2 - \{(Z_m - 1) + 1\}^2 m^2 - (\pi_1 k^2 + \pi_2 m^2) + (Z_3 - 1)k^2}\right]. \tag{3.20}$$

The coefficient of k^2 in the denominator of $iD'^{\mathscr{B}}_{\mu\nu}$ becomes $(Z_3 - \pi_1)\,k^2$. On the other hand, we can find from the bare Lagrangian density in eqn.(3.12) that the transverse part of bare propagator of the A field as

$$iD'^{\mathscr{B}}_{\mu\nu} = -\frac{ig_{\mu\nu}}{k^2 - m^2_{\mathscr{B}}}. \tag{3.21}$$

Comparing eqn.(3.20) and eqn.(3.21), we get,

$$Z_3 = 1 + \pi_1. \tag{3.22}$$

We will find Z'_1 and Z'_2 from the one loop correction of the coupling $A\bar{\omega}\omega$ and ghost propagator respectively and find $g_{\mathscr{B}}$ according to eqn.(3.17). The generic form of Z

factor at one-loop order is

$$Z = 1 + \frac{f(g(\mu))}{\epsilon} \tag{3.23}$$

where $f(g(\mu))$ is the function of $g(\mu)$. Using this form of Z, we can express $g_{\mathscr{B}}$ at one-loop order in eqn.(3.17) with the subtraction point μ as

$$\ln g_{\mathscr{B}} \;=\; \left(\frac{\epsilon}{2}\ln\mu + \sum_{n=1}^{\infty}\frac{G_n(g(\mu))}{\epsilon^n} + \ln g(\mu)\right) \tag{3.24}$$

where $G_n(g(\mu))$ are the functions of $g(\mu)$. The summation over n in the right hand side of the eqn.(3.24) appears due to Taylor expansion of terms like $\ln(1+x)$. $G_n(g(\mu))$'s are the function of g whereas $G(g(\mu), \epsilon)$ designates the sum. Since $g_{\mathscr{B}}$ does not depend on μ, we have

$$\mu\frac{\partial \ln g_{\mathscr{B}}}{\partial\mu} = 0 = \left(\frac{\epsilon}{2} + \frac{\partial g}{\partial\ln\mu}\sum_{n=1}^{\infty}\frac{1}{\epsilon^n}\frac{\partial G_n(g(\mu))}{\partial g} + \frac{1}{g(\mu)}\frac{\partial g}{\partial\ln\mu}\right), \tag{3.25}$$

which yields

$$g(\mu)\frac{\epsilon}{2} + \frac{\partial g(\mu)}{\partial\ln\mu}\left(1 + g(\mu)\sum_{n=1}^{\infty}\frac{1}{\epsilon^n}\frac{\partial G_n(g)}{\partial g}\right) = 0. \tag{3.26}$$

Since $\dfrac{\partial g(\mu)}{\partial\ln\mu}$ is the rate of change of g with respect to $\ln\mu$, this quantity is a physical quantity and it should be finite in the limit $\epsilon\to 0$ [107, 108]. With this demand, we should write in a renormalizable theory

$$\frac{\partial g}{\partial\ln\mu} = -\frac{\epsilon}{2}g(\mu) + \beta(g). \tag{3.27}$$

Equating the coefficients of ϵ to be zero, the first term $-\frac{\epsilon}{2}g(\mu)$ is fixed by matching the $\mathscr{O}(\epsilon)$ term in eqn.(3.26). Using eqn.(3.27), we get from eqn.(3.26)

$$\beta(g) + \left(-\frac{\epsilon}{2}g(\mu) + \beta(g)\right)\left[g(\mu)\left(\frac{1}{\epsilon}\frac{\partial G_1}{\partial g} + \frac{1}{\epsilon^2}\frac{\partial G_2}{\partial g} + \cdots\right)\right] = 0. \tag{3.28}$$

Now equating the coefficient of ϵ^0 in eqn.(3.28) to be zero, the second term, $\beta(g)$ is determined. Hence we get

$$\beta(g(\mu)) = \frac{g^2(\mu)}{2}\frac{\partial G_1(g(\mu))}{\partial g(\mu)}. \tag{3.29}$$

The coefficients of $\frac{1}{\epsilon^n}$ must be zero which determines all the other $G_n(\mu)$ in terms of $G_1(g(\mu))$. For example cancellation of coefficient of $\frac{1}{\epsilon}$ provides

$$g(\mu)\left(\frac{\partial G_1(g(\mu))}{\partial g}\right)^2 = \frac{\partial G_2(g(\mu))}{\partial g}. \tag{3.30}$$

where we have used eqn.(3.29). We will use eqn.(3.29) for the calculation of $\beta(g)$ function here. $G_1(g(\mu))$ is calculated from the one loop calculation which we will see. For the calculation of one-loop β function, it is sufficient to consider the coefficient of $\frac{2}{\epsilon}$ after the loop integration. We consider first the diagrams shown in Fig. 3.2 from which we will get the contribution for Z_3. The loop calculation corresponding to the diagrams in Fig. 3.2 shows that the pole of the propagator of gauge field modifies the result and the sum of the divergent part of one loop amplitude. The coefficient of $\frac{2}{\epsilon}$ for the diagram in Fig. 3.2a becomes

$$\Pi^{3.2a}_{ab,\mu\nu,\epsilon} = -\frac{1}{2}\ \frac{N\delta^{ab}g^2}{16\pi^2}\left[\frac{-19g_{\mu\nu}p^2 + 22p_\mu p_\nu}{6} - 9m^2 g_{\mu\nu}\right], \tag{3.31}$$

where the $\frac{1}{2}$ is taken in order to compensate for identical propagators of gauge bosons in the loop. Here the subscript 'ϵ' of $\Pi_{ab,\mu\nu,\epsilon}$ designates that the right hand side of the equation is the coefficient of $\frac{2}{\epsilon}$. The coefficient of $\frac{2}{\epsilon}$ from the diagrams, shown in Fig. 3.2b and Fig. 3.2c are respectively

$$\Pi^{3.2b}_{ab,\mu\nu,\epsilon} = -\frac{1}{2}\ \frac{N\delta^{ab}g^2}{16\pi^2}\ 6m^2 g_{\mu\nu}, \qquad \Pi^{3.2c}_{ab,\mu\nu,\epsilon} = -\frac{N\delta^{ab}g^2}{16\pi^2}\frac{(-g_{\mu\nu}p^2 - 2p_\mu p_\nu)}{12}. \tag{3.32}$$

Adding the contributions in eqn.(3.31) and eqn.(3.32) we have

$$\Pi^{3.2}_{ab,\mu\nu,\epsilon} = \Pi^{3.2a}_{ab,\mu\nu,\epsilon} + \Pi^{3.2b}_{ab,\mu\nu,\epsilon} + \Pi^{3.2c}_{ab,\mu\nu,\epsilon} = \frac{N\delta^{ab}g^2}{16\pi^2}\left[\frac{5}{3}(p^2 g_{\mu\nu} - p_\mu p_\nu) + \frac{3}{2}m^2 g_{\mu\nu}\right]. \tag{3.33}$$

Now we consider the contributions from the diagrams constructed on the basis of various two, three and four point couplings between the A and B fields. Using the three point couplings AAB and ABB we have constructed the loop diagrams

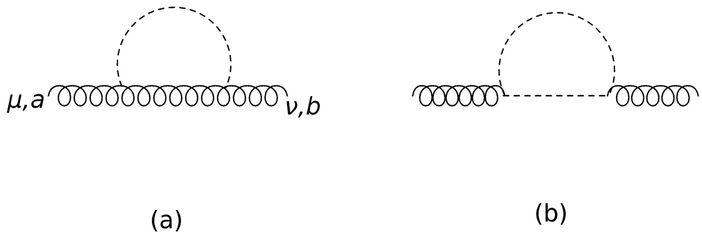

Figure 3.5 Loop formed by AAB and ABB couplings;

shown in Fig. 3.5. The three point coupling AAB contains m hence the vertex rule corresponding to this coupling in eqn.(2.63) contains m. The loop integration for the diagram shown in Fig. 3.5(a) provides logarithmic divergence[1] and we see from the vertex rule of AAB that the coefficient of this divergence goes as m^2 . But the vertex rule ABB coupling contains momentum as shown in eqn.(3.10). Since the propagator of the B field behaves as p^{-2} in the high energy limit, the total dimension of the divergence term in 4 dimensions is $4 + 2 - 2 - 2 = 2$. As a consequence, by power counting we can see that the divergent part of the loop amplitude for Fig.3.5b contains two powers of the external momentum[2] p and mass m^2. We find the appearance of $(p^2 g^{\mu\nu} - p^\mu p^\nu)$ in the divergent part from the calculation. The divergent parts corresponding to the two diagrams in Fig. 3.5 is

$$\Pi^{3.5a}_{ab,\mu\nu,\epsilon} = \frac{N\delta^{ab}g^2}{16\pi^2}3m^2 g_{\mu\nu}, \tag{3.34}$$

$$\Pi^{3.5b}_{ab,\mu\nu,\epsilon} = \frac{N\delta^{ab}g^2}{16\pi^2}\left[(p^2 g_{\mu\nu} - p_\mu p_\nu) + 3m^2 g_{\mu\nu}\right]. \tag{3.35}$$

Adding eqn.(3.34) and eqn.(3.35), we get

$$\Pi^{3.5}_{ab,\mu\nu,\epsilon} = \Pi^{3.5a}_{ab,\mu\nu,\epsilon} + \Pi^{3.5b}_{ab,\mu\nu,\epsilon} = \frac{N\delta^{ab}g^2}{16\pi^2}\left[(p^2 g_{\mu\nu} - p_\mu p_\nu) + 6m^2 g_{\mu\nu}\right]. \tag{3.36}$$

The divergent parts of loop integration corresponding to the diagrams in Fig. 3.6

[1]See the calculation in appendix C

[2]See the calculation in appendix C

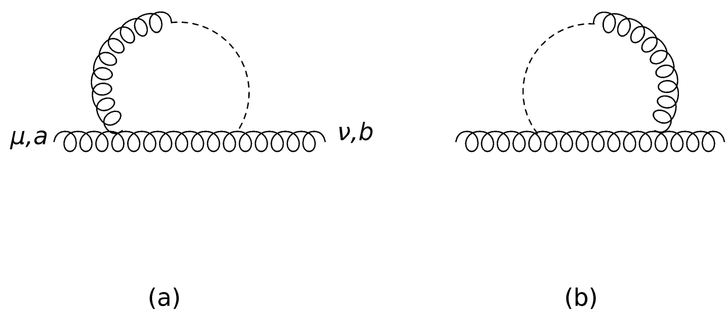

Figure 3.6 Loop formed by AAA, AB and AAB couplings;

contain m^2 appearing only from the vertex rules of the two-point AB coupling and the trilinear AAB coupling. We find from our calculation that the sum of the coefficients of $\frac{2}{\epsilon}$ corresponding to these diagrams is

$$\Pi^{3.6}_{ab,\mu\nu,\epsilon} = 2\Pi^{3.6a}_{ab,\mu\nu,\epsilon} = -\frac{N\delta^{ab}g^2}{16\pi^2}\;\frac{9}{4}m^2 g_{\mu\nu}. \tag{3.37}$$

For similar reasons as given above, we obtain the sum of the coefficients of $\frac{2}{\epsilon}$ corresponding to the diagrams in Fig. 3.7 which is

$$\Pi^{3.7}_{ab,\mu\nu,\epsilon} = \frac{N\delta^{ab}g^2}{16\pi^2}\frac{3}{2}m^2 g_{\mu\nu}. \tag{3.38}$$

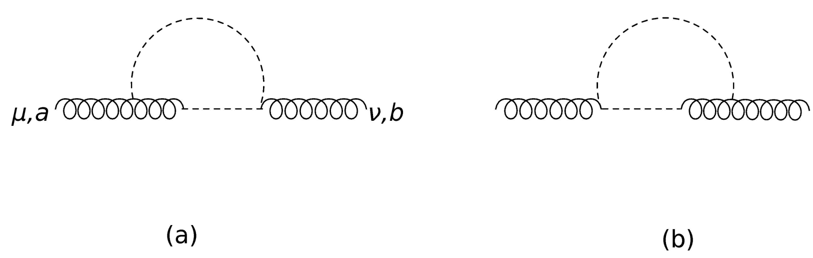

Figure 3.7 Loops formed by AAB, AB and AAB couplings;

Using the AAA, AB and ABB couplings we get the diagrams shown in Fig. 3.8.

The sum of the divergent parts corresponding to them is

$$\Pi^{3.8}_{ab,\mu\nu,\epsilon} = -\frac{N\delta^{ab}g^2}{16\pi^2}\ \frac{3m^2}{2} g_{\mu\nu} \tag{3.39}$$

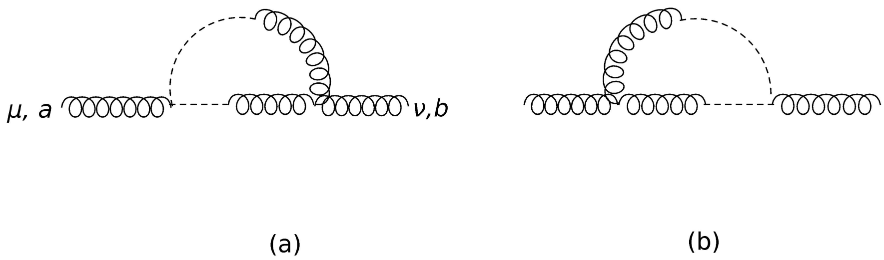

Figure 3.8 Loop formed by AAA, AB, and AAB couplings;

We are now left with only two diagrams which are shown in Fig. 3.9. The four point coupling $AABB$ is used to form it. The diagram in Fig. 3.9b is finite and does not contribute to the coefficients of $\frac{2}{\epsilon}$ in the loop amplitude. The loop calculation for Fig. 3.9a is quite similar to that for Fig. 3.2b because the vertex rule of $AAAA$ in eqn.(2.5) and vertex rule of $AABB$ in eqn.(3.11) do not contain momenta of fields. So the divergent part corresponding to the Fig. 3.9 contains an m^2 due to the pole of the gauge and tensor field propagators, that is

$$\Pi^{3.9a}_{ab,\mu\nu,\epsilon} = \Pi^{3.9}_{ab,\mu\nu,\epsilon} = -\ \frac{N\delta^{ab}g^2}{16\pi^2}\ 9m^2 g_{\mu\nu}. \tag{3.40}$$

There are no more loop diagrams left to calculate. If we sum up the divergent terms corresponding to the diagrams shown in Fig. 3.2 and Fig. 3.5- 3.9, then we have

$$\Pi_{ab,\mu\nu} = \Pi^{3.2}_{ab,\mu\nu,\epsilon} + \sum_{n=3.5}^{3.9} \Pi^{n}_{ab,\mu\nu,\epsilon} = \frac{N\delta^{ab}g^2}{16\pi^2}\left[\frac{8}{3}(p^2 g_{\mu\nu} - p_\mu p_\nu) - \frac{45}{4} m^2 g_{\mu\nu}\right]. \tag{3.41}$$

According to the eqn.(3.22), we can say from the eqn.(3.41) that

$$Z_3 = 1 + \frac{8}{3}\ \frac{Ng^2}{16\pi^2}\frac{2}{\epsilon}. \tag{3.42}$$

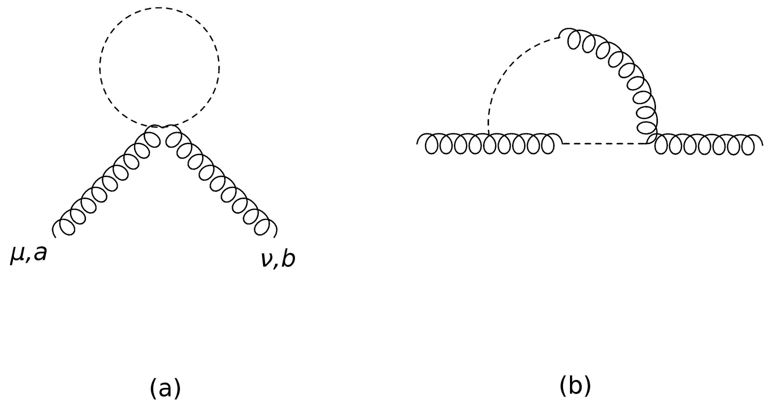

Figure 3.9 (a) Loop formed by $AABB$ couplings; (b) Loop formed by AAB, AB, and AAB couplings

We are now going to consider Z_1' and Z_2' so that we can find the β function from eqn.(3.17). These are obtained from one-loop corrections of the ghost propagator and the trilinear coupling $A\bar{\omega}\omega$.

Diagrams corresponding to the one loop corrections to the propagator and the trilinear coupling are shown in Fig. 3.10.

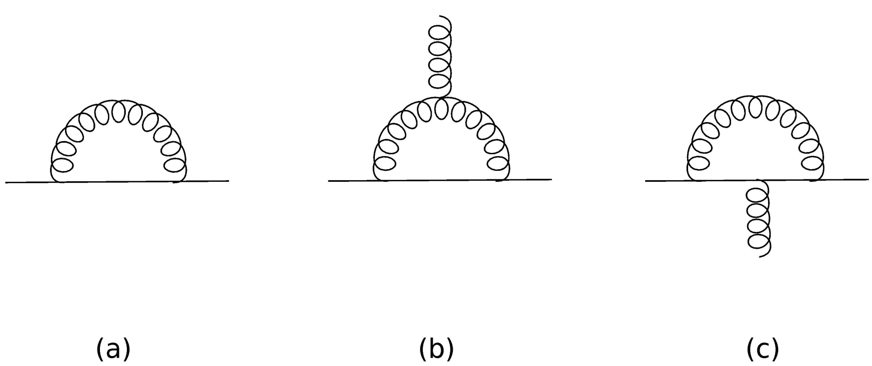

Figure 3.10 One loop contributions to the ghost's self energy and three point couplings among A, $\bar{\omega}$ and ω.

The loop diagrams contain the coupling $A\bar{\omega}\omega$ whose vertex rule is given as

$$iV^{\mu}_{abc} = gf_{abc}p^{\mu}. \tag{3.43}$$

where p^{μ} is the incoming momentum carried by $\bar{\omega}$. This is shown in the Fig. 3.11. Due to the massive gauge fields, we have seen how the divergent term in eqn.(3.33)

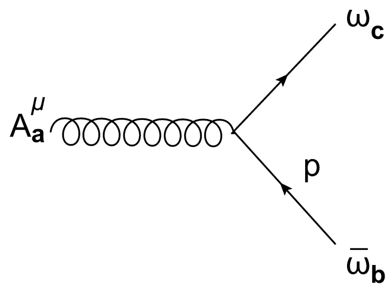

Figure 3.11 Three point vertex of A, ω and $\bar{\omega}$

contains a part having m^2. It becomes necessary to check if the divergent terms fom the loop calculation corresponding to the diagrams shown in Fig. 3.10 contain m^2. We have found[3] that there should not be any term containing m^2 in the coefficient of $\frac{2}{\epsilon}$ and the coefficient becomes the same as found in massless Yang-Mills theory in Feynman 't-Hooft gauge [106]

$$Z'_1 = 1 - \frac{Ng^2}{16\pi^2\epsilon}, \tag{3.44}$$

$$Z'_2 = 1 + \frac{Ng^2}{16\pi^2\epsilon}. \tag{3.45}$$

Using Z_3, Z'_1 and Z'_2 from eqn.(3.42), eqn.(3.44) and eqn.(3.45) in eqn.(3.17), we get

$$g_{\mathscr{B}} = \mu^{\frac{\epsilon}{2}} \frac{\left(1 - \frac{Ng^2}{16\pi^2\epsilon}\right)}{\left(1 + \frac{Ng^2}{16\pi^2}\frac{8}{3}\frac{2}{\epsilon}\right)\left(1 + \frac{Ng^2}{16\pi^2\epsilon}\right)} g(\mu). \tag{3.46}$$

Comparing eqn.(3.46) with eqn.(3.24), we can see

$$G_1 = -\frac{Ng^2}{16\pi^2}\frac{14}{3}. \tag{3.47}$$

[3]See the argument given in appendix C.

Therefore we get,

$$\beta(g) = -\frac{Ng^3}{16\pi^2}\frac{14}{3}. \tag{3.48}$$

Multiplying both side by g in eqn.(3.48), we get

$$\beta(\alpha) = -\frac{14}{3}N\frac{\alpha^2}{2\pi}, \tag{3.49}$$

where $\alpha = \dfrac{g^2}{4\pi}$. Here it can be seen clearly that this topologically massive theory is still asymptotically free though the gauge bosons are now topologically massive. If we compare the behaviour of the gauge coupling constant as a function of the momentum scale for massless and this massive gauge theory, we see that the α decreases more rapidly than in the massless and Proca massive cases. Behaviour of α in both theories is shown in Fig. 3.12.

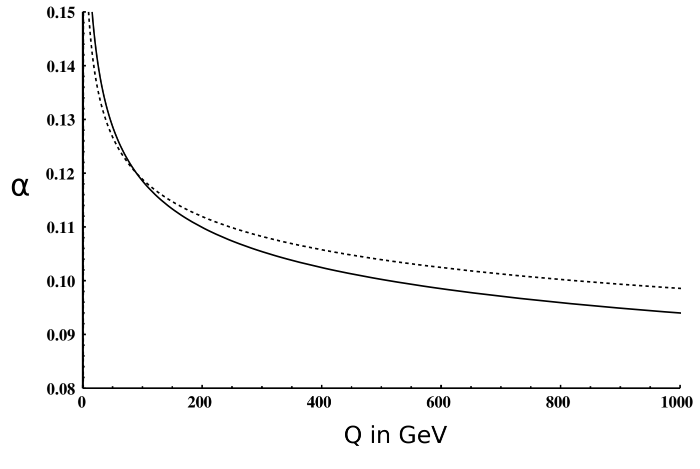

Figure 3.12 The flow of α_s for ordinary (dotted) and topologically massive (solid) SU(3) gauge theory.

Appendices

Appendix C

Loop Calculation

The generic expression of the integration required for calculation of loop-diagram is

$$\begin{aligned} I_s^r(a,D) &= \int \frac{d^D k}{(2\pi)^D} \frac{(k^2)^r}{(k^2-a^2)^s} \\ &= i\frac{(-1)^{r+s}}{(4\pi)^{D/2}} \frac{1}{(a^2)^{s-r-\frac{D}{2}}} \frac{\Gamma(r+\frac{N}{2})\Gamma(s-r-\frac{D}{2})}{\Gamma(\frac{D}{2})\Gamma(s)}. \end{aligned} \tag{C.1}$$

It follows from eqn.(C.1) that

$$\begin{aligned} I_{r+2}^r(a,D) &= i\frac{1}{(4\pi)^{D/2}} \frac{1}{(a^2)^{2-\frac{D}{2}}} \Gamma\left(2-\frac{D}{2}\right) \frac{\left(r+\frac{D}{2}-1\right)\left(r+\frac{D}{2}-2\right)\ldots\frac{D}{2}}{(r+1)!} \\ &= \frac{\left(r+\frac{D}{2}-1\right)\left(r+\frac{D}{2}-2\right)\ldots\frac{D}{2}}{(r+1)!}\ I_2^0(a,D), \end{aligned} \tag{C.2}$$

where

$$I_2^0(a,D) = \frac{i}{(4\pi)^{\left(2-\frac{\epsilon}{2}\right)}} (a^2)^{-\frac{\epsilon}{2}} \Gamma\left(\frac{\epsilon}{2}\right). \tag{C.3}$$

We put $D = 4-\epsilon$ in eqn.(C.3). Putting $D = 4$ in the coefficient of I_2^0 in eqn.(C.2) and using eqn.(C.3) we get

$$I_{r+2}^r = I_2^0. \tag{C.4}$$

For the infinitesimal value of the ϵ, it is given

$$\Gamma(-n+\epsilon) = (-1)^n \left[\frac{1}{\epsilon} - \gamma(n) + \mathcal{O}(\epsilon)\right], \tag{C.5}$$

where $\gamma(n)$ is known as Euler-Mascheroni constant and the last term in the expansion of the Γ contains non-zero positive power of ϵ. So in the limit $\epsilon \to 0$, the last term becomes insignificant. We know

$$\lim_{\epsilon \to 0} x^\epsilon = 1 + \epsilon \ln x + \dots \tag{C.6}$$

Using eqn.(C.3) and eqn.(C.6), we get the leading term in the limit $\epsilon \to 0$,

$$\mu^{\frac{\epsilon}{2}} I_2^0 = i\frac{1}{(4\pi)^2}\left[\frac{2}{\epsilon} - \gamma + \ln 4\pi + f(a^2,\mu)\right], \tag{C.7}$$

where $f(a^2,\mu)$ is a function of a^2 and μ. Now we define ζ_ϵ as

$$\zeta_\epsilon = \frac{2}{\epsilon} - \gamma + \ln 4\pi. \tag{C.8}$$

So, we can conclude from that eqn.(C.1), that I_3^1, I_4^2 provide the same coefficient of $\frac{2}{\epsilon}$ when we put $D = 4$ in all factors other than ζ_ϵ. This result is very useful for calculations. In order to find the beta function of coupling constant it will be sufficient to find the coefficient of $\frac{2}{\epsilon}$ from loop calculation.

C.1 One loop amplitude of Fig. 3.5a and Fig. 3.5b.

We will show here how the m^2 term appears as the coefficient of $\frac{1}{\epsilon}$ in loop calculation from the diagram shown in Fig. 3.5b and in Fig. C.1. We have taken the propagator of $B_a^{\mu\nu}$ field as

$$iD_{\mu\nu,\rho\lambda}(k) \;=\; i\left[\frac{g_{\mu[\rho}g_{\lambda]\nu} + (1-\eta)\frac{k_{[\mu}k_{[\lambda}g_{\rho]\nu]}}{k^2}}{k^2-m^2} - \eta m^2 \frac{k_{[\mu}k_{[\lambda}g_{\rho]\nu]}}{k^4(k^2-m^2)}\right]. \tag{C.9}$$

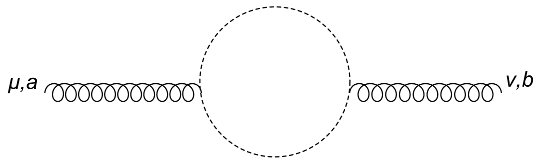

Figure C.1 One loop diagrams using ABB vertex

For the simplicity in calculation , we have chosen $\eta = 1$. The propagator becomes

$$iD_{\mu\nu,\rho\lambda}(k) = i\left[\frac{g_{\mu[\rho}g_{\lambda]\nu}}{k^2 - m^2} - m^2\frac{k_{[\mu}k_{[\lambda}g_{\rho]\nu]}}{k^4(k^2 - m^2)}\right]. \tag{C.10}$$

So the one-loop calculation for the diagram in Fig. C.1 in $D = 4 - \epsilon$ space-time is

$$\Pi^{ab}_{\mu\nu} = \int \frac{d^D k}{(2\pi)^D}\ \pi^{ab}_{\mu\nu}, \tag{C.11}$$

where

$$\begin{aligned}\pi^{ab}_{\mu\nu} \ &= \tfrac{1}{16} \quad g f_{nma}\left[(2k-p)_\mu g_{\rho[\alpha}g_{\beta]\sigma} + p_{[\rho}g_{\sigma][\alpha}g_{\beta]\mu} - p_{[\alpha}g_{\beta][\rho}g_{\sigma]\mu}\right] iD^{\rho\sigma,\rho'\sigma'}(p-k)\times \\ &\qquad g f_{bnm}\left[(p-2k)_\nu g_{\rho'[\alpha'}g_{\beta']\sigma'} - p_{[\rho'}g_{\sigma][\alpha'}g_{\beta']\nu} + p_{[\alpha'}g_{\beta'][\rho'}g_{\sigma']\nu}\right] iD^{\alpha\beta,\alpha'\beta'}(k).\end{aligned} \tag{C.12}$$

The factor $\frac{1}{16} = \frac{1}{4}\times\frac{1}{4}$ comes due to the contraction of two antisymmetric pairs of indices present in two propagators of $B_{\mu\nu}$ field. Now we will see how the different parts of the propagator of B contribute in the coefficient $\frac{2}{\epsilon}$ from counting the power of loop momentum k. It helps us to find the relevant parts of the propagator in our calculation. Writing the propagator of $B^{\mu\nu}$ as

$$iD^{\mu\nu,\rho\lambda}(k) = id_1^{\mu\nu,\rho\lambda}(k) + id_2^{\mu\nu,\rho\lambda}(k), \tag{C.13}$$

where

$$id_1^{\mu\nu,\rho\lambda}(k) \ = \ i\frac{g^{\mu[\rho}g^{\lambda]\nu}}{k^2 - m^2}, \tag{C.14}$$

$$id_2^{\mu\nu,\rho\lambda}(k) \ = \ -m^2\frac{k^{[\mu}k^{[\lambda}g^{\rho]\nu]}}{k^4(k^2 - m^2)}, \tag{C.15}$$

we can express

$$\begin{aligned}\pi^{ab}_{\mu\nu} &= \frac{1}{16} g f_{nma}\left[(2k-p)_\mu g_{\rho[\alpha}g_{\beta]\sigma} + p_{[\rho}g_{\sigma][\alpha}g_{\beta]\mu} - p_{[\alpha}g_{\beta][\rho}g_{\sigma]\mu}\right] \\ & i\left(d_1^{\rho\sigma,\rho'\sigma'}(p-k) + d_2^{\rho\sigma,\rho'\sigma'}(p-k)\right)\times \\ & g f_{bnm}\left[(p-2k)_\nu g_{\rho'[\alpha'}g_{\beta']\sigma'} - p_{[\rho'}g_{\sigma][\alpha'}g_{\beta']\nu} + p_{[\alpha'}g_{\beta'][\rho'}g_{\sigma']\nu}\right] \\ & i\left(d_1^{\alpha\beta,\alpha'\beta'}(k) + d_2^{\alpha\beta,\alpha'\beta'}(k)\right). \end{aligned} \tag{C.16}$$

Our aim is to calculate the divergent part of the integration in eqn.(C.11). So we now see what are the relevant contributions to the divergent part of the integration in eqn.(C.16). We can see from eqn.(C.14) and eqn.(C.15) that $id_1^{\mu\nu,\rho\lambda}(k)$ behaves as $\frac{1}{k^2}$ and $id_2^{\mu\nu,\rho\lambda}(k)$ behaves as $\frac{1}{k^4}$ at high energy. So we can easily see the parts of the integrand providing the divergent part of the integration are those which contain $d_1(k)d_1(p-k)$, $d_1(k)d_2(p-k)$ and $d_1(p-k)d_2(k)$. We can understand now that $d_1 d_1$ and $d_1(k)d_2(p-k)$ or $d_2(k)d_1(p-k)$ behave like $\frac{1}{k^4}$ and $\frac{1}{k^6}$ respectively. The $k^\mu k^\nu$ term in the loop integration contributes as $k^2\eta^{\mu\nu}$ because of

$$\int \frac{d^Dk}{(2\pi)^D}\frac{k^\mu k^\nu}{[k^2-a^2]^2} = \frac{1}{4}\int \frac{d^Dk}{(2\pi)^D}\frac{\eta^{\mu\nu}k^2}{[k^2-a^2]^2} = \eta^{\mu\nu}\frac{1}{4}I_2^1. \tag{C.17}$$

So in order to calculate the divergence the divergent part from the part of the integrand where $d_1(k)d_1(p-k)$ is present, we have to consider the terms of the numerator containing k^{2-n} where $n = 0, 1, 2$ for four dimensional space-time. Whereas it is sufficient to take the terms from the numerator containing k^2 when the parts with $d_1(k)d_2(p-k)$ or $d_2(k)d_1(p-k)$ are considered. We do not consider the part of the integrand containing $d_2(k)d_2(p-k)$, it behaves as $\frac{1}{k^8}$ at high energy, but the maximum power of k from the numerator is 2+4=6; as a consequence there should not be any divergent part in this case. We have used xAct Mathematica-package to know the result of tensor algebra in eqn.(C.16). We get the numerator in the part of the integrand where $d_1(k)d_1(p-k)$ is present

$$
\begin{aligned}
N^{\mu\nu}_{1ab} &= 2N\delta_{ab}\left[2g_{\mu\nu}p^2 + 6k_\mu(2k-p)_\nu + p_\mu(p-6k)_\nu\right] \\
&= 2N\delta_{ab}\left[(2g_{\mu\nu}p^2 + p_\mu p_\nu) + 12k_\mu k_\nu - 6(k_\mu p_\nu + k_\nu p_\mu)\right], \qquad \text{(C.18)}
\end{aligned}
$$

where we have used $f_{abc}f_{dbc} = N\delta_{db}$ for $SU(N)$ group. We have to calculate the integration

$$
\Pi^{\mu\nu}_1\delta_{ab} = \int \frac{d^Dk}{(2\pi)^D}\,\frac{N^{\mu\nu}_{1ab}}{\left[(p-k)^2-m^2\right](k^2-m^2)}. \qquad \text{(C.19)}
$$

Introducing Feynman parameter ζ, we get

$$
\begin{aligned}
\Pi^{\mu\nu}_1\delta_{ab} &= \int_0^1 d\zeta \frac{d^Dk}{(2\pi)^D}\int_0^1 d\zeta\,\frac{N^{\mu\nu}_{1ab}}{\left[(1-\zeta)(k^2-m^2)+\zeta\left\{(p-k)^2-m^2\right\}\right]^2} \\
&= \int \frac{d^Dk}{(2\pi)^D}\int_0^1 d\zeta\,\frac{N^{\mu\nu}_{1ab}}{\left[(k-\zeta p)^2-a^2\right]^2}, \qquad \text{(C.20)}
\end{aligned}
$$

where

$$
a^2 = m^2 - \zeta(1-\zeta)p^2. \qquad \text{(C.21)}
$$

We find from eqn.(C.18) and eqn.(C.19) that we need to find the divergent part of the integration of type

$$
I^{\mu\nu} = \int \frac{d^Dk}{(2\pi)^D}\int_0^1 d\zeta\frac{k^\mu k^\nu}{\left[(k-\zeta p)^2-a^2\right]^2}. \qquad \text{(C.22)}
$$

Shifting the variable $k \to k-\zeta p$, we rewrite the above integration as

$$
I^{\mu\nu} = \int \frac{d^Dk}{(2\pi)^D}\int_0^1 d\zeta\frac{k^\mu k^\nu + \zeta\left(k^\mu p^\nu + k^\nu p^\mu\right) + \zeta^2 p^\mu p^\nu}{\left[k^2-a^2\right]^2}. \qquad \text{(C.23)}
$$

The coefficient of ζ in the integrand of eqn.(C.23) containing k^μ contributes zero after integration because it is odd in k. Hence we are left with

$$
I^{\mu\nu} = \int \frac{d^Dk}{(2\pi)^D}\int_0^1 d\zeta\frac{k^\mu k^\nu + \zeta^2 p^\mu p^\nu}{\left[k^2-a^2\right]^2}. \qquad \text{(C.24)}
$$

Using eqn.(C.17) and integrating eqn.(C.24) over ζ , we get

$$\int \frac{d^D k}{(2\pi)^D} \int_0^1 d\zeta \frac{k^\mu k^\nu + \zeta^2 p^\mu p^\nu}{[k^2 - a^2]^2} = \frac{1}{4} g^{\mu\nu} I_2^1 + \int_0^1 d\zeta \zeta^2 p^\mu p^\nu I_2^0. \tag{C.25}$$

Now using eqn.(C.1), we get

$$I_2^1 = -\frac{1}{(4\pi)^2} (a^2)^{\left(1-\frac{\epsilon}{2}\right)} \frac{D}{2} \Gamma\left(-1 + \frac{\epsilon}{2}\right). \tag{C.26}$$

After integration over ζ, we find the coefficient of $\frac{2}{\epsilon}$ from the integration eqn.(C.25), as

$$C_1^{\mu\nu} = \frac{1}{4} g^{\mu\nu} \left(2m^2 - \frac{p^2}{3}\right) + \frac{1}{3} p^\mu p^\nu. \tag{C.27}$$

We can also find from eqn.(C.18) and eqn.(C.19) that we need to get the divergent part of the integration

$$I_2^{\mu\nu} = -6 \int \frac{d^D k}{(2\pi)^D} \frac{p^\mu k^\nu + p^\nu k^\mu}{[(p-k)^2 - m^2]\,(k^2 - m^2)}. \tag{C.28}$$

We find the coefficient of $\frac{2}{\epsilon}$ from the integration in eqn.(C.28) as

$$C_2^{\mu\nu} = -6 p^\mu p^\nu. \tag{C.29}$$

Finding the contributions to the coefficient of $\frac{2}{\epsilon}$ from the eqn.(C.27), eqn.(C.28) and eqn.(C.29), we get the coefficient of $\frac{2}{\epsilon}$ for the integration in eqn.(C.20) as

$$\Pi_{1,\epsilon}^{\mu\nu} = 2N[(2p^2 g^{\mu\nu} + p^\mu p^\nu) + 12 C_1^{\mu\nu} + C_2^{\mu\nu}], \tag{C.30}$$

$$= 2N[p^2 g^{\mu\nu} - p^\mu p^\nu + 6m^2 g^{\mu\nu}]. \tag{C.31}$$

We can easily observe from the expression of the integrand in eqn.(C.16) that the divergent contribution containing $d_1(k) d_2(p-k)$ has the numerator

$$\begin{aligned} N_{2ab}^{\mu\nu} &= -2g^2 N \delta_{ab} k_\mu k_\nu k_{[\alpha} k^{[\alpha} g_{\beta]}^{\beta]} \\ &= -12 g^2 N \delta_{ab} k_\mu k_\nu k^2. \end{aligned} \tag{C.32}$$

We have now the integration

$$\Pi_2^{\mu\nu}\delta_{ab} = \int \frac{d^D k}{(2\pi)^D}\ \frac{N^{\mu\nu}_{2ab}}{k^4\left[(p-k)^2-m^2\right](k^2-m^2)}, \tag{C.33}$$

which provides the coefficient of $\frac{2}{\epsilon}$

$$\Pi^{\mu\nu}_{2,\epsilon} = -3Ng^{\mu\nu}. \tag{C.34}$$

Same contribution as in eqn.(C.34) is obtained when we consider the part of the integrand containing $d_2(k)d_1(p-k)$:

$$\Pi^{\mu\nu}_{3,\epsilon} = -3Ng^{\mu\nu}. \tag{C.35}$$

So adding up the contributions, we obtain the coefficient of $\frac{2}{\epsilon}$ as

$$\Pi^{ab}_{\mu\nu,\epsilon} = [2(p^2 g^{\mu\nu} - p^\mu p^\nu) + 6m^2 g^{\mu\nu}]\delta^{ab}. \tag{C.36}$$

which is shown in eqn.(3.35) with a factor $\frac{1}{2}$ is taken for the two internal B propagators. Now we consider the diagram shown in Fig. C.2. Unlike the vertex rule for

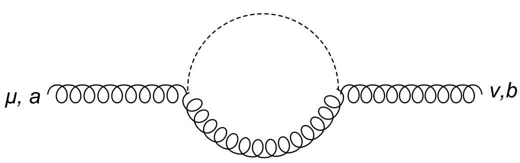

Figure C.2 One loop diagrams using AAB vertex

ABB coupling, AAB vertex rule does not have any momentum but it contains m. So we can easily understand that the required coefficient of $\frac{2}{\epsilon}$ comes from the part containing $d_1(k)d_1(p-k)$. Thus we can write

$$\begin{aligned}
\pi^{ab}_{\mu\nu} &= \frac{1}{4} igm f_{amn}\epsilon_{\mu\sigma\rho\lambda}\ i d_1^{\rho\lambda,\rho'\lambda'}(k)\frac{-ig^{\sigma\sigma'}}{(p-k)^2-m^2} igm f_{mbn}\epsilon_{\sigma'\nu\rho'\lambda'}, && \text{(C.37)}\\
&= \frac{3Ng^2m^2}{(k^2-m^2)\left[(p-k)^2-m^2\right]}\delta^{ab}. && \text{(C.38)}
\end{aligned}$$

So the loop integration becomes I_2^0. Hence here the m^2 term in the coefficient of $\frac{2}{\epsilon}$ appears only due to the vertex rule of AAB coupling. This result is shown in eqn.(3.34).

C.2 One loop corrections in the ghost sector

We are going to see how the divergent part of the loop integration for the one loop correction of ghost propagator and trilinear coupling $A\bar{\omega}\omega$ is independent of m^2 term. First I consider the diagram Fig. C.3a. The loop amplitude in the Feynman 't-Hooft

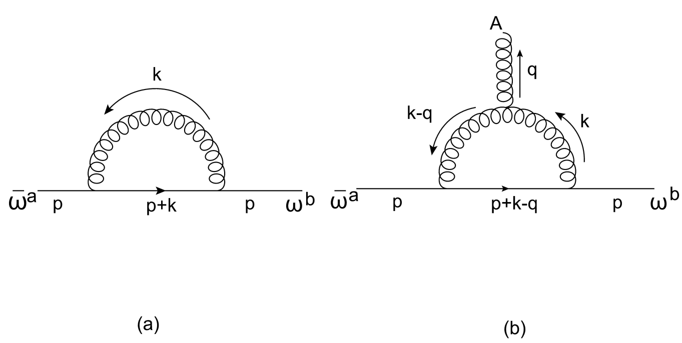

Figure C.3 Diagram for one loop correction of (a) ghost propagator and (b) trilinear coupling $A\bar{\omega}\omega$.

gauge is

$$\pi_{ab} = -ig^2 N\delta_{ab} \int \frac{d^4k}{(2\pi)^4} p_\alpha \left[\frac{g^{\alpha\beta}}{k^2 - m^2} - \frac{m^2 k^\alpha k^\beta}{k^4(k^2 - m^2)} \right] (p+k)_\beta \frac{1}{(p+k)^2}. \quad \text{(C.39)}$$

It is clearly seen from power counting that the part of the integrand containing $k^\alpha k^\beta$ does not provide any divergence. Only the term in the propagator containing $g^{\alpha\beta}$ in the integrand is divergent i.e. the divergence is in

$$\pi^1_{\mu\nu,ab} = ig^2 N\delta_{ab} \int \frac{d^4k}{(2\pi)^4} p_\alpha \left[\frac{g^{\alpha\beta}}{k^2 - m^2} \right] (p+k)_\beta \frac{1}{(p+k)^2}. \quad \text{(C.40)}$$

So the maximum power of k in the numerator is 5. The term containing an odd power of k after introducing Feynman parameters and after the shifting variable provides zero. The next of power of k in the numerator is 4 which is also the power of k in denominator of the integrand. The integral thus I_2^0.

Next we consider the diagram in Fig. C.3b. The loop integration corresponding to it in the Feynman-t'Hooft gauge is

$$\begin{aligned} - & \int \frac{d^4k}{(2\pi)^4} ig^3 f_{aem} f_{cnm} f_{ebn} p_\alpha \left[\frac{g^{\alpha\alpha'}}{(k-q)^2 - m^2} - \frac{m^2 (k-q)^\alpha (k-q)^{\alpha'}}{\{(k-q)^2 - m^2\}(k-q)^4} \right] \\ \times & \left[(q+k)_{\alpha'} g_{\mu\lambda} - (2k-q)_\mu g_{\alpha'\lambda} - (2q-k)_\lambda g_{\alpha'\mu} \right] \frac{1}{(k+p-q)^2} (k+p-q)_{\lambda'} \\ \times & \left[\frac{g^{\lambda\lambda'}}{k^2 - m^2} - \frac{m^2 k^\lambda k^{\lambda'}}{k^4 (k^2 - m^2)} \right]. \end{aligned} \tag{C.41}$$

By counting the power of loop momentum k, we see that the divergent part comes from the integration

$$\begin{aligned} iI^{\mu C.3b}_{abc} = & - \int \frac{d^4k}{(2\pi)^4} ig^3 f_{aem} f_{cnm} f_{ebn} p_\alpha \frac{g^{\alpha\alpha'}}{(k-q)^2 - m^2} \left[k_{\alpha'} g_{\mu\lambda} - 2k_\mu g_{\alpha'\lambda} + k_\lambda g_{\alpha'\mu} \right] \\ & \times \frac{1}{(k+p-q)^2} k_{\lambda'} \frac{g^{\lambda\lambda'}}{k^2 - m^2} \end{aligned} \tag{C.42}$$

$$= \int \frac{d^4k}{(2\pi)^4} ig^3 f_{aem} f_{cnm} f_{ebn} \frac{p_\alpha (k^2 g^{\alpha\mu} - k^\alpha k^\mu)}{[(k-q)^2 - m^2](k^2 - m^2)(k+p-q)^2}. \tag{C.43}$$

Introducing the Feynman parameters ζ_1, ζ_2 and ζ_3, we get the the divergent part of loop integration in $D = 4 - \epsilon$ dimension as

$$\begin{aligned} i\Gamma^\mu_{abcC.3b} &= ig^3 f_{aem} f_{cnm} f_{ebn} \int_0^1 d\zeta_1 \int_0^1 d\zeta_2 \int_0^1 d\zeta_3 \int \frac{d^Dk'}{(2\pi)^D} \delta \left(1 - \sum_{n=1}^3 \zeta_n \right) \frac{p_\alpha (k'^2 g^{\alpha\mu} - k'^\alpha k'^\mu)}{[k'^2 - a^2]^3} \\ &= ig^3 f_{aem} f_{cnm} f_{ebn} \frac{3}{4} \int_0^1 d\zeta_1 \int_0^1 d\zeta_2 \int_0^1 d\zeta_\int \frac{d^Dk'}{(2\pi)^D} \delta \left(1 - \sum_{n=1}^3 \zeta_n \right) \frac{p_\alpha k'^2 g^{\alpha\mu}}{[k'^2 - a^2]^3}, \end{aligned} \tag{C.44}$$

where $k' = k - \zeta_2 q - \zeta_3 (q-p)$ and $a^2 = \zeta_1 m^2 + \{\zeta_2 q - \zeta_3 (q-p)\}^2$. Here we have used eqn.(C.17). The integration over k' is I_3^1 according to eqn.(C.1). It is clearly seen that the coefficient of $\frac{2}{\epsilon}$ does not m^2. Next we consider the diagram shown in Fig. 3.10 and Fig. C.4. The loop integration corresponding to Fig. C.4 is

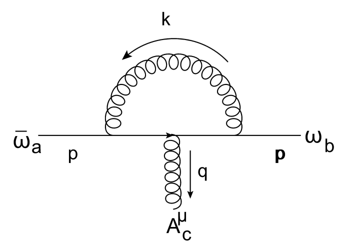

Figure C.4 Diagram for one loop correction of trilinear coupling $A\bar{\omega}\omega$.

$$\begin{aligned} I^{\mu C.4}_{abc} &= - \; i f_{amn} f_{cne} f_{meb} \int \frac{d^4k}{(2\pi)^4} p_\alpha (p+k)^\mu (k+p-q)_{\alpha'} \left[\frac{g^{\alpha\alpha'}}{k^2-m^2} - \frac{m^2 k^\alpha k^{\alpha'}}{k^4(k^2-m^2)} \right] \\ & \quad \times \; \frac{1}{(p+k)^2 (k+p-q)^2}. \end{aligned} \tag{C.45}$$

Introducing the Feynman parameters ζ_1, ζ_2, and ζ_3, we get the divergent part of loop integration in $D = 4 - \epsilon$ dimension as

$$\begin{aligned} i\Gamma^{\mu C.4}_{abc} &= - \; i f_{amn} f_{cne} f_{meb} \int_0^1 d\zeta_1 \int_0^1 d\zeta_2 \int_0^1 d\zeta_3 \int \frac{d^D k'}{(2\pi)^D} \delta \left(1 - \sum_{n=1}^{3} \zeta_n \right) \frac{p_\alpha k'^\mu k'^\alpha}{[k'^2 - a^2]}, \\ &= - \; \frac{1}{4} i f_{amn} f_{cne} f_{meb} \int_0^1 d\zeta_1 \int_0^1 d\zeta_2 \int_0^1 d\zeta_3 \int \frac{d^D k'}{(2\pi)^D} \delta \left(1 - \sum_{n=1}^{3} \zeta_n \right) \frac{p^\mu k'^2}{[k'^2 - a^2]}, \end{aligned} \tag{C.46}$$

where $k' = k + \zeta_2 p + \zeta_3 (p-q)$ and $a^2 = \zeta_1 m^2 + [\zeta_2 p + \zeta_3 (p-q)]^2$. The integration over loop momentum k in eqn.(C.46) is also I^1_3 which does not provide m^2 in the divergent part. As a consequence, Z'_1 and Z'_2 are same as found in the massless Yang-Mills theory [106] which we have used in eqn.(3.44) and eqn.(3.45).

Chapter 4

Conclusions

In this thesis, we have worked on topologically massive models where the Yang-Mills gauge field acquires mass without breaking the global symmetry. We have considered elastic scattering of massive non-Abelian gauge bosons in 3+1 dimensions. Because of the mass gap, cluster decomposition property of S-matrix holds in this model. We have seen in the first chapter how mass-gap also plays the role in the interpretation of confinement of gluons in QCD. The topologically massive model provides the CP conservation which is necessary in QCD.

We wanted to see if in this model provides the unitarity of $2 \to 2$ elastic scatterings among massive bosons at tree level remains unitarity. With the purpose, we considered $SU(2)$ gauge theory for simplicity. It is a well known fact that if we take Proca massive gauge bosons in a pure Yang-Mills model, then unitarity is violated. This cannot cause any problem in the electroweak sector of the Standard model where we consider $WW \to WW$ scattering process. Because the non-linear interactions among gauge and Higgs fields cause the total amplitude behaving as required for unitarity i.e. unitarity is not violated. In the non-Abelian topologically massive model, we have considered various couplings among gauge and Kalb-Ramond fields. We have found that total amplitude of the scattering process $\mathcal{M}$ behaves as $\mathscr{O}(E^0)$ in the leading order, which ensures unitarity. Since the model is renormalizable, the unitarity of the models is guaranteed at every order of quantum correction.

Next we have seen a beautiful characteristic of topologically massive Yang-Mills theory. We know that the asymptotic freedom exists in the pure Yang-Mills theory, which says that the gauge coupling constant decreases with the increase of energy scale. We see this behaviour by calculating the β function. But if we include the interactions among matter and gauge fields, then the rate of decrease becomes slower. Since we considered various interactions among the YM and KR fields, it became interesting to see the behaviour of gauge coupling in the topologically massive model for $SU(N)$ gauge theory. We have observed an interesting behaviour which is different from the pre-existing notion of the contribution of matter field in beta function. The beta function in this model becomes more negative than usual massless Yang-Mills theory.

Bibliography

[1] C. N. Yang, R. L. Mills, Phys. Rev. **96**, 191(1954) 1

[2] S. Weinberg Phys. Rev. Lett. **19** (1967) 1264 1

[3] A. Salam,Weak and Electromagnetic Interactions,in Elementary Particle Physics: Relativistic Groups and Analyticity, edited by N.Svartholm,(Almqvist and Wiksell, Sweden, 1968). 1

[4] S. Glashow, Nucl. Phys. **22**, 579(1961) 1

[5] T. J. Allen, M. J. Bowick, A. Lahiri Mod. Phys. Lett. **A6**, 559(1990) 1

[6] A. Lahiri Phys. Rev. **D55**, 5045(1997). 1, 20, 21, 34, 37

[7] A. Lahiri Phys. Rev. **D63**, 105002(2001). 1, 20, 21, 33, 37

[8] M. Kalb, P. Ramond Phys. Rev. **D9**, 2273(1973). 1, 13, 22

[9] P. W. Higgs, Phys. Rev. Lett. **13**, 508-509 (1964). 2

[10] F. Englert, R. Brout, Phys. Rev. Lett. **13**, 321 (1964). 2

[11] G. S. Guralnik, C. R. Hagen, T. W. B. Kibble, Phys. Rev. Lett. **13**, 585 (1964). 2

[12] H. Fritzch, M. Gell-Mann and H. Leutwyler, Phys. Lett. **B47**, 365(1973). 2

[13] S. Weinberg, Phys. Rev. Lett. **31**, 494(1973). 2

[14] T. Muta, *Foundations of Quantum Chromodynamics: An introduction to Prturbative Methods in Gauge Theories*, World Scientific(2009) 2

[15] M. Shifman , *Advanced topics in quantum field theory*, Cambridge University Press(NY), 2012 2, 13

[16] D.J. Gross, F. Wilczek, Phys. Rev. Lett. **30**, 1343(1973). 2, 83, 84

[17] H.D. Politzer, Phys. Rev. Lett. **30**, 1346(1973). 2, 83, 84

[18] E. Reya, Phys. Rep. **14C**, 129(1974). 2

[19] S. Coleman, D. J. Gross, Phys. Rev. Lett. **31**, 851(1973). 2

[20] A. Zee, Phys. Rev. **D7**, 3630(1973). 2

[21] J. Frankel, J. C. Taylor, Nucl. Phys. **B109**, 439(1976). 2

[22] D. J. Gross, Rev. Mod. Phys. **77**, 837(2005). 2

[23] 't Hooft, Nucl. Phys. **B254**, 11(1985). 2

[24] C. Patrignani *et al.* (Particle, Data Group), Chin. Phys. C, **40**, 100001(2016). 3

[25] S. Weinberg , *The quantum theory of fields, Vol-II,* Cambridge University Press(NY), 1996 4, 13, 37

[26] J. D. Bjorken, Phys. Rev. **179**, 1547(1969). 4

[27] H. Georgi, H. D. Politzer, Phys. Rev. **D9**, 416(1974) 4

[28] A. J. Buras, Rev. Mod. Phys. **52**, 199(1980). 4

[29] R. P. Feynman, "*The Behaviour of Hadron Collisions at Extreme Energies*". High Energy Collisions: Third International Conference at Stony Brook, N.Y. Gordon and Breach(1969). 4

[30] Y. Nambu, G Jona-Lasinio Phys. Rev. **122**, 345 (1961); Phys. Rev. **124**, 246(1961). 5

[31] L. N. Cooper, Phys. Rev, **104**, 1189(1956). 5

[32] J. Bardeen, L. N. Cooper and J. R. Schrieffer, Phys. Rev. **108**, 1175(1957). 5

[33] N. N. Bogolyubov, Sov. Phys. JETP, **7**, 41(1958)[Zh. Eksp. Teor. Fiz.34, 58(1958)][Front. Phys. 6, 399(1961)]. 5

[34] P. D. B. Collins, Phys. Rept. 1, 103(1971) 5

[35] A. C. Irving, R. P. Worden, Phys. Rept. **34**, 117(1977). 5

[36] D. Ebert, R. N. Faustov and V. O. Galkin, Phys. Rev. D79, 114029(2009), arXiv:0903.5183[hep-ph]. vii, 6

[37] G. Veneziano, Nuovo. Cim. **A30**, 457(1970). 7

[38] Cheuk-Yin Wong, *Introduction to High-Energy Heavy-Ion Collisions*, World Scientific Pte. Ltd.(1994). 8

[39] L. Susskind, Nuovo. Cim. **A69**, 3(1970). 8

[40] A. A. Abrikosov, Journal of Physics and Chemistry of solids, **2**, 199(1957). 9

[41] V. L. Ginzburg, L. D. Landau, JETP (USSR), **20**, 1064(1950). 9

[42] H. B. Nielsen, P. Olesen, Nucl. Phys. **B61**, 45(1973). 9

[43] P. Goddard, J. Goldstone, C.Rebbi and C. B. Thorn, Nucl. Phys. **B56**, 109(1973).

[44] S. Coleman, *Aspect of Symmetry*, Cambridge University Press(NY), (1985). 13

[45] G. 't Hooft, Nucl. Phys. B190, 455(1981). 13

[46] G. 't Hooft, arXiv:0010225[hep-th](2000). 13

[47] A. Vilenkin, E. P. S. Shellard, *Cosmic Strings and other topological defects*, Cambridge University Press(NY), 1994. 14

[48] E. Cremmer, J. Scherk Nucl. Phys. **B72**, 117(1974). 18

[49] H. Ruegg, M. Ruiz-Altaba, Int. J. Mod. Phys. **A19**, 3265 (2004). 18, 19

[50] R. Jackiw, Annals Phys. **140**, 372(1982); Annals Phys. **281**, 409(2000). 19

[51] R. Jackiw, *Topological investigation of quantized gauge theories*, Les Houches Summer School, North-Holland(1983). 19

[52] C. Becchi, A. Rouet, R. Stora, Comm. Math. Phys. 42,127(1975). 25

[53] I. V. Tyutin, Lebedev Institute Preprint N39(1975). 25

[54] L. D. Faddeev, A. A. Slavnov, *Gauge Fields, Introduction to Quantum Theory,* Perseus Books, Cambridge, Massachusetts(1991). 25

[55] I. Ojima, Nucl. Phys. **B143**, 340(1978). 26

[56] J. Goldstone, A. Salam and S. Weinberg, Phys. Rev. **127**, 965(1962). 27

[57] T. Kugo, I. Ojima, Prog. Theor. Phys. **66**, 1(1979). 28

[58] S. Weinberg, *The Quantum Theory of Fields, Vol-1*, Cambridge University Press(NY)(1995). 23, 29

[59] F. Strocchi, *An Introduction to Non-Perturbative Foundation of Quantum Field Theory*, Oxford Univ. Press(UK)(2013). 29

[60] F. Strocci, Phys. Lett. **B62**, 60.(1976). 29

[61] R. Hagg, D. Kastler, J. Math. Phys. **5**, 848(1964).

[62] K. Nishijima, Int. J. Mod. Phys. **A9**, 457(1994).

[63] M. Chaichian, K. Nishijima Eur. Phys. J. **C47**, 737(2006).

[64] M. Veltman, Nucl. Phys. **B7**, 637(1968). 33

[65] M. Veltman, Nucl. Phys. **B21**, 288(1970). 33

[66] Ken-Ichi Shizuya, Nucl. Phys. B121, 125(1977). 33

[67] H. Umezawa, Nucl. Phys. 23, 399(1961). 33

[68] J. M. Cornwall, Phys. Rev. **D26**, 1453(1982). 33

[69] J. M. Cornwall, J. Papavassiliou and D. Binsoi, *The Pinch Technique and its Application to Non-Abelian Gauge Theories*, Cambridge Univ. Press(UK)(2011). 33

[70] G. Curci, R. Ferrari, Nuovo Cim. **A32**, 151(1975). 33

[71] I. Ojima, Z. Phys. **C13**, 173(1982). 34

[72] J. Thierry-Mieg, L. Baulieu, Nucl. Phys. **B197**, 477(1982), Nucl. Phys. **B228**, 259. 21

[73] R. Kumar, R. P. Malik, Eur. Phys. J. **C71**, 1710(2011). 21

[74] R. Kumar, R. P. Malik, Europhys. Lett. 94, 11001(2011). 21

[75] E. Wichmann, J. H. Crichton, Phys. Rev. **132**, 2788(1963). 29

[76] H. Araki, K. Hepp and D. Ruelle, Helv. Phys. Acta **35**, 164(1962). 29

[77] W. Greiner, J. Reinhardt, *Field Quantization*, Springer(1996).

[78] L. D. Faddeev, arXiv:0911.1013[math-ph](2009). 29

[79] S. Weinberg, Phys. Rev. **140**, B516.(1965).

[80] G. 't Hooft, *Gauge theories with unified weak, electromagnetic and strong interactions*, in Proc EPS Int. Conf. on High energy Physics, Palermo, June(1975).

[81] J. Zinn-Justin in Trends in Elementary Particle Theory-International Summer Institute on Theoretical Physics in Bonn 1974 (Springer-Verlag, Berlin, 1975). 37

[82] B. W. Lee, J. Zinn-Justin, Phys. Rev. **D5**, 3121(1972); Phys. Rev. **D5**, 3121(1972). 37

[83] O. Piguet, S. P. Sorella, *Algenraic Renormalization, Perturbative Renormalization, Symmetries and Anomalies*, Springer(1995). 37

[84] P. A. Grassi, Nucl. Phys. B462, 524(1996). 37

[85] M. Veltman, Nucl. Phys. **B22**, 397(1970).

[86] Kei-Ichi. Kondo, Phys. Rev. D87, 025017(2013).

[87] S. Joglekar Annals. Phys. **83**, 427(1973). 39, 42, 44

[88] C. E. Vayonakis Lett. Nuovo. Cim **17**, 383(1976). 39, 42, 44

[89] B. Lee, C. Quigg, and H. B. Thacker, Phys. Rev. **D16**, 1519(1977). 39, 42, 44

[90] A. Lahiri, D. Mukhopadhyay, Unitarity in $WW \to WW$ elastic scattering in topologically massive $SU(2)$ gauge theory, arXiv:1107.1501[hep-ph]. 40

[91] B. de. Wit, J. Smith, *Field Theory In Particle Physics*, North Holland Physics(NY)(1986). 44

[92] H. Veltman, M. Veltman Act. Phys. Polon **B22**, 669(1991). 42, 44

[93] W. Kilian, *Electroweak Symmetry Breaking-The Bottom-Up Approach*, Springer(NY)(2003). 44

[94] J. M. Cornwall, D. N. Levin, G. Tiktopoulos, Phys. Rev. **D10**, 1145 (1974). 42

[95] J. Horejsi, *Introduction to Electroweak Inification, Standard Model from Tree Unitarity*, World Scientific(1994). 42

[96] J. S. Bell, Nucl. Phys. **B60**, 427(1973). 50

[97] C. H. Llewellyn Smith, Phys. Lett. **B46**, 233 (1973). 50

[98] K. Gottfried, Tung-Mow Yan, *Quantum Mechanics: Fundamentals*, Springer(NY)(2003). 67

[99] J. J. Sakurai, *Mordern Quantum Mechanics*, Pearson Education Limited(2013). 67

[100] L. I. Schiff, Quantum Mechanics, Tata-MacGraw-Hill Education Pvt. Ltd(2014). 48, 67

[101] Wu. Ki. Tung, *Group Theory in Physics*, World Scientific Pvt. Ltd.(1985). 67

[102] F. Englert and R. Brout Phys. Rev. Lett. **13**, 321(1967). 50

[103] P. W. Higgs Phys. Rev. Lett. **13**, 508(1964). 50

Act. Phys. Polon **B8**, 475(1977).

[104] M. Chanowitz, Zuoz 1998, Hidden symmetries and Higgs phenomena, arXiv:9812215[hep-ph](1998)

,

[105] D. Mukhopadhyay, A. Lahiri, Phys. Rev. **D90**, 025015, arXiv:1407.3148[hep-ph]. 83

[106] C. Itzykson, Z. B. Zuber, *Quantum Field Theory*, McGraw-Hill Book Co.(1986). 95, 107

[107] M. Srednicki, *Quantum field Theory*, Cambridge Univ. Press(2007). 89

[108] S. Pokorski, Gauge Field Theories, Cambridge Univ. Press(1987). 89

[109] J. de Boer, K. Skenderis, P. van Nieuwenhuizen, A. Waldron, Phys. Lett. **B367**, 175(1996). 85